FORENSIC ANALYSIS OF INK ON DOCUMENTS USING DIRECT ANALYTE-PROBED NANOEXTRACTION COUPLED TECHNIQUES

Vivian Huynh, B.S.

Dissertation Prepared for the Degree of

DOCTOR OF PHILOSOPHY

UNIVERSITY OF NORTH TEXAS

May 2016

APPROVED:

Teresa Golden, Major Professor
Guido Verbeck, Committee Member
Francis D'Souza, Committee Member
Martin Schwartz, Committee Member
Gabriel Watts, External Committee Member
Michael Richmond, Chair of the Department of Chemistry
Costas Tsatsoulis, Dean of the Robert B. Toulouse Graduate School

Huynh, Vivian. Forensic analysis of ink on documents using direct analyte-probed nanoextraction coupled techniques. Doctor of Philosophy (Chemistry-Analytical Chemistry), May 2016, 169 pp., 16 tables, 53 illustrations, references, 253 titles.

Analzying questioned documents in a nondestructive nature has been an issue for the forensic science community. Using nondestructive techniques such as video spectral comparator does not give reliable information due to the variations in gray or color levels that are distinguished differently by analysts. Destructive techniques such as chromatography give dependable, qualitative and quantitative, information but involves altering the evidentiary value of these questioned documents. The paradox of document examination becomes a problem when document evidence is involved, especially when trying to preserve its evidentiary value and critical data is needed. Thus, a nondestructive technique has been developed to solve the loopholes in document examinations.

Direct analyte-probed nanoextraction (DAPNe) is a nanomanipulation technique that extracts ink directly off the document for further examination. A watermark is left, at most, post-extraction. DAPNe utilizes a tip emitter, pre-filled with a solvent, which is controlled in x-, y-, and z-coordinates via joystick controller and aspirates/extracts using a pressure injector. The versatility of this technique lies within the solvent chemistry and its capability to be coupled to various types of instrumentation. The extraction solvent can be altered to target specific components in the ink. For example, a chelator may be added to target metal ions found in ancient inks or methanol may be added to target certain organic resins and binding agents found in modern inks. In this study, DAPNe has been coupled to nanospray ionization mass spectrometry, fluorescence microscopy, Raman spectroscopy, matrix-assisted laser desorption ionization mass spectrometry, and laser

ablation to solve questioned document concerns in the area of falsified or forged documents, redacted documents, and aging studies.

ACKNOWLEDGEMENTS

First, I would like to thank my research advisor Teresa Golden and my co-advisor Guido Verbeck for all of their support, guidance, motivation, inspiration, and most of all their enthusiasm for this project. I enjoyed working for them and gained endless experience from the past several years working at UNT's laboratory of imaging mass spectrometry. I would also like to express gratitude towards Francis D'Souza, Martin Schwartz, and Gabriel Watts for taking the time to be a part of my committee and their guidance throughout my time in the graduate program. I would also like to acknowledge the National Institute of Justice grant for funding this research project.

I would like to recognize the Golden and Verbeck research group for everything that they have taught me, laughs that they have given me, and especially the meaningful friendships that were created throughout my graduate career. I would like to give a special thanks to Charlie Williams for her guidance, Casey Thurber for running SEM for me, Roberto Aguilar for soft landing silver nanoparticles for my samples, Mandy Phelps for teaching me how to use MALDI-MS, Jason Hamilton for teaching me how to operate LA-ICP-MS, and Phillip Mach and Zachary Sasiene for all their hard work in laser ablation.

Above all, I would like to thank my mom, brother, and my best friend for their love and motivation. Thank you mom for everything that you have done to mold me into the person I am today. Your hard work and motivation has defiantly influenced me to follow in your footsteps. Thank you Stanley and Thao for your encouraging words and being there for me, especially in those times of doubts and stressful moments. My greatest love and special thanks to you all!

TABLE OF CONTENTS PAGE

LIST OF TABLES

LIST OF FIGURES

CHAPTER 1

INTRODUCTION

1.1 Research Motivation

Direct analyte-probed nanoextraction (DAPNe) is a new and innovative technique for direct *in-situ* nano-sampling of analytes at trace and ultra-trace levels. This genuine method has been utilized for many different forensic applications for the past six years [1–4] and continues to transcend. DAPNe is advantageous due to its attractive features in requiring minimal to no sample preparation, ability to extract a volume as low as 300 nL, its minimal to nondestructive nature, and most importantly, its potential to be coupled to many different types of instrumentation. The aforementioned features have allowed the forensic science community to expand and advance in their techniques and methods of analysis for evidence investigations.

DAPNe has been implemented on various case studies including trace analysis of energetic materials [5], drug residues from latent fingerprints [6], trace particles found on fibers [2], and ultra-trace analysis of illicit drugs from transfer of an electrostatic lift [3]. The versatility of this technique has also been expanded towards biological studies such as lipid [7,8] and single cell [9–11] analyses. One area, in the field of forensics, which has yet to be established by DAPNe is ink on document investigations.

My dissertation focuses on developing a direct sampling method via DAPNe coupled to a variety of instruments for the forensic analysis of ink on documents. This means of analysis will aid forensic document examiners in the area of document fraud and forgery including, but not limited to, plagiarized ancient manuscripts, forging checks, banknotes, contracts, and government official documents.

Document fraud has become an increasing and prominent issue affecting both developed and developing countries. Criminal activity involving falsified documents can result in medical malpractice, altered wills, patent disputes, tax and insurance fraud, wrongful terminations, copyright cases, identity theft, and many other unlawful activities [12]. Forensic document examiners have used several techniques to distinguish fabricated from authentic documents. These common techniques are not favorable due to two reasons: (1) nondestructive techniques preserve the integrity of the document but may not give significant or reliable information and (2) destructive techniques involve altering the document in a harmful manner but produces critically important and dependable information. The paradox of document examination becomes a problem when document evidence is involved, especially when trying to preserve its evidentiary value and critical data is needed. These destructive and nondestructive methods are described hereinafter and summarized in Table 1.1.

Methods	Type of Technique	Destructive process
Video Spectral Comparison	Microscopy, Fluorescence	Not destructive, lacks reliable information
Thin-layer Chromatography	Separation	Requires destructive removal of ink from document
High Performance Liquid Chromatograph	Separation	Requires destructive removal of ink from document
Gas Chromatography	Separation	Requires destructive removal of ink from document
Capillary electrophoresis	Separation	Requires destructive removal of ink from document
Desorption Electrospray Ionization	Direct Analysis	Require large amount of surface area
Direct Analysis in Real Time	Direct Analysis	Require large amount of surface area
Liquid Extraction Surface Analysis	Direct Analysis	Workstation size limitation
Matrix-Assisted Laser Desorption Ionization	Direct Analysis	Sample holder limitation
Secondary Ion Mass Spectrometry	Direct Analysis	Sample holder limitation

Table 1.1. Summary of techniques used to analyze ink on documents.

Traditional and nondestructive methods involve visual examination of the document by microscopy and video spectral comparison (VSC). VSC utilizes light sources, typically 400-700 nm, to identify different variations in the inks or visualize hidden security features. Although nondestructive, this method is limited to analyzing solely visual characteristics of inks. VSC relies on visual comparison of gray levels and fails to discern between inks in suspected alterations [13]. Other common analytical techniques used, but destructive, include thin-layer chromatography (TLC) [14,15], high performance liquid chromatrography (HPLC) [13–16], gas chromatography (GC) [15,17], and capillary electrophoresis [18,19]. Sample preparation for these separation techniques involve micropunching holes [20], cutting strips [15,21,22], or pulling ink-bearing fibers from the document [23]. Those pieces are then placed into a solvent in order to diffuse the

ink from the paper for further analysis. Although these techniques give reliable and significant information, they are destructive.

There are also many types of direct analysis methods, with a concept similar to DAPNe, which have been performed on ink from documents. These types of techniques are advantageous due to its simplicity and lack of required sample preparation. Another positive characteristic of using a direct analysis technique is its ability to analyze ink directly from the document. This reduces sample preparation time and does not require the ink to be destructively removed from the document, unlike separation techniques, prior to analysis. These methods include desorption electrospray ionization (DESI), direct analysis in real time (DART), and liquid extraction surface analysis (LESA). DESI provides a rapid and direct approach to ultra-trace analysis by releasing charged droplets onto the surface for ionization of analytes [24]. DART is another high throughput surface method that releases excited state gas molecules for ionization of the analytes on the surface [25]. LESA uses an automated sampling probe for direct analysis [26]. LESA is the most similar technique to DAPNe in that they both interact directly with the surface at the liquid junction. DESI and DART requires a large amount of surface area for analyte ionization and in turn are more destructive. LESA currently has an enclosed workstation with limited workspace which confines document size. Although LESA has a less destructive means of analysis, document constriction of its workstation limits the analysis of documents as a whole. LESA is not as versatile as DAPNe when coupled to different instrumentation due to its enclosed workstation and computerized extractions.

Mass spectrometric methods such as laser desorption ionization mass spectrometry (LDI-MS), matrix-assisted laser desorption ionization-MS (MALDI-MS), and secondary ion mass spectrometry (SIMS) are also considered direct analysis techniques. Utilizing MS techniques

instead of chromatographic separation reduces both time and solvent needs [21,27,28]. Similarly to the abovementioned direct analysis techniques, one major drawback with implementing MS methods is also the limitation of sample space. Weyermann et al. [29] analyzed 30 black gel pen inks using LDI-MS, where the sample was fixed to a solid steel plate with glue. Even though the samples were directly analyzed without the addition of a matrix, reducing preparation time, the samples were cut in order to be fitted to the plate. Similarly, Wu et al. [15] cut 5 cm ink entries into small pieces and extracted the ink by 1.0 mL of dimethyl formamide (DMF) for 12 h and then filtered through a 0.22 μm Millipore film prior to LDI-MS analysis, both destructive and time-consuming. LDI and MALDI techniques are limited to the size of the sample plate and can have an extended sample preparation time. Denman et al. [30] analyzed 24 blue ballpoint pens using time-of-flight (ToF)-SIMS and prepared the samples by drawing a 3 cm line on paper with each spectral analysis performed over a 100 × 100 μm raster area. Although surface analysis by ToF-SIMS provides ballpoint pen ink discrimination and is nondestructive, like the previous techniques, it is also limited to the size of the sample holder.

Harming the document or altering it from its pristine state is not favorable, especially when examining evidence. DAPNe applied to ink on document analysis is advantageous due to its large sampling space and its ability to extract ultra-trace amounts of sample. This allows documents to not be cut, in order to be fitted to the sample holder, and also provides minimal to no destruction post-analysis. The remarkable ability of DAPNe-NSI-MS is its ease of coupling to other instrumentation such as nanospray ionization mass spectrometry, fluorescence microscopy, Raman spectroscopy, laser ablation, and matrix-assisted laser desorption ionization mass spectrometry to benefit the determination of fraud and document forgery. This advantage provides an immediate and effective way of conducting chemical analysis for ink on document analysis.

Thus, implementing DAPNe coupled instruments to investigate counterfeit documents as a nondestructive and innovative technique is favorable.

1.2 Significance of Study

The significance of this research can have an immediate impact for forensic investigations. The analysis of trace residue within document and ink samples could pinpoint or eliminate potential suspects, and lead to acceptable court resolution. Chemical signature data from the extracted residue can offer an ink database to group and characterize documents. The majority of inks offer chemical signature pointing to manufacturing that could be acquired using this method, thus linking group and distribution chains together with documents.

This research focuses on the development, optimization, and validation of a methodology using DAPNe coupled NSI-MS, fluorescence microscopy, Raman spectroscopy, laser ablation, and MALDI-MS to analyze forged documents. Several ancient inks from the Middle Ages and many modern inks have been analyzed on paper (including printer ink). These high-throughput techniques are simple and almost no sample preparation is required.

1.3 Characterization of Counterfeit Documents

The genesis of ink history began forty centuries ago and have significantly advanced through time, past the age of stone inscription and clay tablet [31]. This section discusses the transition of ink formulas and writing instruments derived from different eras. Table 1.2 summarizes some significant events of commonly used inks that have revolutionized writing.

Time Period	Ink Type	Location
3500BC-300AD	Indian Ink or Carbon Black Ink	China and Egypt
450AD-1900s, still used today.	Iron Gall ink	Europe
1770s	First Patent for colored ink was developed	England
1780s	Steel pen points begin to replace quill feathers.	England
1870s	Fountain Pen	United States
1940s	Ballpoint pens	United States

Table 1.2. Summary of some historical ink events [14,31–33].

1.3.1 Ancient inks

Iron gall ink has made a huge impact in Western history, from the late Middle Ages until the early part of last century [33,32]. It was heavily used for many significant events from the 5th to as recent as the 19th century (Table 1.2). Many artists such as Leonardo da Vinci, Van Gogh, and Rembrandt drew with Iron gall ink. Musical artists, like Bach, composed with it. The black ink on the Dead Sea Scrolls and even a drafted version of the Constitution of the United States was found to be written with Iron gall ink. Other inks used were carbon-based such as India and Japanese Sumi-e ink. These inks smudged easily and did not adhere well to the paper. The popularity of Iron gall ink was due to its adherent and smudge-proof properties to paper as well as its use of natural ingredients used to make the ink formula.

Iron gall ink is first made by crushing galls obtained from oak trees to acquire gallotannic acid. Water is then added to gallotannic acid to break the ester links, forming gallic acid (Figure 1.1) [34].

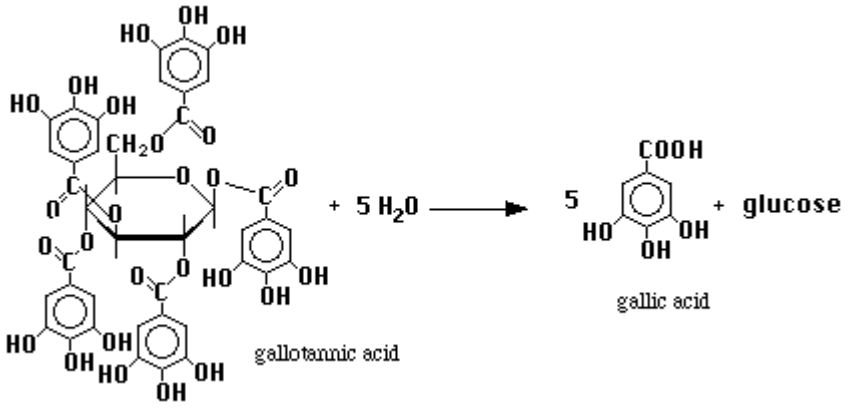

Figure 1.1. Water inducing the breaking of ester links from gallotannic acid, forming gallic acid [33].

Finally, water and vitriol (iron (II) sulfate) are added to the mixture followed by adding a suspension agent, gum Arabic from acacia trees [32]. The final product produced is Iron gall ink (equation 1.1).

$$\text{Gallic} + FeSO_4 \cdot H_2O + \text{water} \rightarrow \text{Iron gall ink} \qquad (1.1)$$

Other metal-complexes such as calcium, zinc, copper, and manganese could also be found in Iron Gall inks. These metals contribute to the corrosive nature of Iron gall inks, inducing a color change of black to brown which often fades over time. Adversely, the chemical changes obtained from Iron gall ink over time also contributes to the uniqueness and originality of the manuscript's credibility. The historical documents created throughout ancient history are now and have been regenerated as "authentic pieces".

Plagiarizing ancient documents is difficult due to mimicking the ink chemistry of natural aging that occurs over time with both the ink and paper. Acceleration of aging ink may have a different physical appearance than naturally aged ink. Analytical techniques are implemented to determine the components found in authentic documents compared to counterfeit documents. By

adding a chelator to the extraction solvent, DAPNe can effectively chelate and characterize the metal complexes from Iron gall ink [35]. Not limited to just inorganic analytes, DAPNe can also be used to characterize organic components in carbon-based inks. Carbon-based inks were made by acquiring carbon black or from finely pulverized pin ash (obtaining a black color) and then adding lamp oil which contained gelatin. These oils are considered binding agents which include glycols, such as polyethylene glycol (PEG) or diethylene glycol that can be characterized using a method of analysis. Counterfeiters will try to mimic historical documents by creating the ink themselves and applying heat or UV light to age the document [36]. DAPNe-NSI-MS can also be used to monitor the aging process of certain components of ink (e.g., monitoring the oxidation of PEG), narrowing the time period of when the ink was placed on paper [4,35]. Most times, ingredients and paper used to create false manuscripts are not from the correct era or have used an ingredient in the inks that was not used during that time period. This gives document analysts the opportunity to determine the loopholes mistakenly made by con artists creating counterfeit documents.

1.3.2 Modern Inks

The metal content in current inks have decreased due to its destructive and corrosive properties. Common modern pens used today are ballpoint, gel, and rollerball pens which all have different mechanisms for depositing inks [23]. These inks contain many dyes and binding agents to optimize pigment and color stability from pen to paper. Some common dyes and binding agents found in inks are shown in Table 1.3. Ballpoint pens with oil-based inks were first introduced in the 1940s, presenting a new kind of writing apparatus and ink. Before this time, water-based inks were used with fountain and dip pens [37]. Polyethylene glycol (PEG)-based inks began replacing the oil-based ink formulas in 1952. Advancing through history, many different pen apparatuses

and ink formulas were introduced; but PEG has managed to remain constant in many ink formulations today. The polar nature of PEG has allowed a wider range of dyes to be used and were found to adhere firmly to cellulose fibers where inks can neither be smudged nor transferred [38]. It also helps pigments to stay dispersed in solution. The molecular structure of PEG contains a repeating oxyethylene unit (-C_2H_4O-), making the oligomer distribution spaced 44 u apart [39]. The structural formula of PEG is $H(C_2H_4O)_nOH$, where n represents the number of repeating units. For mass spectral analysis, PEG ions are observed to have proton, sodium, or potassium adducts, $[HO(C_2H_4O)_nH + H]^+$, $[HO(C_2H_4O)_nH + Na]^+$, or $[HO(C_2H_4O)_nH + K]^+$, respectively [40].

Dyes and Binding agents	Molecular Formula	Molecular Mass (g/mol)
Diethylene Glycol	$C_4H_{10}O_3$	106.12
Basic Violet 1	$C_{29}H_{28}N_3NaO_7S_2$	617.67
Basic Violet 2	$C_{22}H_{24}ClN_3$	365.90
Acid Yellow 36	$C_{18}H_{16}N_3NaO_3S$	377.39
Diethylene Phthalate	$C_{12}H_{14}O_4$	222.24
Ethoxy Diglycol	$C_6H_{14}O_3$	134.18
Glycerol	$C_3H_8O_3$	92.09
Hexylene Glycol	$C_6H_{14}O_2$	118.17
2-Phenoxyethanol	$C_8H_{10}O_2$	138.16
Polyethylene Glycol, n=5-44*	$HO[CH_2CH_2O]_nH$	44 u per monomer
Propylene Glycol	$C_3H_8O_2$	76.09
Tripropylene Glycol	$H[OC_2H_3(CH_3)]_3OH$	192.25
Triethylene Glycol	C6H14O4	150.17
Triethanolamine	$C_6H_{15}NO_3$	149.19
Crystal Violet	$C_{25}N_3H_{30}Cl$	407.97
Rhodamine B	$C_{28}H_{31}ClN_2O_3$	479.02
Rhodamine 6G	$C_{28}H_{31}N_2O_3Cl$	479.02
Pigment Violet 23	$C_{34}H_{22}Cl_2N_4O_2$	589.47
Brilliant Green	$C_{27}H_{33}N_2HO_4S$	482.64
Methlyene Blue	$C_{16}H_{18}N_3SCl$	319.85
Methyl Green	$C_{16}H_{17}ClN_4O_2S$	653.24
Pigment Red 12	$C_{25}H_{20}N_4O_4$	440.45
*where n represents the number of monomers.		

Table 1.3. Common dyes and binding agents found in modern inks [15,23,35,41].

The progression of these instruments also allow inks to be used in many diverse ways such as handwriting text, printing text, and producing government official documents. Although these advancements are positive, security issues arise from some subjects in the public falsifying breeder documents and impersonating someone else. In order to avoid this issue and make the production of forged documents more difficult, these inks have been secured by adding markers that make the ink unique and proprietary to the government. England was the first to use fluorescent brighteners as antifraud tracers and markers as distinction agents between authentic and counterfeit paper moneys and postage stamps [42]. Karanikas et al. [42] focuses their research work on developing an easy to use "antifraud digital printing system" to distinguish the original from the counterfeit items. These markers can be anything from adding rare-earth elements to organic modifiers, thus making forged documents more difficult to produce.

1.4 Fluorescent Nature of Dyes

Dyes are fluorescent chemical compounds that can re-emit light upon light excitation, strongly absorbing light in the visible region. Dyes typically have structures with several combined aromatic groups, plane, or cyclic molecules with several π bonds, giving them fluorescent properties. The aromatic structure of dyes have delocalized electron systems via certain atomic configurations called chromophore groups [43]. These configurations include, alternate single and double bonds with nitrogen, carbon, oxygen, and sulfur atoms.

Ink pens have been distinguished from one another by comparing its fluorescent intensities. This is accomplished through nondestructive techniques such as VSC and microscopy. Due to the inks fluorescent nature, analyzing forged document with Raman spectroscopy are more difficult. This is because dyes contain structural characteristics that are present in the chromophore, such as electron donating groups (e.g., –OH, $–NH_2$, $–OCH_3$) that may increase the quantum yield. The

fluorescence interference is an issue because it can cover the anticipated chemical footprints of the sample. To overcome this, a laser, with a wavelength deviated from the visible region (400-700 nm), must be used. This will reduce fluorescence interference from both the paper and ink. While a 532 nm laser would produce poor data, using a laser with a wavelength of 780 nm and above will suffice [35,44,45].

1.5 Collisional-Induced Dissociation of Isomeric Dyes

Differentiating isomeric dyes in mass spectra is difficult due to the same peak produced, as illustrated in Figure 1.2. Dyes with the same isomeric structure, such as Rhodamine B and Rhodamine 6G, will produce the same parent ion (m/z 443) when using mass spectrometric techniques [36]. Collisional-induced dissociation (CID) must be implemented to distinguish the Rhodamine structures.

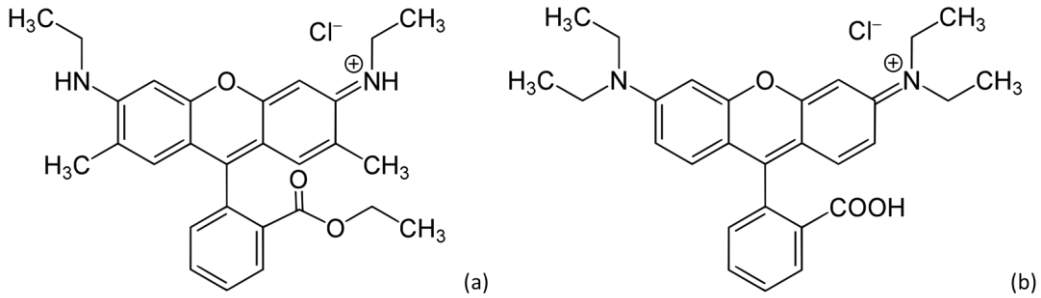

Figure 1.2. Isomeric structures of (a) Rhodamine 6G and (b) Rhodamine B.

CID selects a particular ion to fragment that is bombarded with a certain amount of energy. This creates fragments derived from the isolated molecular (parent) ion, known as daughter ions. When CID is conducted on Rhodamine B, isolating *m/z* 443, *m/z* 415 and 399 daughter ions are created. The daughter ion *m/z* 399 is not seen when CID is conducted on Rhodamine 6G dye. The peak at *m/z* 399 results from a loss of CO_2 from Rhodamine B dye.

1.6 Solvent Chemistry

The extraction solvent used when conducting extractions with DAPNe influences which component of the ink is being extracted and the intensities of the molecular ion peaks in a mass spectrum. For example, if PEG and Crystal Violet were components found in the same ink pen, different solvents may be used to extract each component individually. Crystal Violet is more soluble in cholorform and PEG is more soluble in methanol. Therefore, depending on which solvent is used as the extraction solvent, the intensities of the targeted component may change. In a previous study, EDTA was incorporated into the extraction solvent in order to chelate Fe and Mn ions from iron gall ink [35]. Being able to extract different components from the same ink entry, using one inclusive technique, illustrates the versatility of DAPNe.

The variation of peak intensities, affected by the extraction solvent used, can be compared by converting the relative peak intensities into points via a rating scale, as shown in Table 1.4. The peak intensities are first normalized and then assigned points based on the rating scale. The rating scale is based on normalizing to 100 but this can relatively be altered. For example, when analyzing Crystal Violet, two peaks *m/z* 372 and 358 are produced. If the intensities of *m/z* 372 and 358 were 12 and 61 respectively, then the total points would be 7 for that particular solvent used to extract Crystal Violet dye from the document. When using a different solvent, the total points will vary. The higher the total points, the more optimal that solvent is.

Relative Peak Intensities	Points
<10	0
11-19	1
20-29	2
30-39	3
40-49	4
50-59	5
60-69	6
70-79	7
80-89	8
90-100	9

Table 1.4. A rating scale used to convert relative peak intensities into points [4].

1.7 Aging Studies

Inks begin to age and oxidize as soon as it is dispensed on the paper surface due to solvent loss, resin polymerization, and dye degradation [46]. Ink dating has been a highly concerned and interested topic for document examiners. The ability to date documents via age determination would greatly aid investigations of backdating frauds. For aging studies to be successful, common agents found in inks must be monitored (e.g., PEG and/or Rhodamine Dye) over time.

PEG is a great candidate for short-term aging studies because it easily oxidizes. It is susceptible to radical oxidative attack. This leads to the thermal degradation of PEG producing low molecular weight products. As thermal degradation continues, the amount of low molecular weight products increase [47]. L. Boughen et al. [48] determined that after a few years of PEG in a capped bottle, the degraded PEG had a strong aldehyde/ketone odor and it had become a paste (like toothpaste). J. Glastrup et al. [49] heated PEG 4000 for 2-4 h which has in some cases led to the formation of a liquid that would not solidify after cooling. They have shown that this liquid more resembled PEG 600 than the original PEG 4000. Furthermore, the ratio of PEG changes over time as the production of low molecular weight products increase. This increase correlates with

the age increase of PEG. The variation in the peak intensities can be monitored by using the relative peak area (RPA) formula in Equation 1.2.

$$RPA_i = \frac{A_i}{A_{tot}} x100 \tag{1.2}$$

where A_i is the area of the peak at *m/z*=i and A_{tot} is the summation of all the significant signals, including molecular ion and degradation products [4,35]. The RPA equation may be used for oxidative mass spectrometric studies.

Monitoring the oxidation of dyes would be ideal for long term aging studies due to its fairly stable structure. Dyes could take decades to oxidize a significant amount. In 2005, Siegel et al. [36] analyzed documents from 1996, 1974, and 1961. These documents contained Crystal Violet dye from analyzing the blue ink. The more methyl groups Crystal Violet loses, the more it is oxidized. Significant degradation products of Crystal Violet was observed from the documents from 1974 and 1961 (Figure 1.3).

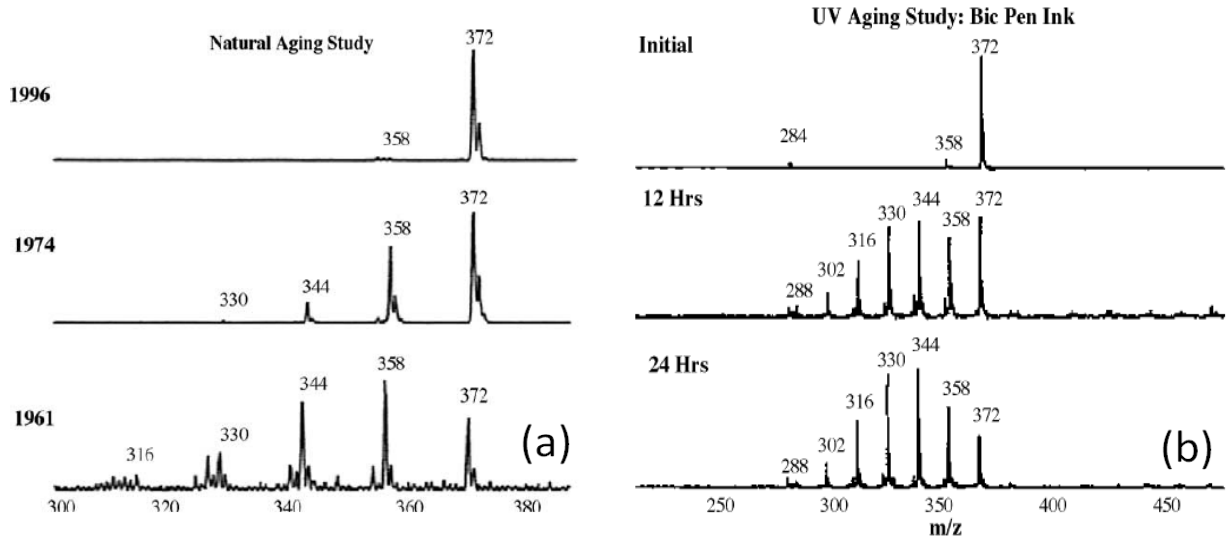

Figure 1.3. Aging studies conducted on (a) naturally aged documents and (b) UV aged documents [36].

The documents from 1996, 1974, and 1961 lose 1, 3, and 4 methyl groups respectively from the parent ion (*m/z* 372). The methyl group lost from the 1996 document was at very low intensity. Siegel et al. also determined that irradiating blue ink for 12 hours with UV light yielded six degradation products. After 24 hours, the same number of peaks were still apparent but the intensity of the parent peak decreased over time.

As demonstrated by Siegal et al., degradation products are produced as the ink oxidizes. The longer the ink oxidizes the parent peak also start to decrease/disappear. Thus, the ratio of the peaks change over time. By establishing a library of aging studies conducted on documents, in different environments using endless amounts of inks and paper, would aid forensic document examiners in narrowing the time frame of document forgery.

1.8 References

[1] J.M. Brown, W.D. Hoffmann, C.M. Alvey, A.R. Wood, G.F. Verbeck, R.A. Petros, One-bead , one-compound peptide library sequencing via high-pressure ammonia cleavage coupled to nanomanipulation / nanoelectrospray ionization mass spectrometry, Anal. Biochem. 398 (2010) 7–14. doi:10.1016/j.ab.2009.10.044.

[2] N.L. Ledbetter, B.L. Walton, P. Davila, W.D. Hoffmann, R.N. Ernest, G.F.V. Iv, et al., Nanomanipulation-Coupled Nanospray Mass Spectrometry Applied to the Extraction and Analysis of Trace Analytes Found on Fibers *, J. Forensic Sci. 55 (2010) 1218–1221. doi:10.1111/j.1556-4029.2010.01406.x.

[3] N. Wallace, E. Hueske, G.F. Verbeck, Science and Justice Ultra-trace analysis of illicit drugs from transfer of an electrostatic lift, Sci. Justice. 51 (2011) 196–203. doi:10.1016/j.scijus.2010.11.004.

[4] V. Huynh, K.C. Williams, T.D. Golden, G.F. Verbeck, Investigation of falsified documents via direct analyte-probed nanoextraction coupled to nanospray mass spectrometry, fluorescence microscopy, and Raman spectroscopy, Analyst. 140 (2015) 6553–6562. doi:10.1039/C5AN01026H.

[5] K. Clemons, J. Dake, E. Sisco, G.F. Verbeck, Trace analysis of energetic materials via direct analyte-probed nanoextraction coupled to direct analysis in real time mass spectrometry, Forensic Sci. Int. 231 (2013) 98–101. doi:10.1016/j.forsciint.2013.04.022.

[6] K. Clemons, R. Wiley, K. Waverka, J. Fox, E. Dziekonski, G.F. Verbeck, Direct analyte-probed nanoextraction coupled to nanospray ionization-mass spectrometry of drug residues from latent fingerprints, J. Forensic Sci. 58 (2013) 875–880. doi:10.1111/1556-4029.12141.

[7] P.J. Horn, N.R. Ledbetter, C.N. James, W.D. Hoffman, C.R. Case, G.F. Verbeck, et al., Visualization of lipid droplet composition by direct organelle mass spectrometry, J. Biol. Chem. 286 (2011) 3298–3306. doi:10.1074/jbc.M110.186353.

[8] P.J. Horn, U. Joshi, A.K. Behrendt, K.D. Chapman, G.F. Verbeck, On-stage liquid-phase lipid microextraction coupled to nanospray mass spectrometry for detailed , nano-scale lipid analysis, Rapid Commun. Mass Spectrom. 26 (2012) 957–962. doi:10.1002/rcm.6194.

[9] M.S. Phelps, G.F. Verbeck, A lipidomics demonstration of the importance of single cell analysis, Anal. Methods. 00 (2015) 1–3. doi:10.1039/C5AY00379B.

[10] M.S. Phelps, D. Sturtevant, K.D. Chapman, G.F. Verbeck, Desorption / Ionization-Direct Organelle Mass Spectrometry : A Technique for the Detailed Analysis of Single Organelles, Am. Soc. Mass Spectrom. 10.1007/s1 (2015) 1–7. doi:10.1007/s13361-015-1232-9.

[11] M. Phelps, J. Hamilton, G.F. Verbeck, Nanomanipulation-coupled nanospray mass spectrometry as an approach for single cell analysis, Rev. Sci. Instrum. 85 (2014) 124101. doi:10.1063/1.4902322.

[12] K.R. Brunelle, Richard L.; Crawford, Advances in the Forensic Analysis and Dating of Writing ink, Charlies C. Thomas Publisher, LTD., Springfield, 2003.

[13] C.D. Adam, S.L. Sherratt, V.L. Zholobenko, Classification and individualisation of black ballpoint pen inks using principal component analysis of UV–vis absorption spectra, Forensic Sci. Int. 174 (2008) 16–25. doi:10.1016/j.forsciint.2007.02.029.

[14] C. Neumann, R. Ramotowski, T. Genessay, Forensic examination of ink by high-performance thin layer chromatography-The United States Secret Service Digital Ink

Library, J. Chromatogr. A. 1218 (2011) 2793–2811. doi:10.1016/j.chroma.2010.12.070.

[15] Y. Wu, C.X. Zhou, J. Yu, H.L. Liu, M.X. Xie, Differentiation and dating of gel pen ink entries on paper by laser desorption ionization- and quadruple-time of flight mass spectrometry, Dye. Pigment. 94 (2012) 525–532. doi:10.1016/j.dyepig.2012.03.005.

[16] M.I. Kher, A.A.; Green, E.V.; Mulholland, Evaluation of principal components analysis with high-performance liquid chromatography and photodiode array detection for the forensic differentiation of ballpoint pen inks, J. Forensic Sci. 46 (2001) 878–883.

[17] S.L. LaPorte, G.M.; Wilson, J.D.; Cantu, A.A.; Mancke, S.A.; Fortunato, The identification of 2-phenoxyethanol in ballpoint inks using gas chromatography/mass spectrometry--relevance to ink dating, J. Forensic Sci. 49 (2004) 155–159.

[18] C. Vogt, J. Vogt, a. Becker, E. Rohde, Separation, comparison and identification of fountain pen inks by capillary electrophoresis with UV-visible and fluorescence detection and by proton-induced X-ray emission, J. Chromatogr. A. 781 (1997) 391–405. doi:10.1016/S0021-9673(97)00621-3.

[19] C. Cruces-Blanco, L. Gámiz-Gracia, a. M. García-Campaña, Applications of capillary electrophoresis in forensic analytical chemistry, TrAC - Trends Anal. Chem. 26 (2007) 215–226. doi:10.1016/j.trac.2006.12.007.

[20] L. Ng, L.K.; Lafontaine, P.; Brazeau, Ballpoint pen inks: characterization by positive and negative ion-electrospray ionization mass spectrometry for the forensic examination of writing inks, J. Forensic Sci. 47 (2002) 1238–1247.

[21] M. Gallidabino, C. Weyermann, R. Marquis, Differentiation of blue ballpoint pen inks by

positive and negative mode LDI-MS, Forensic Sci. Int. 204 (2011) 169–178. doi:10.1016/j.forsciint.2010.05.027.

[22] Y.-Z. Liu, J. Yu, M.-X. Xie, Y. Liu, J. Han, T.-T. Jing, Classification and dating of black gel pen ink by ion-pairing high-performance liquid chromatography, J. Chromatogr. A. 1135 (2006) 57–64. doi:10.1016/j.chroma.2006.09.031.

[23] M.R. Williams, C. Moody, L.-A. Arceneaux, C. Rinke, K. White, M.E. Sigman, Analysis of black writing ink by electrospray ionization mass spectrometry., Forensic Sci. Int. 191 (2009) 97–103. doi:10.1016/j.forsciint.2009.07.003.

[24] R.G. Takats, Z.; Wiseman, J.M.; Cooks, Ambient mass spectrometry using desorption electrospray ionization (DESI): instrumentation, mechanisms and applications in forensics, chemistry, and biology, J. Mass Spectrom. 40 (2005) 1261–1275.

[25] R.B. Cody, J.A. Laramee, H.D. Durst, Versatile New Ion Source for the Analysis of Materials in Open Air under Ambient Conditions, Anal. Chem. 77 (2005) 2297–2302. doi:10.1021/ac050162j.

[26] M.R.L. Paine, P.J. Barker, S.J. Blanksby, Characterising in situ activation and degradation of hindered amine light stabilisers using liquid extraction surface analysis-mass spectrometry., Anal. Chim. Acta. 808 (2014) 190–8. doi:10.1016/j.aca.2013.09.039.

[27] R.B. Cole, Electrospray and MALDI Mass Spectrometry: Fundamentals, Instrumentation, Practicalities, and Biological Applications, Second, John Wiley & Sons, Inc., Hoboken, 2010.

[28] J. Coumbaros, K.P. Kirkbride, G. Klass, W. Skinner, Application of time of flight secondary

ion mass spectrometry to the in situ analysis of ballpoint pen inks on paper, Forensic Sci. Int. 193 (2009) 42–46. doi:10.1016/j.forsciint.2009.08.020.

[29] C. Weyermann, L. Bucher, P. Majcherczyk, W. Mazzella, C. Roux, P. Esseiva, Statistical discrimination of black gel pen inks analysed by laser desorption/ionization mass spectrometry, Forensic Sci. Int. 217 (2012) 127–133. doi:10.1016/j.forsciint.2011.10.040.

[30] J.A. Denman, W.M. Skinner, K.P. Kirkbride, I.M. Kempson, Organic and inorganic discrimination of ballpoint pen inks by ToF-SIMS and multivariate statistics, Appl. Surf. Sci. 256 (2010) 2155–2163. doi:10.1016/j.apsusc.2009.09.066.

[31] D.N. Carvalho, Forty Centuries of Ink, 1st ed., The Banks Law Publishing Co., New York, 1904.

[32] A.S. Lee, P.J. Mahon, D.C. Creagh, Raman analysis of iron gall inks on parchment, Vib. Spectrosc. 41 (2006) 170–175. doi:10.1016/j.vibspec.2005.11.006.

[33] L. Fruen, The Real World of Chemistry, 6th ed., Kendall/Hunt Publishing, Dubuque, 2002.

[34] G. Adami, A. Gorassini, E. Prenesti, M. Crosera, E. Baracchini, A. Giacomello, Micro-XRF and FT-IR/ATR analyses of an optically degraded ancient document of the Trieste (Italy) cadastral system (1893): A novel and surprising iron gall ink protective action, Microchem. J. 124 (2016) 96–103. doi:10.1016/j.microc.2015.07.020.

[35] V. Huynh, U. Joshi, J.M. Leveille, T.D. Golden, G.F. Verbeck, Nanomanipulation-coupled to nanospray mass spectrometry applied to document and ink analysis, Forensic Sci. Int. 242 (2014) 150–156. doi:10.1016/j.forsciint.2014.06.037.

[36] J. Siegel, Jay; Allison, John; Mohr, Donna; Dunn, The use of laser desorption / ionization

mass spectrometry in the analysis of inks in questioned documents, Sci. Justice. 249 (2005) 425–429. doi:10.1016/j.talanta.2005.03.028.

[37] B.S. Kelly, J.S.; Lindblom, ed., Scientific Examination of Questioned Documents, CRC Press, Boca Raton, 2006.

[38] S. Thompson, Tim; Black, ed., Forensic Human Identification, CRC Press, Boca Raton, 2006.

[39] J.L. Koenig, Spectroscopy of Polymers, Second, Elsevier, New York, 1999.

[40] R.W. Jones, J.F. McClelland, Analysis of writing inks on paper using direct analysis in real time mass spectrometry, Forensic Sci. Int. 231 (2013) 73–81. doi:10.1016/j.forsciint.2013.04.016.

[41] J.D. Dunn, J. Allison, The Detection of Multiply Charged Dyes Using Matrix-Assisted Laser Desorption／Ionization Mass Spectrometry for the Forensic Examination of Pen Ink Dyes Directly from Paper, J. Forensic Sci. 52 (2007) 1205–1211. doi:10.1111/j.1556-4029.2007.00535.x.

[42] E.K. Karanikas, N.F. Nikolaidis, E.G. Tsatsaroni, Novel digital printing ink-jet inks with “antifraud markers” used as additives, Prog. Org. Coatings. 75 (2012) 1–7. doi:10.1016/j.porgcoat.2012.04.002.

[43] F. Coman, Virginia; Copaciu, Instrumental Thin-Layer Chromatography, Elsevier, Cluj-Napoca, 2015.

[44] M. Hoehse, A. Paul, I. Gornushkin, U. Panne, Multivariate classification of pigments and inks using combined Raman spectroscopy and LIBS, Anal. Bioanal. Chem. 402 (2012)

1443–1450. doi:10.1007/s00216-011-5287-6.

[45] L. Heudt, D. Debois, T.A. Zimmerman, L. Köhler, F. Bano, F. Partouche, et al., Raman spectroscopy and laser desorption mass spectrometry for minimal destructive forensic analysis of black and color inkjet printed documents, Forensic Sci. Int. 219 (2012) 64–75. doi:10.1016/j.forsciint.2011.12.001.

[46] B. Weyermann, Céline; Spengler, The potential of artifical aging for modelling of natural aging processes of ballpoint ink, Forensic Sci. Int. 180 (2008) 23–31.

[47] S. Han, C. Kim, D. Kwon, Thermal/oxidative degradation and stabilization of polyethylene glycol, Polymer (Guildf). 38 (1997) 317–323. doi:10.1016/S0032-3861(97)88175-X.

[48] L. Boughen, J. Liggat, G. Ellis, Thermal degradation of polyethylene glycol 6000 and its effect on the assay of macroprolactin., Clin. Biochem. 43 (2010) 750–3. doi:10.1016/j.clinbiochem.2010.02.012.

[49] J. Glastrup, Degradation of polyethylene glycol. A study of the reaction mechanism in a model molecule: Tetraethylene glycol, Polym. Degrad. Stab. 52 (1996) 217–222. doi:10.1016/0141-3910(95)00225-1.

CHAPTER 2

INTRUMENTATION

For the experiments performed in this research, the main instrumentation used was mass spectrometric and microscopic techniques. In addition, various lasers and transitional stages were incorporated for the sampling of the inks. This chapter covers the main theory and operation of these techniques.

2.1 Mass Spectrometry Instrumentation

Mass spectrometry (MS) is an analytical technique used to identify the elemental composition of a sample or molecule by means of separating gaseous ions corresponding to its mass and charge [1]. MS instrumentation consists of three main components: an ion source, a mass analyzer, and a detector. These pieces have been significantly revolutionized in the 20th century and continues to advance. In 1918, the first electron impact source was invented by Dempster [2]. Later on, time-of-flight mass analyzers and quadrupole ion traps were developed in the 1950s. Currently, miniaturizing the mass spectrometer has become the new and prevailing topic. One great quality about MS is that it is a versatile tool with very low limits of detection. There are many types of ion sources and mass analyzers that can be paired for a variety of sample types and applications.

2.1.1 Ionization Sources

2.1.1.1 Electrospray and Nanospray Ionization

One of the most versatile ionization techniques, introduced in 1984 by Yamashita, Fenn, and Aleksandrov et al., is electrospray [3]. Currently, electrospray ionization mass spectrometry

(ESI-MS) is a widely used technique in biological, pharmaceutical, and forensic research. Electrospray is a soft ionization method that uses applied voltage to form droplets from the introduced sample. The mass spectra of electrospray usually have reduced fragment ions, which can be formed in a triple quadrupole, an ion trap, an ICR cell, or in the field-free regions of magnetic sector mass spectrometers. The mechanism of electrospray ionization process is divided into three different stages: (1) droplet formation, (2) droplet fission, and (3) gaseous ion formation (Figure 2.1) [4].

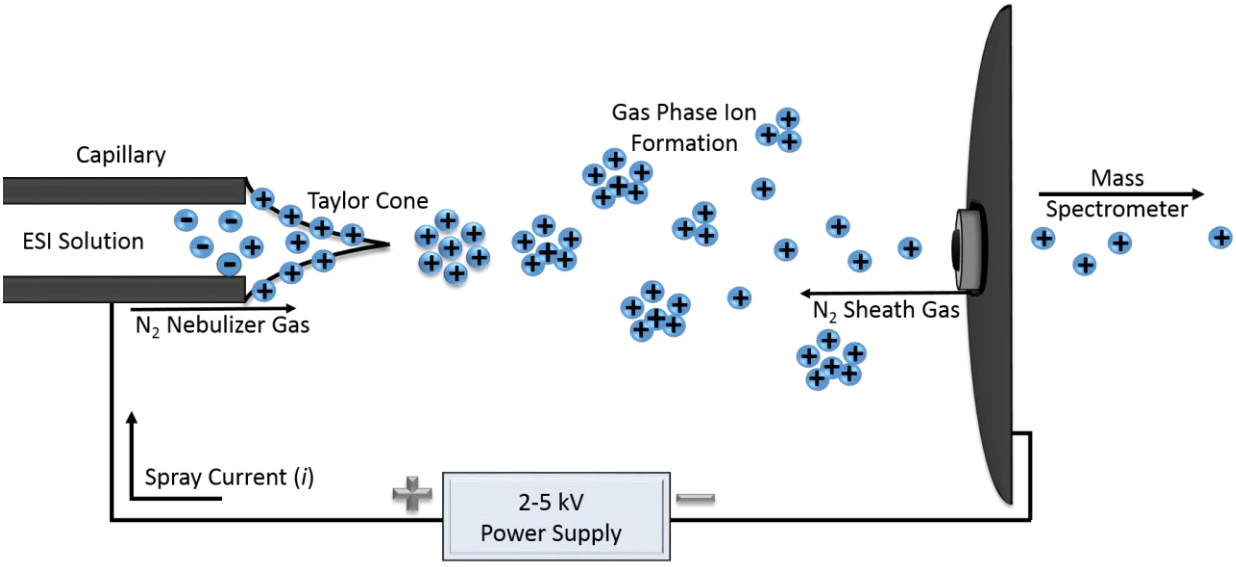

Figure 2.1. Schematic of electrospray ionization mechanism.

As the solution is delivered to the tip of the electrospray capillary (i.d. of typically 100 µm) using an external pump, with a controlled flow rate (1-10 µL), an electric field is induced by applying a potential (2-5 kV). The potential applied can either be positive or negative. Assuming a positive potential, positive ions from the solution will surface and accumulate at the tip. Thus, the ions are drawn out in a downfield direction creating a Taylor cone. At an optimal applied electrostatic force, the Taylor cone will be drawn to a filament which produces positive charged

droplets. These first generation droplets have an initial diameter of more than 1 μm [5]. The production of charged droplets is known as the budding process or Coulomb explosion where the surface tension is exceeded by the applied electrostatic force, creating smaller droplets. The Rayleigh limit is reached when the charged droplet becomes unstable due to solvent evaporation. The Rayleigh limit determines the charge of the droplet which affects the tension of the liquid subjected to electrospray. The equation for the Rayleigh limit of charge (q_R) is shown in Equation (2.1) in terms of surface tension (γ), droplet radius (R), and ε_0 representing the permittivity of the vacuum [6]. Thus, solution parameters of surface tension and the final droplet radius is affected by the maximum charge available.

$$q_R = 8\pi(\gamma \varepsilon_0 R^3)^{1/2} \tag{2.1}$$

Solvent evaporation needs to occur within the initial stage of charged droplets to induce charge density for fission to occur. The droplets then result in an increase in concentration of both analyte and salt. The initial droplet size can be decreased even more by adding compounds that increase the conductivity of the solution known as charge carriers (e.g., acetic acid and ammonium acetate).

The voltage applied depends on the system used to transfer ions to the mass analyzer and the type of mass analyzer itself. For a quadrupole mass spectrometer, the applied voltage for the sprayer and ion source at the ground potential can be up to 5 kV. The accelerating voltage is restricted to 3-5 kV during electrospray operation for most magnetic sector mass spectrometers, leading to a voltage of 8-10 kV (with respect to ground) for the sprayer [7]. At the right potential, a corona discharge will take place between the electrospray capillary and its counterelectrode. During this process, a conductive region will form when the strength of the electric field around a conductor is high enough to cause electrical breakdown. In other words, the spectrum will

represent ions present in the solution that is dispersed into charged droplets. In contrast, the spectrum will represent the products of ion-molecule reactions resulting from a corona discharge [7].

M. S. Wilm and M. Mann theorize droplet diameter of about 180 nm for a capillary with an i.d. of 1-3 µm. The setting for flow rate is an important element that can affect droplet diameter and droplet charging efficiency. Increasing the flow rate for a given sample concentration does not affect the sensitivity of the spectrum. In turn, the sensitivity decreases when the flow rate is increased (in terms of mass flow). Both effects attributed to increasing the flow rate lead to lower ionization efficiency, according to the scaling laws in Equations (2.2) and (2.3).

$$\text{Diameter} \propto [\text{flow}]^{1/3} \tag{2.2}$$

$$\text{Current} \propto [\text{flow}]^{1/2} \tag{2.3}$$

Table 2.1 shows the relationship between different elements of electrospray ionization and flow rate using a 3 µM sample with 1% acetic acid. As the flow rate decreases the number of charges per droplet and droplet diameter decreases; while the ratio of charges to sample molecules increases. There is only one sample molecule per aerosol droplet. It is reasonable to assume that molecules undergoing less competition for charge will release ions from droplets more readily. Competition from the primary aerosol may be nonexistent when using a low flow rate. The ion signals become lower and unstable when the flow rate is increased too much (upper limit is 10-20 µL/min).

Flow Rate (µL/min)	6	0.2	0.006
Droplet Diameter (µm)	1	0.3	0.1
Charges per droplet	15,000	2,700	500
Charges: sample molecules	16:1	90:1	500:1

Table 2.1. Relationship between some important elements in electrospray ionization [7].

The mechanism of nanospray ionization mass spectrometry (NSI-MS) is similar to the mechanism of ESI. The main difference between both mechanisms is that NSI produces a finer electrospray plume, leading to better ionization efficiency and sensitivity with less ion suppression effects [8, 9]. This is because nanospray uses a much smaller needle and lower flow rate which negates the need to have an external pump. Thus, no extensive solvent evaporation is required. A regular electrospray device uses approximately 0.3-mm-o.d., 0.1-mm-i.d. stainless steel tubing, or a coaxial arrangement of fused silica and stainless steel [7]. A nanospray device, on the other hand, utilizes a narrow i.d. of 10 to 50 µm fused silica capillary. Nanospray also has a higher tolerance for salt contamination than electrospray by at least one order of magnitude [8]. Nanospray uses a lower applied voltage to help reduce problems with corona electrical discharges [10].

NSI-MS is a very useful technique for trace analysis or where the amount of sample is limited (trace 1 ppb - 100 ppm, ultra-trace < 1 ppb). This is allowed by the subnanoliter sample consumption and sensitivity in the attomole range. A. Berlioz-Barbier et al. [11] incorporated nanospray in a new methodology to quantify traces of two pharmaceuticals in benthic invertebrates. The method, nanoliquid chromatography-nanospray-tandem mass spectrometry, was sensitive enough to detect levels as low as 18 ng/g and 128 ng/g for carbamazepine and fluoxetine, respectively, with a recovering yield greater than 85% for the two targeted compounds. In another study conducted by J. J. Gaumet et al. [12], NSI-MS successfully analyzed precursors and nanoscale metal chalcogenide clusters (1.5 nm in diameter cluster). In comparison to ESI-MS,

there are many advantages to using NSI-MS. It uses low sample consumption, low flow rates, no sheath gas requirements which decreases activation collisions in the ionization source and only requires pmol/µL [13].

2.1.1.2 Matrix-assisted laser desorption ionization

Matrix-assisted laser desorption ionization (MALDI) is an ionization method that produces exact mass information for irradiated molecular species. This technique is most often used for species ranging in molecular mass from a few thousand to several hundred thousand Da. The sample preparation for MALDI is minimal. This involves a low concentration of analyte dispersed in a matrix that is deposited on a stainless steel plate or glass slide. The plate is then placed in a vacuum chamber where the laser irradiates the sample (Figure 2.2)

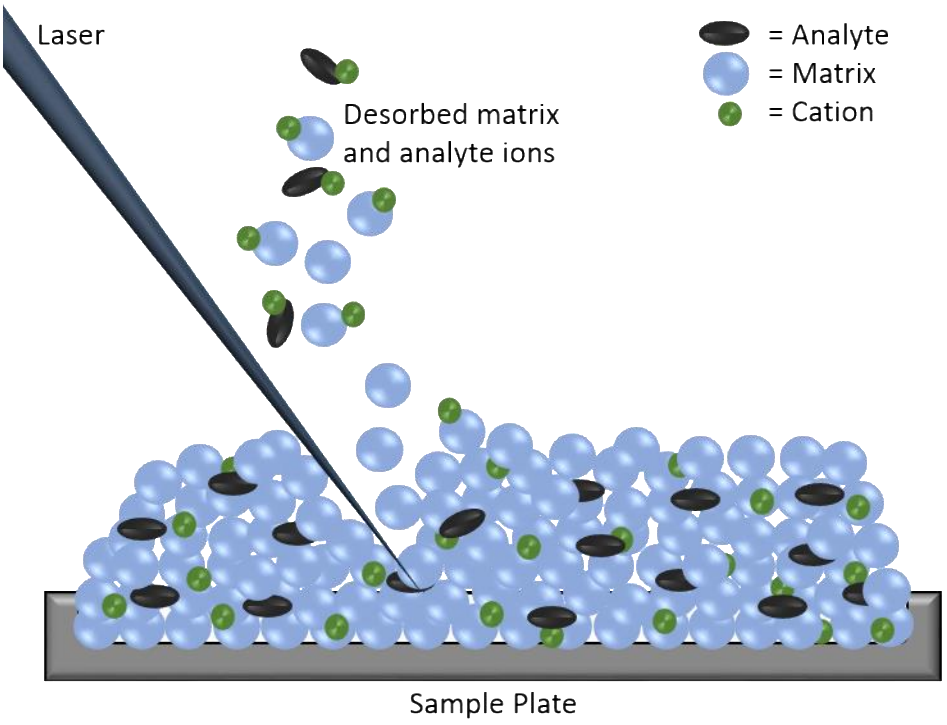

Figure 2.2. Diagram of the MALDI process.

In Figure 2.2 the analyte is dispersed uniformly in the matrix. The pulsed laser then strikes the sample, creating desorption of a plume of matrix, analyte and other ions. This is created when the matrix and analyte are desorbed and ionized. It is important to note that the matrix must strongly absorb the laser radiation. The process has not yet been completely understood. The theory of the mechanism is thought to first desorb the analyte and become neutral molecules and then be ionized by transferring energy from the matrix (i.e., proton transfer reactions with protonated matrix ions).

2.1.2 Mass Analyzers

Mass analyzers are the component of the mass spectrometer that separates ionized masses based on mass-to-charge ratios (*m/z*). Once separated, the ions are then outputted to the detector which is later converted to digital output. There are several types of mass analyzers that can be used depending on the application, cost, and desired resolution and performance. Mass resolving power is defined in Equation (2.4).

$$R = \frac{m}{\Delta m} \tag{2.4}$$

where m is the mass of the first peak and $\Delta m=(m_2-m_1)$ is the difference in peaks at full width half height. Table 2.2 below compares different mass analyzers and their characteristic advantages and disadvantages. Each mass analyzer has its own benefits and limitations, but a single mass analyzer is not ideal for all applications.

Mass Analyzer	Typical Mass Range and Resolution	Advantages	Disadvantages
Quadrupole	Range *m/z* 3000 Resolution 2000	Good quantitation in heavy matrix Tolerant of high pressures Easily adaptable to ESI Ease pos/neg mode switching Small size Low cost	Mass range limited to m/z 3000 Poor adaptability to MALDI Low duty cycle Low sensitivity and full scan Poor high mass sensitivity
Ion Trap	Range *m/z* 2000 Resolution 1500	Fast Sensitive full scan for MS and MS/MS Excellent high mass sensitivity Small size Simple design, low cost Medium resolution Easily adaptable to MALDI Well-suited for tandem MS Easy for pos/neg ions	Currently has limited mass range commercially available Ability to handle heavy matrix
Magnetic Sector	Range *m/z* 20,000 Resolution 10,000	Capable of high resolution Capable of exact mass Medium mass range	Not tolerant to high pressures Expensive Massive size Relatively slow scanning speed
Time-of-flight (TOF)	Range *m/z* ∞ Resolution 350	Highest mass range Very fast scan speed Simple design, low cost Ease of adaptation to MALDI	Low resolution Difficulty of adaptation to electrospray
TOF-reflectron	Range *m/z* ∞ Resolution 1500	Good resolution Very fast scan speed Simple design, low cost	Good resolving power Limited *m/z* range Lower sensitivity than TOF
Fourier transform-mass spectrometry	Range *m/z* 10,000 Resolution 30,000	High resolution Well-suited for tandem MS^n($n \leq 4$)	High vacuum required Superconducting magnet required, expensive Massive size

Table 2.2. Comparisons of Mass Analyzers [1, 7, 14].

2.1.2.1 Quadrupole

In the early 1950s, Wolfgang Paul and Helmut Steinwedel (German physicists) developed the quadrupole mass spectrometer [15]. A schematic of a quadrupole is shown in Figure 2.3, consisting of four parallel metal rods. These hyperbolic rods, serving as electrodes, have alternating positive and negative charges. The radio frequency (RF) voltage with a DC offset voltage is applied and manipulated for a given ratio of voltages, isolating a specific range of mass-to-charge (*m/z*) values. Only ions within this *m/z* range will obtain a stable trajectory to reach the

detector. Ions obtaining an unstable trajectory, outside the chosen *m/z* range, collide with the rods and are not detected.

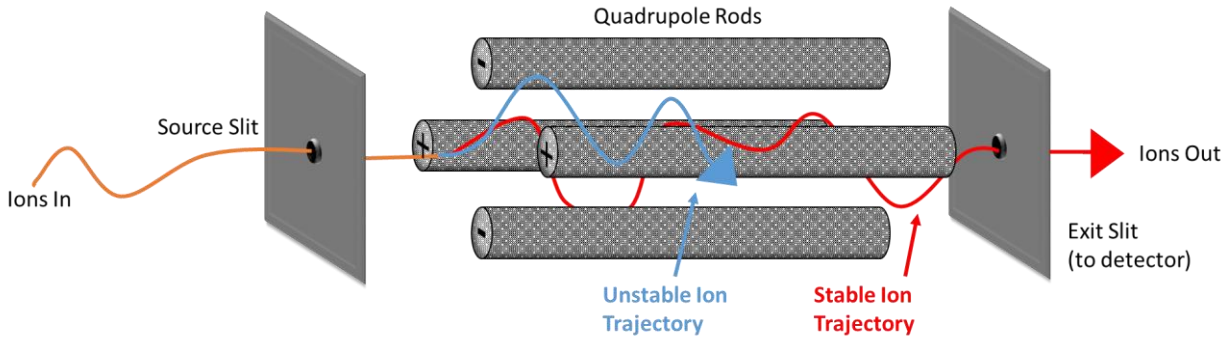

Figure 2.3. Schematic of quadrupole mass analyzer.

Quadrupole mass spectrometers are more rugged than most mass spectrometers, compact, and cost effective. They are typically used for molecules with low mass and can analyze up to *m/z* 3000 [1, 7, 14]. Another advantage of utilizing a quadrupole is its ability to analyze an entire mass spectrum in less than 100 ms, at high scan rate [16]. The resolution of a quadrupole is limited to 1 u, but provides good quantitation in heavy matrix, tolerant of high pressures, and easily adaptable to electrospray ionization.

2.1.2.2 Quadrupole Ion Trap

Ion trap mass analyzers are rugged, compact, and less costly compared to other mass analyzers and have the capability to achieve low detection limits [17, 15]. They are most often paired with electrospray ionization and MALDI sources. Gaseous cations and anions are formed within the ion trap for an extended amount of time by electric and magnetic fields (up to 15 min for stable ions). The tradeoff for trapping the ions for long periods of time (milliseconds to days) is that the ions will start to fall apart spontaneously which could lead to alterations in mass spectra. Figure 2.4 is a schematic of an ion trap mass spectrometer consisting of a central ring electrode

with two grounded endcap electrodes. A variable radio frequency voltage is applied to the central ring electrode to control the orbits of stabilized and destabilized ions. Increased radio frequency voltage leads to stabilizing the orbits of heavier ions and destabilizing the orbits of lighter ions. Destabilized ions will collide with the wall of the ring electrode. The appropriate *m/z* value can be selected and the ions correlating with that range will circulate in a stable orbit within the cavity surrounded by the ring [17].

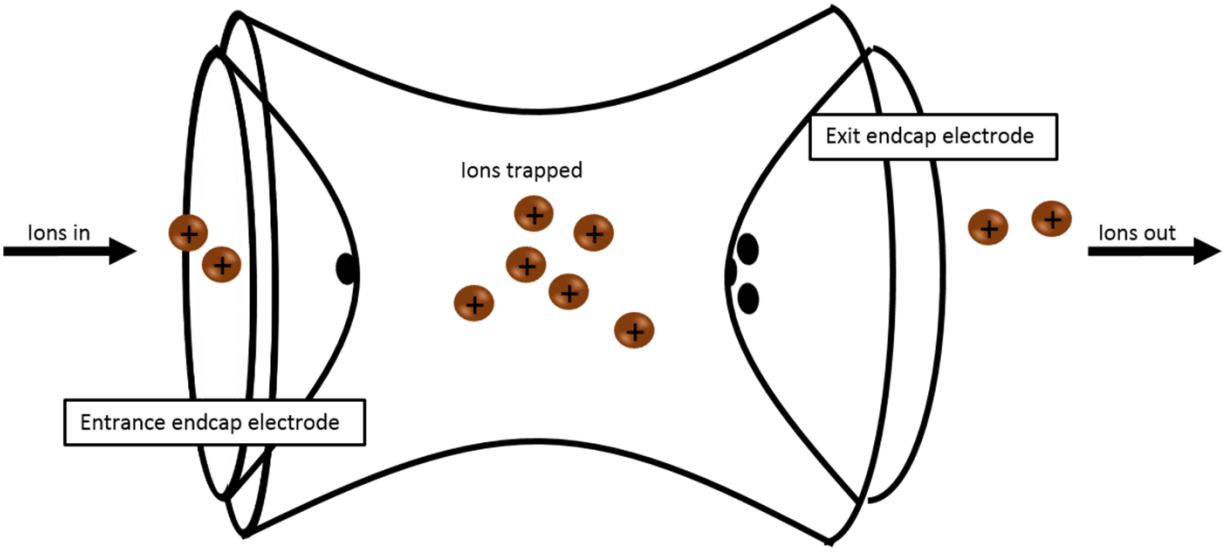

Figure 2.4. Schematic of ion trap mass spectrometer.

Ions in order by mass can be sequentially ejected from the ion trap by a technique called mass-selective ejection. This involves increasing the radio frequency voltage applied to the ring electrode in a linear ramp [17]. The trapped, but destabilized ions, will leave the ring electrode cavity through openings in the lower end cap. The stabilized, trapped ions, will then pass through to the detector. The main benefits of using a quadrupole ion trap as a mass analyzer is that it is highly sensitive and is compact. The limitations include poor quantitation, poor dynamic range, and subject to space charge effects and ion molecule reactions. Space charge effects or also known

as ion-ion repulsion is the cause of limiting the dynamic range of the ion trap, but there are additional elements that can help supplement this issue, which includes auto-ranging. Even though the ion trap does not have the ability to analyze a sample that co-elutes with a matrix; it is fast, has sensitive full scan spectra for MS and MS/MS, excellent high mass sensitivity, low price, and has the ability to conclude a structure using MS^n.

2.1.2.3 Orbitrap

The orbitrap mass analyzer has been proven to be a robust tool for mass spectrometry, delivering high resolving power and mass accuracy (±0.003) [18]. The orbitrap has good sensitivity and high mass resolving power, can reach up to 300,000. It is established on the orbital trapping and analyzing injected ion populations through use of electrostatic fields. Figure 2.5 illustrates the mechanism of ion selection. The orbitrap consists of two electrodes, central spindle-like and outer barrel-like, that are connected to independent voltage supplies. Trapped ions cycle around the inner electrode on elliptical trajectories due to their electrostatic attraction to the inner electrode (i.e., applying a voltage between the two electrodes). Ion packets are injected tangentially into the field between the two electrodes. Ions will agglomerate towards the inner electrode until the desired orbit is reached. The orbit is controlled by various electric field strength via voltage adjustment. Ions of specific mass-to-charge ratio oscillate along the inner electrode in a ring-like trajectory. They will move with different rotational frequencies but with the same axial frequency.

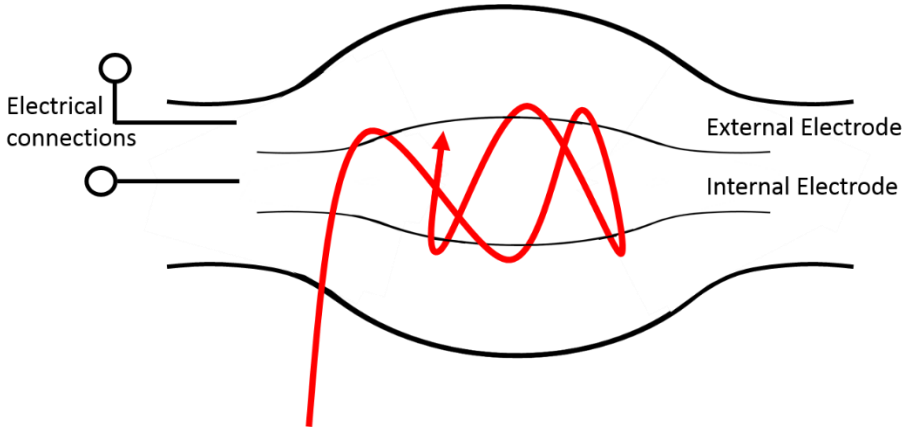

Figure 2.5. Schematic of orbitrap mass analyzer.

The ions must be trapped in the radial plane, making the ψ-motion (r) of ions important. Thus, the equation for the motion of trajectory is show in Equation (2.5).

$$r = \frac{2qV}{qE} \tag{2.5}$$

where r is the radius of the electrostatic analyzer and radius of the ion trajectory though the analyzer, qV is the ion kinetic energy before injection, and qE is the force due to the electric field (directed radially inward towards r=0) experienced by the ion [18]. Therefore, ion trajectories are determined by their kinetic energy at a given electric field strength.

2.2 Direct Analysis

2.2.1 Laser Ablation[1]

Lasers play an essential role in our everyday lives. The word “laser” itself originated from the acronym “light amplification by stimulated emission of radiation”. Lasers have been used is printers, computers, scanners, communication systems, and even for medical use. Maiman

developed the laser in 1960, for chemists, as a new laboratory tool [19]. Chemical lasers are used to initiate and control chemical reactions as well as irradiation.

The process of forming a laser beam can be understood by considering four processes (Figure 2.6): (a) pumping, (b) spontaneous emission (fluorescence), (c) stimulated emission, and (d) absorption [17]. Pumping occurs when an electrical discharge, passage of an electrical current, or exposure to an intense radiant source excites the active species of a laser. In Figure 2.6a, two electrons are excited to two different energy levels but relax to the same metastable excited state. During this transition an undetectable quantity of heat is produced. During spontaneous emission of radiation, the electrons in its excited electronic state may lose energy. Stimulated emission described in Figure 2.6c occurs when excited laser species are struck by photons with homologous energies. During this event, these collisions cause the excited species to relax immediately to the ground state while emitting a photon of the exact same energy as the photon that encouraged this process. The wavelength of the fluorescence radiation is given by Equation (2.6).

$$\lambda = \frac{hc}{E_y - E_x} \tag{2.6}$$

Figure 2.6d illustrates the process of absorption that competes with stimulated emission. In this process, two photons of the same energies are absorbed to produce the metastable excited state shown in Figure 2.6d(3). It is important to note that the absorption process is the same as the pumping process.

[1] Contents from this section was retrieved from Skoog/Holler/Crouch. Principles of Instrumental Analysis, 6E. © 2007 Brooks/Cole, a part of Cengage Learning, Inc. Reproduced by permission. www.cengage.com/permissions

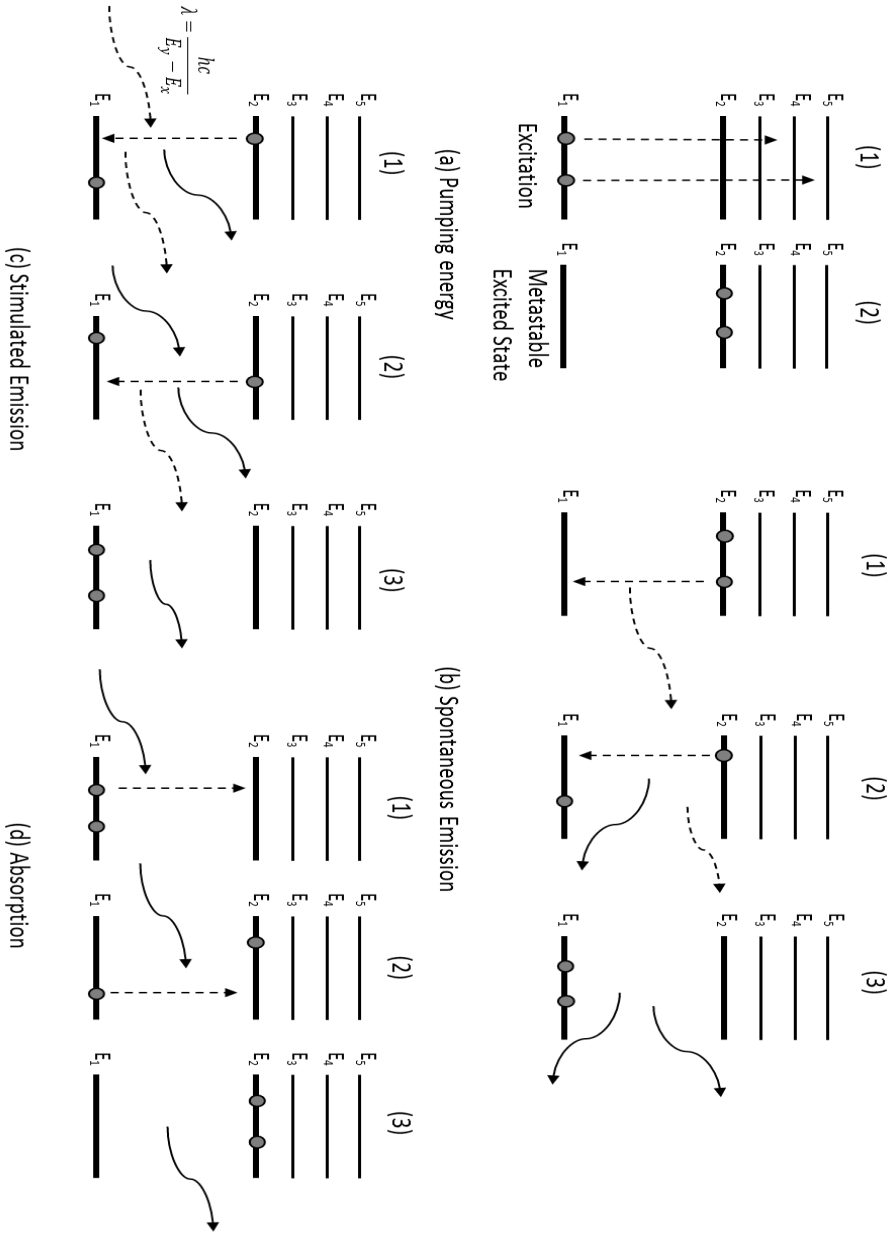

Figure 2.6. The processes of laser action illustrating (a) pumping, (b) spontaneous emission, (c) stimulated emission, and (d) absorption.[2]

[2] This figure has been redrawn from Skoog/Holler/Crouch. Principles of Instrumental Analysis, 6E. © 2007 Brooks/Cole, a part of Cengage Learning, Inc.Reproduced by permission. www.cengage.com/permissions.

Population inversion and light amplification, in a laser, is achieved when the number of photons produced by stimulated emission exceeds the number lost by absorption [17]. This occurs when the conditions of population inversion are met. Population inversion is a process induced by pumping in which there are more particles in the higher energy state than in the lower energy state. Figure 2.7 illustrates the effect of incoming radiation with a noninverted and inverted population. Both populations contain nine molecules in higher and lower energy states. In Figure 2.7a, three molecules transition to the excited state through absorption and then relax immediately. Three photons are absorbed to produce three additional excited molecules. A net attenuation of the beam by one photon may result from the radiation, stimulating emission from two photons from the excited molecules. The inverted population shows six molecules transitioning to higher energy levels through stimulated emission, producing a net gain in emitted photons. This is because two molecules are being pumped into virtual states, followed by relaxation to E_1, creating a population inversion. If molecule absorbs a photon (with the proper energy) in its excited state, it will then relax and emit a second photon perfectly identical to the first. Therefore, placing this system between two mirrors traps the photons that are being created. Thus, a lasing beam is created.

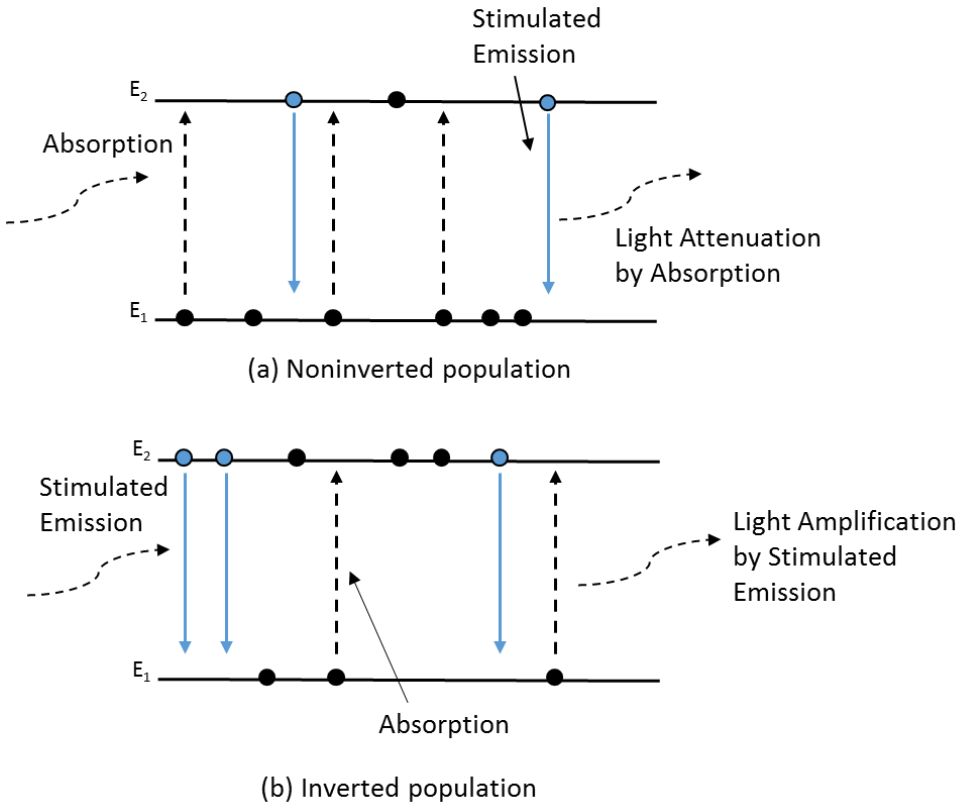

Figure 2.7. Illustration of light attenuation by absorption and light amplification by stimulated emission through (a) noninverted population and (b) inverted population.[3]

There are many type of laser techniques that can be used for different scientific applications, including laser ablation (LA). Laser ablation uses a laser beam to irradiate a sample in order to remove material from a solid sample, sometimes liquid. In Figure 2.8, a sample is placed on the target plate prior to irradiation with a pulsed laser. Once the high power pulsed laser becomes focused onto the sample, the material will result into a plume. A plume consists of broken chemical bonds, energetic fragments, neutral atoms, molecules, and ions. It is important to note that this phenomenon only occurs when the laser fluence exceeds the ablation threshold value for

[3] This figure has been redrawn from Skoog/Holler/Crouch. Principles of Instrumental Analysis, 6E. © 2007 Brooks/Cole, a part of Cengage Learning, Inc. Reproduced by permission. www.cengage.com/permissions.

the material. The ejected material absorbs most of the energy from the ablation process. Therefore little to no thermal damage is conducted on the rest of the sample. The ablated material is then removed from the chamber by purging with gas. Laser ablation is commonly coupled with inductively coupled plasma mass spectrometry (LA-ICP-MS). After the LA process, the ablated particulates are transported to the source (plasma torch) of the ICP-MS for ionization of the sampled mass. The ablated material entering the plasma torch are then introduced to the mass spectrometer detector as excited ions for elemental and isotopic analysis.

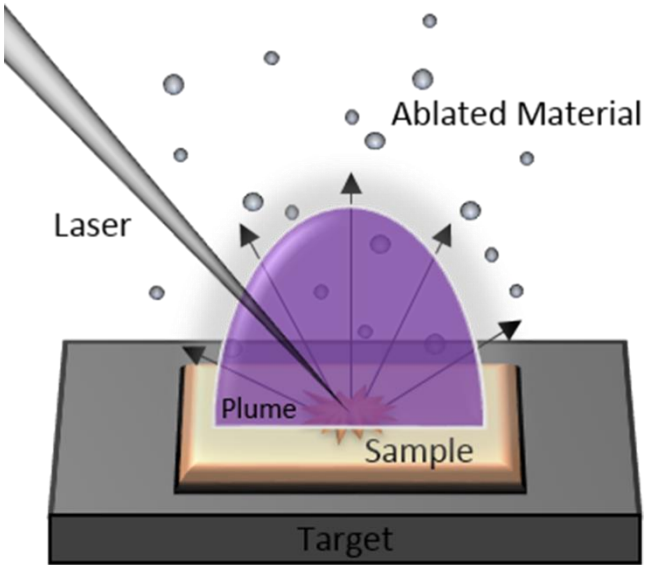

Figure 2.8. Schematic of laser ablation mechanism.

2.2.2 Fluorescence Microscopy

2.2.2.1 Jablonski Diagram

Energy levels are used to describe the photoluminescent phenomenon of molecules such as absorption, fluorescence, and phosphorescence which is also known as a Jablonski diagram (Figure 2.9). S_1 and T_1 represent the singlet and triplet electronic energy states, respectively. After absorption of high enough energy, the electrons from the molecule transitions from the ground state to the excited levels, promoting electrons. Relaxation will take place by transitioning to the lowest available energy state in a few pico-seconds then transitioning to triplet state. In this state, there will be a spin flipping delay period of several nanoseconds known as the fluorescence lifetime. Fluorescence is a molecular phenomenon where a substance is excited by absorbing light and then emits fluorescent light. The molecule will then relax down to its original state, the ground state, while releasing energy in the form of a photon shift.

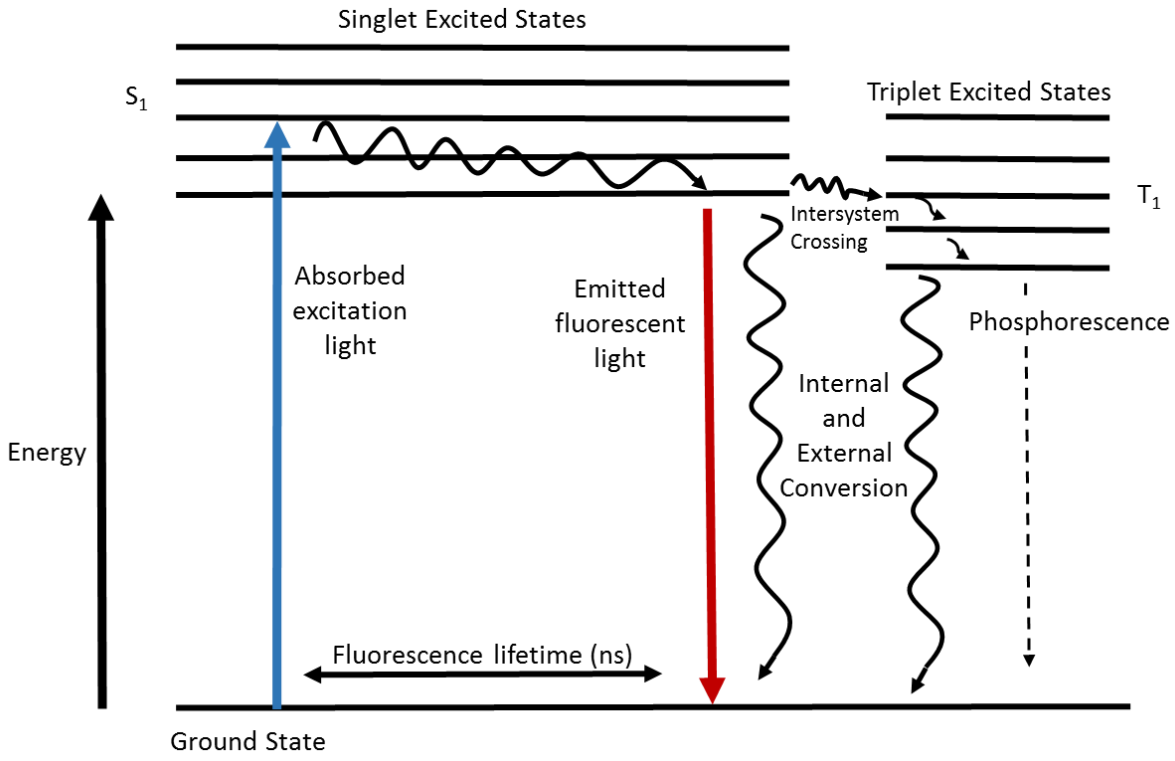

Figure 2.9. Jablonski energy diagram of fluorescence and phosphorescence.

When a molecule transitions, without emission of radiation, to a lower energy electron state undergoes a process called internal conversion. This process is not well understood but is defined as a crossover between singlet-singlet or triplet-triplet [17]. On the other hand, external conversion occurs when an excited electronic state is deactivated. This process involves interaction and energy transfer between excited molecules and solvents or other solutes. Since external conversion is a deactivation process, reducing number of collisions between particles, can typically enhance fluorescence.

Deactivation of electronic states can happen further with intersystem crossing which leads to phosphorescence (also a deactivation process). Intersystem crossing occurs when there is a shift between different multiplicity states (e.g., the most common process is $S_1 \rightarrow T_1$). After crossing to

the triplet state, internal or external conversion or phosphorescence could take place. Phosphorescence differs from fluorescence due to its slower time scale in re-emitting absorbed radiation. This phenomenon causes a lower intensity that could happen several hours after the start of the original excitation.

2.2.2.2 Microscopy

Molecules that undergo fluorescence are known as fluorophores. A fluorophore is a fluorescent chemical compound that can re-emit a photon upon excitation. Fluorophores typically contain conjugated aromatic groups along with electron donating groups (e.g., -OH, $-NH_2$, $-OCH_3$) that may increase the quantum yield. Fluorophores have been used as tracers or markers in biological compounds by covalently bonding them to macromolecules. They have also been used as dyes for staining certain structures like enzymes and probes for DNA. Fluorophores only absorbs light energy of a specific wavelength, re-emiting light at a longer wavelength.

A fluorescence microscope utilizes this phenomenon to observe the fluorescent variations of different samples. Figure 2.10 is a schematic of today's most common epifluorescence microscope. It utilizes an episcopic light to illuminate the sample. The fluorescence filters only filter out excitation light scattering back from the sample. The filter cubes include epi-fluorescence interference and absorption filter combinations. They include an excitation filter, dichromatic beamsplitter, and a barrier filter to satisfy the excitation and emission requirements of the fluorescent compounds. The dichroic beam splitter reflects the excitation light into the objective and filters out the back-scattered excitation light by another factor of 10 to 500. The filter cubes are easily interchanged to match the spectral excitation and emission characteristics of chromophores in samples.

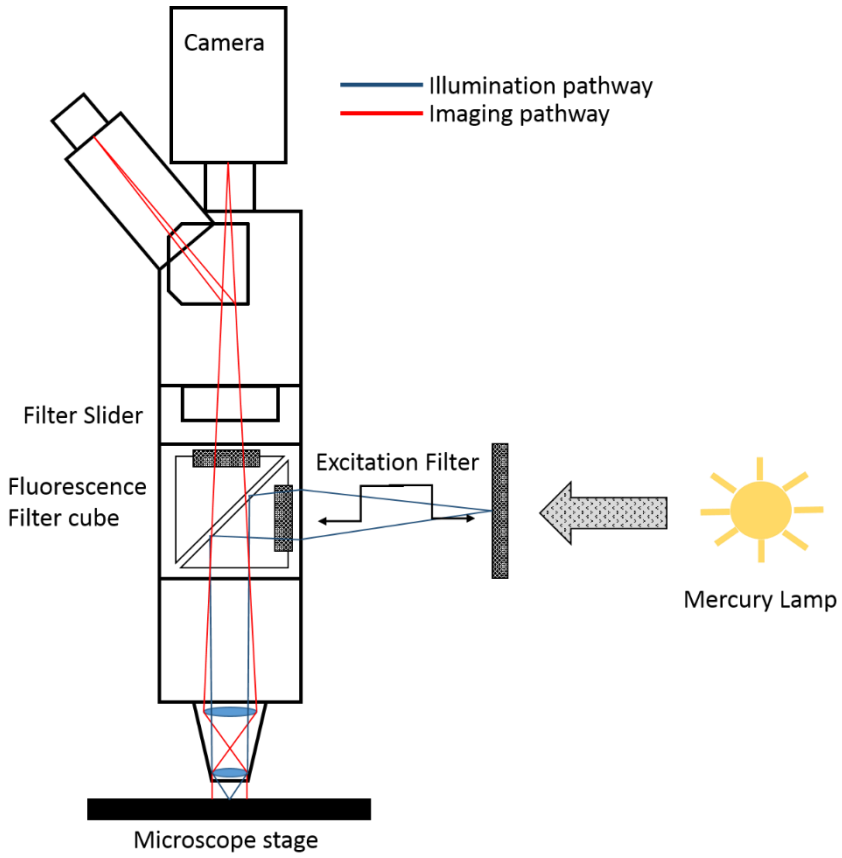

Figure 2.10. Schematic of Fluorescence Microscope.

2.2.2 Raman Spectroscopy

Figure 2.11 shows the mechanism of Rayleigh and Raman scattering. The heavy arrow on the far left represents the energy change in the molecule as it interacts with a photon. The energy of the photon (hv_{ex}) is equal to the increase in energy. It is important to note that a molecule can assume many virtual states (depending on the frequency of the radiation from the source) between the ground state and the lowest (first) electronic excited state and this process is not quantized [17]. The second, narrow, arrow represents what would occur if a molecule encountered a photon that was in its first vibrational level of electronic ground state. The probability of this occurring is much smaller, only a tiny fraction occurs at room temperature. The middle set of arrows characterize the

changes that produce Rayleigh scattering where the larger arrow is the most probably pathway. Although no energy is lost in Rayleigh scattering, elastic scattering occurs between the photon and the molecule when they collide. During elastic scattering, the kinetic energy of a particle is preserved in its center-of-mass. The interaction of other particles modifies its direction of propagation. Lastly, on the far right is the energy change that produce stokes and anti-stokes shift in Raman scattering. The energy for Rayleigh scattering is $E=h\nu_{ex}$ and the energy for Raman scattering is $E=h\nu_{ex} \pm \Delta E$. $\pm \Delta E$ is the energy of the first vibrational level of the ground state, $h\nu_v$. Stokes shifts are depicted by $-\Delta E$ and anti-stokes are represented by $+ \Delta E$. In addition, ΔE also represents the energy of absorption if the bond were IR active. Concluding that the Raman frequency shift and the IR absorption frequency are identical [17].

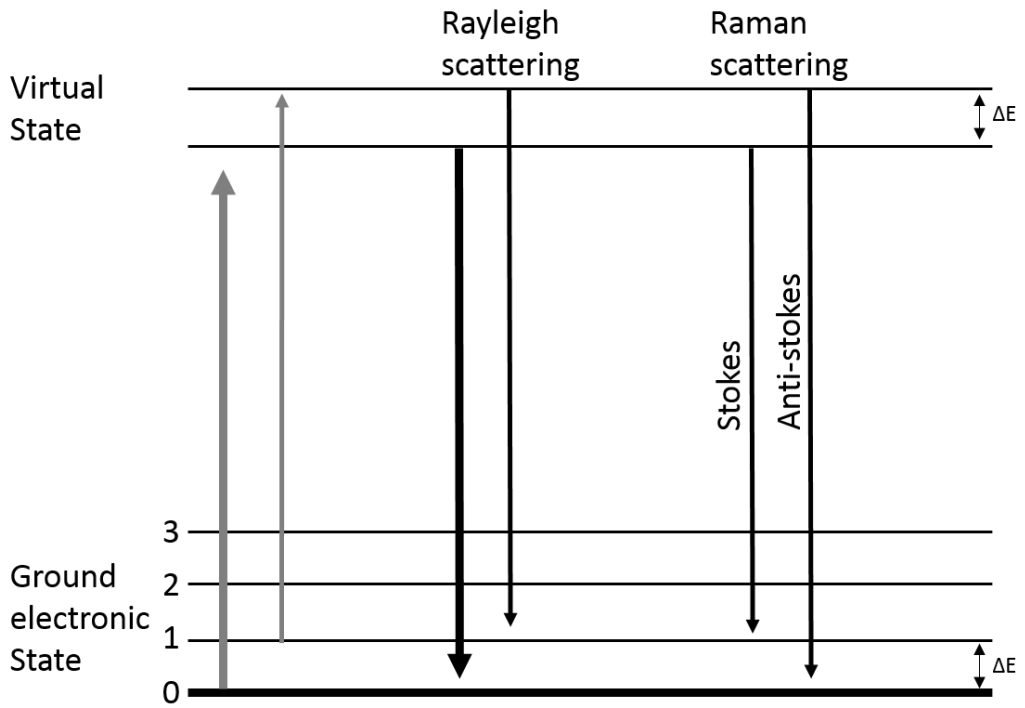

Figure 2.11. Mechanism of Rayleigh and Raman scattering.

Scattered radiation from irradiating a sample with a laser source can be measured using a Raman Spectrometer illustrated in Figure 2.12. A sample is first placed on the microscope stage where it will come in contact with an incident laser and scatter at all angles. Using a laser source is important because it produces a high enough intensity to produce Raman scattering with a reasonable signal-to-noise ratio. Five of the most common lasers used are argon ion (488.9 or 514.4 nm), Krypton ion (530.9 or 647.1 nm), helium-neon (632.8 nm), diode (785 or 830 nm), and Nd-YAG 1064 nm) [17]. Short wavelength lasers such as argon and krypton ion emit in the blue and green region of the spectrum and produce Raman lines that are nearly three times more intense than those excited by a longer wavelength source (e.g., Helium-neon). Although that is a major advantage, short wavelength lasers produce significant fluorescence. Fluorescence interference is a major issue for Raman spectroscopy because it can cover the anticipated chemical footprints of the sample. Using a wavelength that does not fluoresce the sample can fix this problem [20]. Longer wavelength sources are advantageous because it can operate at a much higher power (up to 50 W) without causing photodecomposition of the sample and they are not energetic enough to populate a significant number of fluorescence-producing excited electronic energy states in most molecules [17]. The Nd-YAG laser is most effective in eliminating fluorescence. There are also features in the software that can help reduce this issue.

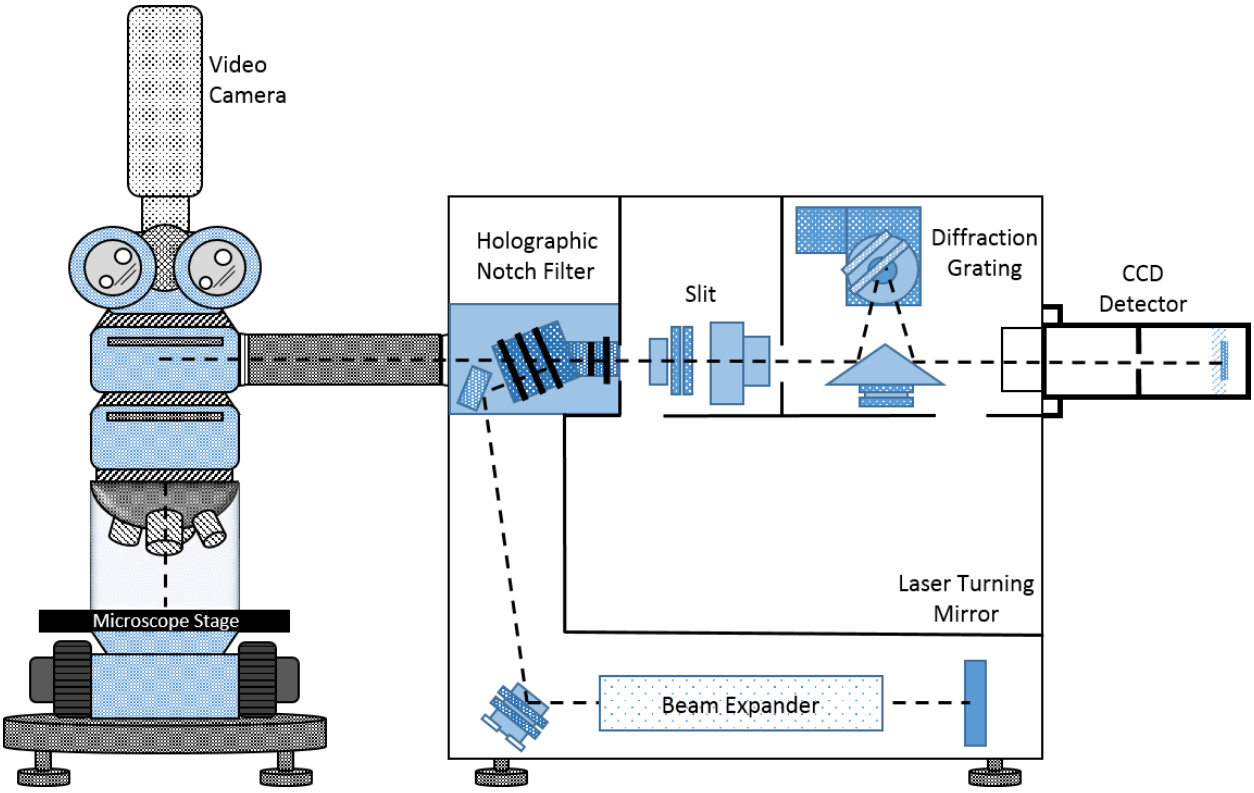

Figure 2.12. Schematic of XR Almega Raman spectrometer.

Double- and triple-grating monochromators are high-quality wavelength filter devices used to separate the weak Raman lines from the intense Rayleigh-scattered radiation. Holographic notch filters and holographic gratings have improved significantly and virtually eliminated the need for multiple-grating monochromaters [17]. Notch filters also provide good stray light rejection. Thus, the combination of notch filters and monochromators are commercially available and most often used for Raman spectrometers. The Raman scattered light is first disperse using the diffraction grating. A diffraction grating contains many grooves that also affect the resolution. The higher the groove density of the grating (grooves per millimeter), the higher the spectral resolution. Typically, between 3600 gr/mm and 1800 gr/mm are gratings used for high and low resolution respectively. The light then proceeds to charge-coupled devices (CCD) which have also been recently advanced. A CCD is a silicon-based multichannel array detector. They are most often used for Raman

spectroscopy because they are extremely sensitive to light which can enhance inherently weak Raman signal.

2.2.3 Nanomanipulation

Direct analyte-probed nanoextraction coupled to nanospray ionization mass spectrometry (DAPNe-NSI-MS) is a technique that extracts ultra-trace amounts of analyte and has allowed the forensic science community to use extremely small sample volumes with increased sensitivity and resolution [21, 22, 23]. DAPNe consists of a nanomanipulator fixed on the stage of a high-powered microscope that contains positioner(s) that is/are piezoelectric-controlled and coupled to a pressure injector (Figure 2.13). The nanomanipulator can move along the x, y, and z axis via joystick controller and can aspirate/extract using the pressure injector. The range of motion for the nanomanipulator is 12 mm for x and z axis and 28 mm for the y axis. The translational resolution is 5 nm in fine mode and 100 nm in course mode. The nanospray tip is coated with AuPd and has an i.d. of 1 ± 0.02 µm. It is easily removable and pre-filled with an extraction solvent (5-10 µL) before extracting samples.

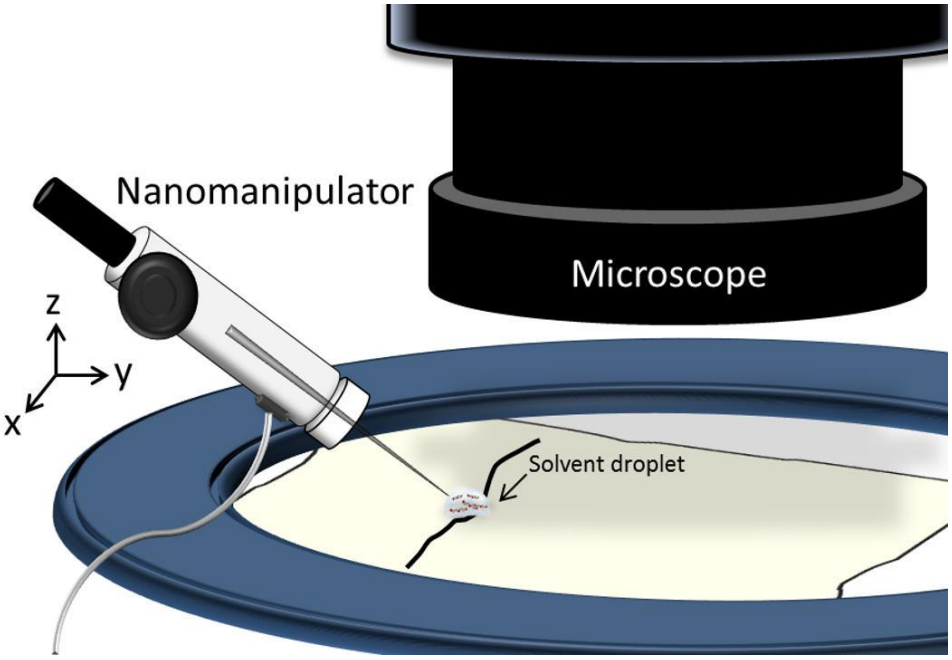

Figure 2.13. Schematic of nanomanipulator on stage of microscope.

Nanomanipulation has already been proven to be a valuable technique. The nanomanipulator is able to extract trace cocaine particles directly from a single rayon fiber and extract ultra-trace drug residues retrieved from an electrostatic lifting process [24, 22]. The cleavage and extraction of peptides from resin beads and extracting the lipid contents directly from organelle preparations of plant tissues has been proven to be successful using the nanomanipulator [21, 23]. Nanomanipulation can be effectively coupled to nanospray ionization mass spectrometry providing picomolar sensitivity and having the capability to analyze femtograms to attograms of material [22]. Nanospray ionization has been able to reduce the required sample volume to as low as 300 nL. Once the extraction is complete, the sample can be directly analyzed using MS, thereby reducing the sample preparation procedure and time.

For the aformentioned reasons, DAPNe is ultimately a nondestructive technique when applied to ink on documents. Figure 2.14 is a schematic that defines the nondestructive term for extraction. After each sampling, a miniscule amount of analyte is removed from the ink.

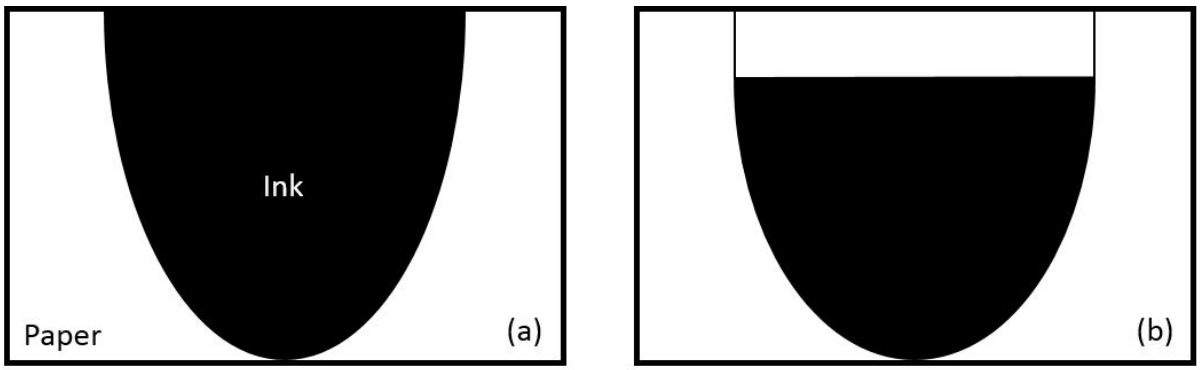

Figure 2.14. Schematic of the ink on paper (a) before extraction and (b) after extraction.

Although some ink is removed, there is ink that still remains. This allows for DAPNe to resample the document if needed. Destructive techniques destroy part of the document as well as removes all the ink from the well. By applying DAPNe to ink on document analysis, forensic document examiners are allowed to revisit the sample if needed.

2.3 References

[1] J. K. Lang, Handbook on Mass Spectrometry: Instrumentation, Data and Analysis, and Applications, New York: Nova Science Publishers, Inc., 2009.

[2] J. Griffiths, "A brief history of mass spectrometry," *Analytical chemistry,* vol. 80, pp. 5678-5683, 2008.

[3] M. S. Wilm and M. Mann, "Electrospray and Taylor-Cone theory, Dole's beam of macromolecules at last?," *International Journal of Mass Spectrometry and Ion Processes,* vol. 136, pp. 167-180, 1994.

[4] S. J. Gaskell, "Electrospray: Principles and Practice," *Journal of Mass Spectrometry,* vol. 32, pp. 677-688, 1997.

[5] A. P. Bruins, T. R. Covey and J. D. Henion, "Ion Spray Interface for Combined Liquid Chromatography/Atmosperic Pressure Ionization Mass Spectrometry," *Analytical Chemistry,* vol. 59, pp. 2642-2646, 1987.

[6] A. Cooper, C. M. Johnson, J. H. Lakey and M. Nollmann, "Heat does not come in different colours: Entropy-enthalpy compensation, free energy windows, quantum confinement, pressure perturbation calorimetry, solvation and the multiple causes of heat capacity effects in biomolecular interactions," *Biophysics Chemistry,* vol. 93, no. 2-3, pp. 215-230, 2001.

[7] R. B. Cole, Electrospray and MALDI mass spectrometry: Fundamentals, instrumentation, practicalities, and biological applications, Hoboken, New Jersey: John Wiley & Sons, Inc., 2010.

[8] R. Juraschek, T. Dulcks and M. Karas, "Nanoelectrospray--More Than Just a Minimized-Flow Electrospray Ionization Source," *Journal of the American Society for Mass Spectrometry*, vol. 10, pp. 300-308, 1999.

[9] A. Tycova and F. Foret, "Capillary electrophoresis in an extended nanospray tip-electrospray as an electrophoretic column," *Journal of Chromatography A,* vol. 1388, pp. 274-279, 2015.

[10] B. M. Ham and A. MaHam, Analytical chemistry: A chemist and laboratory technician's toolkit, Hoboken, New Jersey: John Wiley & Sons, Inc., 2016.

[11] A. Berlioz-Barbier, R. Baudot, L. Wiest, M. Gust, J. Garric, C. Cren-Olive and A. Bulete, "MicroQuEChERS–nanoliquid chromatography–nanospray–tandem mass spectrometry for the detection and quantification of trace pharmaceuticals in benthic invertebrates," *Talanta,* vol. 132, pp. 796-802, 2015.

[12] J. J. Gaumet and G. Strouse, "Nanospray mass spectrometry technique for analysing nanomaterials from molecular precursors up to 1.5 nm in diameter cluster," *Materials Science and Engineering C,* vol. 19, pp. 299-304, 2002.

[13] M. Phelps, J. Hamilton and G. F. Verbeck, "Nanomanipulation-coupled nanospray mass spectrometry as an approach for single cell analysis," *Review of Scientific Instruments,* vol. 85, pp. 124101-124105, 2014.

[14] G. Siuzdak, Mass spectrometry for biotechnology, Waltham, MA: Academic Press, 1996.

[15] W. Paul, "Electromagnetic traps for charged and neutral particles," *Rev. Mod. Phys.,* vol. 62, p. 531, 1990.

[16] P. Miller and M. Denton, "The quadrupole mass filter: Basic operating concepts," *J. Chem. Educ.,* vol. 63, pp. 617-623, 1986.

[17] D. A. Skoog, F. J. Holler and S. R. Crouch, Principles of instrumental analysis, Belmont, CA: David Harris, 2007.

[18] R. H. Perry, R. G. Cooks and R. J. Noll, "Orbitrap mass spectrometery: Instrumentation, ion motion and applications," *Mass Spectrometry Reviews,* vol. 27, pp. 661-699, 2008.

[19] D. L. Rousseau, "Laser chemistry," *Journal of Chemical Education,* vol. 43, pp. 566-570, 1966.

[20] V. Huynh, K. C. Williams, T. D. Golden and G. F. Verbeck, "Investigation of falsified documents via direct analyte-probed nanoextraction coupled to nanospray mass spectrometry, fluorescence microscopy, and Raman spectroscopy," *Analyst,* vol. 140, pp. 6553-6562, 2015.

[21] J. M. Brown, W. D. Hoffmann, C. M. Alvey, A. R. Wood, G. F. Verbeck and R. A. Petros, "One-bead, one compound peptide library sequencing via high-pressure ammonia cleavage coupled to nanomanipulation/nanoelectrospray ionization mass spectrometry," *Analytical Biochemistry,* vol. 398, pp. 7-14, 2010.

[22] N. M. Wallace, E. E. Hueske and G. F. Verbeck, "Electrostatic lifting-coupled with nanomanipulation nanospray ionization for the analysis of illicit drugs," *Science and Justice*, vol. 51, pp. 196-203, 2011.

[23] P. J. Horn, U. Joshi, A. K. Behrendt, K. D. Chapman and G. F. Verbeck, "On-stage liquid-phase lipid microextraction coupled to nanospray mass spectrometry for detailed, nano-scale lipid analysis," *Rapid Communications in Mass Spectrometry*, vol. 26, pp. 957-962, 2012.

[24] N. L. Ledbetter, B. L. Walton, P. Davila, W. D. Hoffmann, R. N. Ernest and G. F. Verbeck, "Nanomanipulation-coupled nanospray mass spectrometry applied to the extraction and analysis of trace analytes found on fibers," *Journal of Forensic Sciences,* vol. 55, pp. 1218-1221, 2010.

CHAPTER 3

NANOMANIPULATION COUPLED TO NSI-MS APPLIED TO DOCUMENT AND INK ANALYSIS[4]

3.1 Abstract

A method for the extraction and analysis of ink samples was developed using microscopy with direct analyte-probed nanoextraction coupled to nanospray ionization mass spectrometry (DAPNe-NSI-MS) for localized chemical analysis of document inks. Nanomanipulation can be effectively coupled to nanospray ionization mass spectrometry providing picomolar sensitivity, and the capability to analyze ultra-trace amounts of material and reduce the required sample volume to as low as 300 nL. This new and innovative technique does not leave destructive footprints on the surface of a document. To demonstrate the breadth of this technique, analysis of inks from various eras were tested, iron gall ink and modern inks, as well as the capability to detect the oxidative products of polyethylene glycol (PEG), a common binding agent. The experimental results showed that DAPNe-NSI-MS was able to chelate iron(II) and manganese(II) ions of iron gall ink and organic components of modern and carbon-based inks. Regardless of whether the ink composition is modern or ancient, organic or inorganic, this new instrumental approach is able to identify and characterize the ingredients by modifying the extraction solvent, illustrating the potential diversity of the DAPNe technique.

[4] Contents of this chapter have been previously published from V. Huynh, U. Joshi, J. M. Leveille, T. D. Golden, and G.F. Verbeck *Forensic Science International* 242 (2014) 150-156. Reproduced with permission from Elsevier.

3.2 Introduction

Developing an analytical technique for the study of antique and ancient documents must satisfy the specific requirement of integrity preservation during ink extraction. Ink analysis is of great importance whenever there is a question regarding verification or age determination of documents under differing conditions such as temperature, humidity, light and pest exposure, and any chemical alterations that may occur over time [1,2]. However, a major problem arises when obtaining accurate results without altering the original contents of the document; hence, a minimal to nondestructive approach is of great necessity. Numerous procedures have been used for the extraction and analysis of ink from documents. Traditional, nondestructive methods involve a visual examination of the document by microscopy and/or video spectral comparison (VSC) [3,4]. Thin-layer chromatography (TLC) is also a widely used method because it is inexpensive and shows good discrimination, but its discrimination is reduced for many gel inks, only to verify their pigmented nature [3,5,6]. However, the subjective nature of these techniques limit their usefulness. VSC relies on a visual comparison of grey levels and fails to discern between inks in suspected alterations, and TLC results are dependent on either simple side-by-side comparisons of color bands or retention factors calculated by an analyst [5,7–9]. Common procedures such as use of a micro punch [10], removal of ink-bearing fibers from the paper containing ink [11], or cutting a small strip from the document [8,12,13] have been used for the extraction of ink from manuscripts. Although TLC [5,6], high performance liquid chromatography (HPLC) [12,15,16], and capillary electrophoresis (CE) [17,18] are common analytical methods for the separation and analysis of ink components, a less destructive approach using nanospray ionization—mass spectrometry would provide a quantitative and qualitative advantage. By eliminating the need for chromatographic separation, both time and solvent needs can be significantly reduced [6,8,19–21]. The advent of a

new approach using microscopy with direct analyte-probed nanoextraction coupled to nanospray ionization mass spectrometry (DAPNe-NSI-MS) has allowed the forensic science community to use extremely small sample volumes for trace analyses with increased sensitivity and resolution [22–25]. Nanomanipulation has already been proven to be a valuable technique. The nanomanipulator is able to extract trace cocaine particles directly from a single rayon fiber and extract ultra-trace drug residues retrieved from an electrostatic lifting process [23,24]. The cleavage and extraction of peptides from resin beads and extracting the lipid contents directly from organelle preparations of plant tissues has been proven to be successful using the nanomanipulator [22,25]. Nanomanipulation can be effectively coupled to nanospray ionization mass spectrometry providing picomolar sensitivity and having the capability to analyze femtograms to attograms of material [24]. Nanospray ionization has been able to reduce the required sample volume to as low as 300 nL. Once the extraction is complete, the sample can be directly analyzed using MS, thereby reducing the sample preparation procedure and time. The key advantage of using the nanomanipulation technique for the extraction of ink is that the process does not leave visible destructive footprints on the surface of the document, which enables the analyst to retain the document in its original form. This innovative approach is able to facilitate the analysis of modern inks and inks from different eras. Modern ink is made from organic pigments and dyes with sometimes small amounts of metal present, along with solvents and other additives [10]. Compositions using carbon were utilized four to six thousand years ago (India ink), and Japanese Sumi ink came later during the 1300– 1400B.C. period [26,27]. Carbon-based inks are typically made out of ground soot or charcoal with other additives and binding agents to form a liquid, whereas commercially available India inks use shellac and borax [28]. Another popular ink, iron gall, was developed during the Middle Ages and consists primarily of tannins obtained from plant

galls mixed with iron(II) sulphate and natural gum [29,30]. The ink contains a large amount of iron(II) ions along with some significant Zn, Mn, Ca, and Mg ions [31]. Unfortunately, free iron ions present in the iron gall ink can cause corrosion of the paper and results in damaged historical manuscripts. Identifying the cause of corrosion can lead to the proper treatment and preservation of historical documents; in this case, the phytate process has been used to stabilize documents written with iron gall inks [32]. The metal ions present in iron gall ink can be efficiently extracted using chelating agents and subsequently analyzed. Regardless of whether the ink composition is modern or ancient, organic or inorganic, this new approach is able to identify and characterize the components, illustrating the potential diversity of the extraction chemistries. The focus in the present study is to develop an analytical tool and scheme for the direct extraction and analysis of components in ink using DAPNe-NSI-MS. This approach presents a minimally invasive procedure for the extraction and analysis of inks from questioned documents.

3.3 Materials and methods

3.3.1 Reagents and solvent preparation

Millipore water was obtained from Milli-Q Plus (Millipore; Billerica, MA) with 18 MΩ resistivity. The glacial acetic acid, ethylenediaminetertraacetic acid (EDTA), and potassium hydroxide (KOH) were purchased from Mallinckrodt Baker Inc. (Phillis-burg, NJ). Optima LC/MS methanol from Fischer Scientific (Fair Lawn, NJ) was used and iron gall ink was purchased from John Neal Books (Greensboro, NC). Sharpie ultra-fine point permanent markers (red, blue and black) were purchased from Newell Rubbermaid office products (Oak Brook, IL), the Japanese Sumi ink was purchased through Shopatron, Inc. and Yasutomo and Company (Burlingame, CA) and Higgins Calligraphy India inks were purchased from Chartpak Inc. (Leeds, MA). The extraction solvent for iron gall ink consisted of 0.0021 g of EDTA dissolved in 4 mL of water and

350 mL of 0.2 M KOH. The solution was then stirred for complete dissolution of EDTA and denoted as the EDTA extraction solvent. The extraction solvent for carbon-based inks and modern inks was made using 1:1 MeOH:H_2O (v:v) and 1% glacial acetic acid (MeOH/H_2O/1%Ac).

3.3.2 Instrumentation

The mass spectrometric analysis was done on a LCQ DECA XP Plus and TSQ 7000 (Thermo Finnegan; San Jose, CA), both equipped with an electrospray and nanospray ionization source (Proxeon Biosystems; Odense, Denmark). The nanomanipulator consisted of an L200 nanomanipulator (Zyvex; Richardson, TX) mounted on a Nikon AZ 100 (Nikon Instruments Inc.; Melville, NY) microscope stage. The nanomanipulator setup used for extraction has been described in detail in previous articles [22–25]. A PE2000b four channel pressure injector (MicroData Instrument Inc.; S. Plainfield, NJ) was used to inject and extract solvent.

3.3.4 Direct extraction analytical scheme

A schematic representation of the nanopositioner maneuvered over the document, using a joystick controller, is shown in Fig. 3.1(a). Nanospray capillary tip was loaded with 10 mL of the extraction solvent and inserted into the nanopositioner. A small droplet was made with 2 mL of Millipore water on top of the letter for extraction. The droplet is injected with a tiny amount of extraction solvent using an injection pressure of 15 psi and allowed to sit for 15–20 s, letting the ink dissolve into the droplet. The droplet is then extracted with a fill pressure of 35 psi. The extracted solvent is directly analyzed in the mass spectrometer without any further modification. Fig. 3.1(b) illustrates the direct extraction of ink from a document placed on top of the Nikon AZ 100 microscope stage.

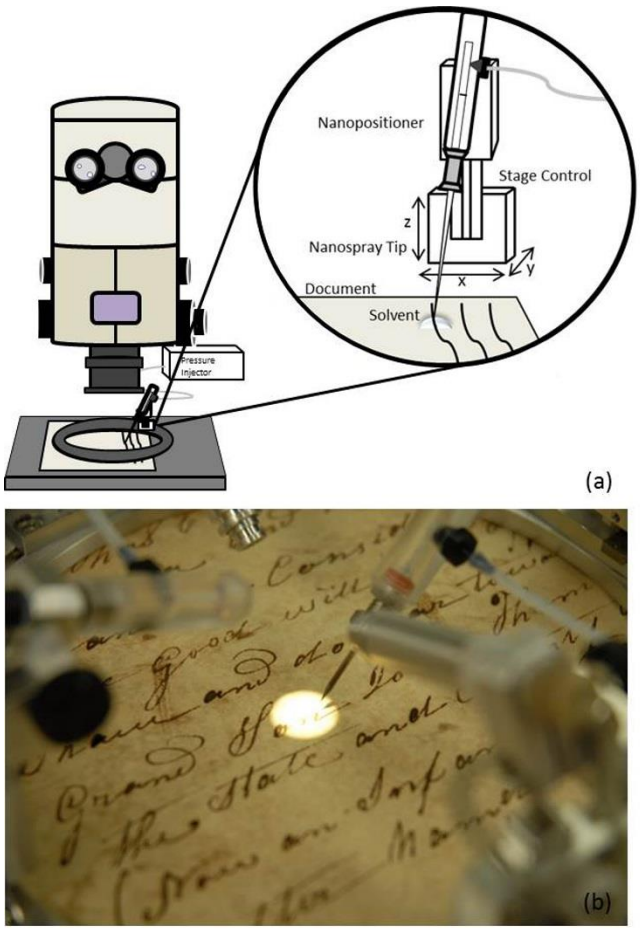

Figure 3.1. (a) A schematic of the Nikon AZ 100 microscope and nanomanipulator with the nanospray tip maneuvered on top of the document. (b) The document to be analyzed placed on the microscope stage with the nanopositioner maneuvered where the extraction is to be done.

3.3.5 Iron gall ink classification

The electrospray ionization method was used for the initial identification of peaks in iron gall ink and then tested on a document using the DAPNe-NSI-MS. A 1 mg/mL solution of iron gall ink was prepared in water. A background spectrum was collected using a 1:1 (v:v) mixture of the EDTA and MeOH/H_2O/ 1%Ac extraction solvents. After the background was collected, 500 mL of the iron gall ink solution was added to 500 mL of the 1:1 (v:v) EDTA:MeOH/H_2O/1%Ac solvent solution and analyzed in negative ionization mode since both EDTA and metal-EDTA

complexes have negative charge. A spray voltage of 3.5 kV and a flow rate of 5 mL/min were used for ESI–MS, spray voltages of 2.5 kV were used for DAPNe-NSI-MS and mass range of m/z 130 to 500 was used for all spectra.

3.3.6 Organic dyes and carbon based inks classification

The nanospray ionization technique identified and characterized the resins and vehicles in Sharpie Ultra-fine permanent markers (red, blue, and black), India ink (MPN: 4415, 4425, and 44314) and Japanese Sumi ink. The extractions were analyzed in positive mode and had a set extraction voltage of 2.5 kV. The scan ranges for the dyes and Japanese Sumi ink were m/z 50 to 500 and m/z 100 to 1000 for the carbon based inks.

3.3.7 Oxidation of polyethylene glycol

The oxidation of polyethylene glycol (PEG) was simulated by applying incandescent heat every 4 h up to 24 h on waterproof and non-waterproof India inks (MPN: 4415 and 4425), where a sample was taken between each 4 h increment. The maximum temperature resided between 37 and 40˚ C with a 60 W bulb.

3.4 Results and discussion

3.4.1 Solvent selection

An appropriate solvent should be selected to optimize extraction and the integrity of the document. The extraction solvent can be modified to target different chemistries in different inks. An EDTA extraction solution was proven to chelate iron(II) and manganese(II) ions, and MeOH/H_2O/1%Ac successfully extracted organic components of ink. Other extraction solvent components such as dichloromethane (DCM), acetonitrile (ACN), ethanol and dimethylformamide

(DMF) can be used for inks [33]. In addition, an appropriate chelator may be added to the extraction solvent for targeting a particular metal. Weyermann et al. analyzed Blue Parker® ballpoint pen entries extracted with DCM [34] and LaPorte et al. used ACN as the extraction solvent for over 600 black and blue ballpoint inks from 60 different companies [35]. Li et al. analyzed 30 black gel pen ink samples collected from different factories in China, spanning different brands for any given factory, in which all were extracted by methanol [36]. DMF showed successful ink extractions from 69 red ink pastes of seals which contained dyes or pigments as colorants, hydrocarbon, plant or mineral oil as vehicles, and other additives [33]. The compatibility of extraction solution with the MS and dissolution of the ink are the limitations of the solvent selection. The nanospray ionization solvents and the solvent extraction technique are valuable assets and more efficient than other minimally destructive techniques. LDI-MS is a harmful technique due to the ink entry paper being cut into small pieces prior to analysis [8,13]. However, Matthews et al. has shown promise with imperceptible damage to the surface of the document by removing a single ink bearing paper fiber [9]. The technique involves an individual extricating a fiber loose and then obtaining it by tweezers, increasing the potential for human error. DAPNe-NSI-MS is very competent due to its precise movements using a joystick controller. Although both techniques are almost equally nondestructive compared to each other, removing single ink bearing paper fibers is more time consuming and less efficient during sample extraction. Moreover, Giurato et al. uses a home-modified AP/MALDI-MS system for the investigation of organic dyes and pigments used to print books from the early 1900s [37]. The sample preparation involves depositing a matrix aerosol over 2– 3 mm^2 surface area, waiting for the solvent to evaporate and matrix to crystallize before analysis. No visible alterations were observed on the analyzed regions, making this technique eligible for comparison. DAPNe-NSI-MS requires only femtograms to

attograms of material and a sample volume as low as 300 nL; conversely, the ionization process of AP/MALDI-MS requires excess matrix to be maintained and utilizes a larger sampling area.

3.4.2 Determination of iron gall ink from a document

Iron gall ink has been characterized in Fig. 3.2 and the ions summarized in Table 3.1. The background spectrum obtained a distinct peak at m/z 291.00, as shown in Fig. 3.2(a). The results obtained indicate that iron gall ink has iron(II) and manganese(II) ions present, confirming that both metal ions can be efficiently chelated using EDTA (Fig. 3.2(c)) [38]. These results are consistent with the study conducted by Wagner and Bulska on written heritage using laser ablation inductively coupled mass spectrometry [39]. Despite the fact that the ink contains more iron than manganese, the spectrum shows relatively higher intensity of manganese complex. This may be that most of the iron has been oxidized leaving less iron for chelation.

3.4.3 Determination of organic dyes from a document

Sharpie ultra-fine point permanent markers were used to study the extraction of organic dyes. Currently, red pen ink is known to contain one or both Rhodamine B and Rhodamine 6G dyes. During photodegradation, Rhodamine B and Rhodamine 6G would expect to lose CO_2 (m/z 399) and an ethyl group (m/z 415), respectively [40,41]. Fig. 3.3(a) indicates that the red Sharpie contains Rhodamine 6G where m/z 443.24 is the parent peak and m/z 415.10 represents the loss of an ethyl group. Basic Blue 7 is a commonly used dye for blue inks which gives a peak at m/z 478.00 as shown in Fig. 3.3(b). A peak at m/z 372.53 signifies the extraction of another commonly used blue dye called Basic Violet 3 and gradual N-demethylation for Basic Violet 3 produces peaks at m/z 330.60 and 316.00 [10]. Unfortunately, no specific dye peaks could be assigned to the

extraction of black ink but diethylene glycol (DEG) was successfully extracted and gave a peak at m/z 129.80.

3.4.4 Determination of carbon based ink from a document

All the analyzed carbon-based inks contained polyethylene glycol (PEG), except the Japanese Sumi ink. Polyethylene glycols are commonly used as binders and thickening agents in the recipe of ink pens [13]. The PEG ions were detected as sodiated and protonated species ($[M + Na]^+$ and $[M + H]^+$) with a distinctive separation of 44 amu between each PEG signal [11,13]. The separation of 44 amu is derived from the monomeric ions of PEG ($–OCH_2CH_2–$) ions. Each ink is shown to produce a footprint that uniquely characterizes it. In Fig. 3.4(a), the waterproof drawing ink (4415) contains the only protonated PEG peak at m/z 327.09, [HO(C2H4O)7H + H]+. The non-waterproof India ink (4425) produces a signal at m/z 156.89 which indicates another binding agent, ethoxy diglycol with a sodium adduct, in addition to PEG (Fig. 3.4(b)). The waterproof calligraphy ink (44314) is shown to only contain PEG as its main binding agent, shown in Fig. 3.4(c). Fig. 3.5 confirms that Japanese Sumi ink contains diethylene glycol and ethoxy diglycol as its main binder and thickening agent. The peaks present at m/z 129.86 and m/z 156.89 verify sodiated adducts of diethylene glycol and ethoxy diglycol, respectively.

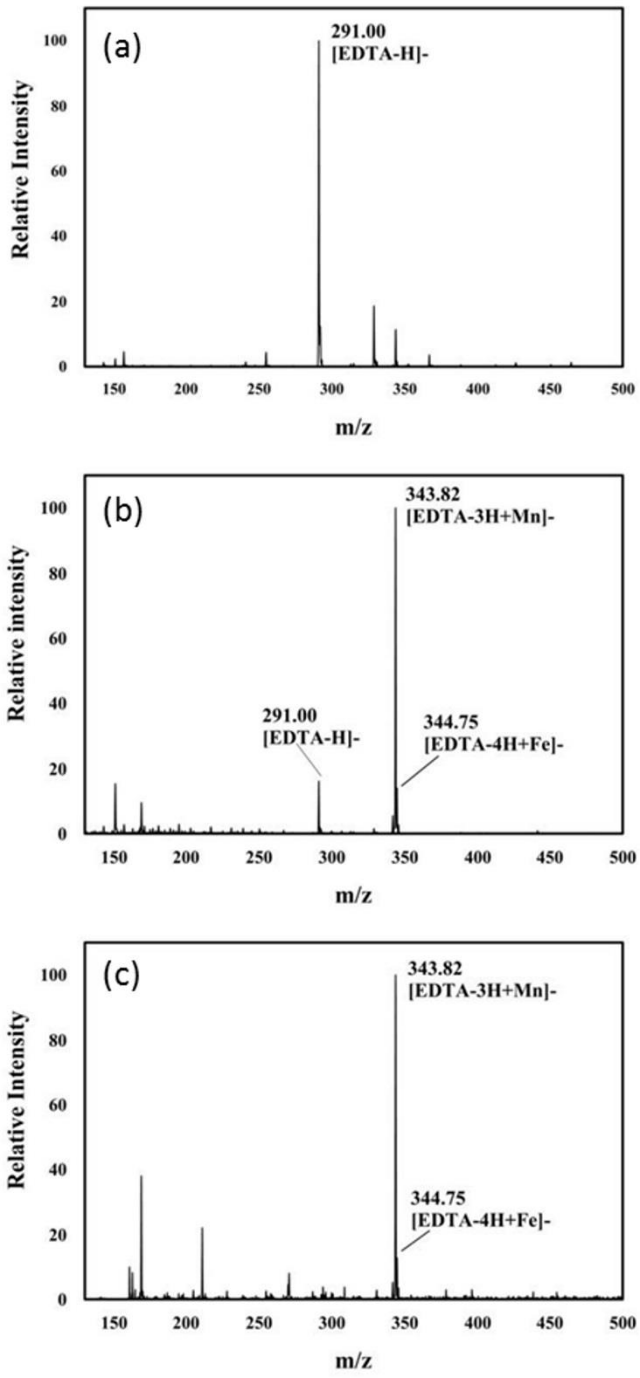

Figure 3.2. (a) Background spectrum of EDTA extraction solution. (b) ESI-MS spectrum of prepared iron gall ink solution. (c) NSI-MS spectrum of iron gall ink extracted from paper.

Method	Ion	*m/z*	Relative Intensities
ESI-MS	$[EDTA-H]^-$	291.00	16.57
	$[EDTA-4H+Fe]^-$	344.75	13.13
	$[EDTA-3H+Mn]^-$	343.82	99.57
DAPNe-NSI-MS	$[EDTA-H]^-$	291.00	5.54
	$[EDTA-4H+Fe]^-$	344.75	12.32
	$[EDTA-3H+Mn]^-$	343.82	99.37

Table 3.1. Summarized ions and components in iron gall ink obtained by an EDTA extraction solvent using ESI-MS and DAPNe-NSI-MS.

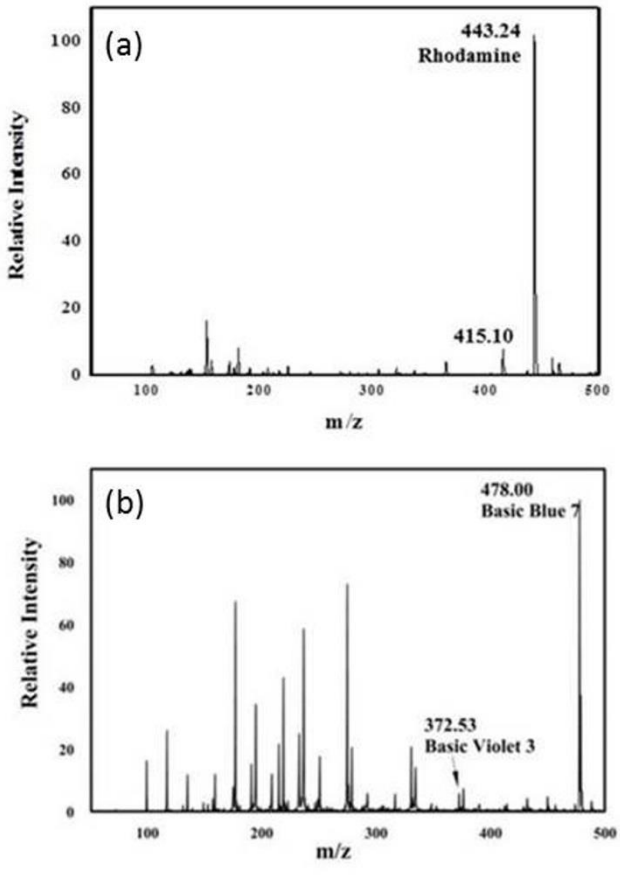

Figure 3.3. NSI-MS spectra of (a) red Sharpie showing the presence of Rhodamine 6G and (b) blue Sharpie indicating Basic Blue 7 and Basic Violet 3.

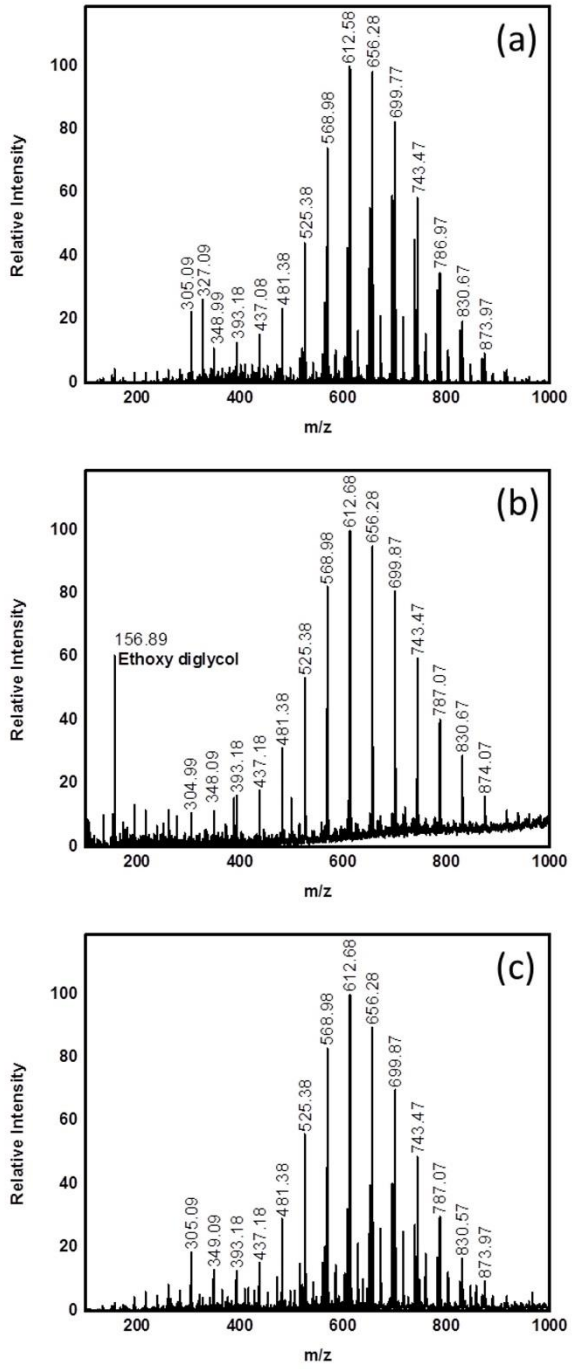

Figure 3.4. Mass spectra of India inks: (a) waterproof drawing ink (4415), (b) non-waterproof ink (4425), and (c) waterproof calligraphy ink (44314).

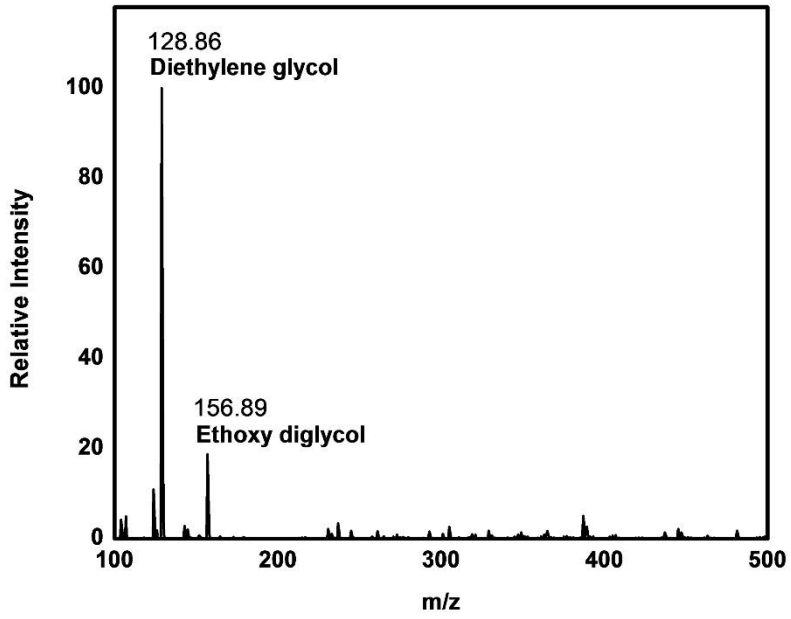

Figure 3.5. Mass spectrum of Japanese Sumi ink showing two binding agents.

3.5. Oxidation of PEG in carbon-based inks

The degradation of PEG in 4415 (waterproof ink) and 4425 (non-waterproof ink) was observed as heat was applied over time. Applying incandescent light to ink strokes speed up the process of aging, inferring a simulated aging study [1]. The degradation was calculated by the relative peak area (RPA) for each peak, defined as:

$$RPA_i = \frac{A_i}{A_{tot}} x100\% \quad (3.1)$$

where Ai is the area of the peak at m/z = i and A_{tot} is the summation of all the significant signals, including molecular ion and degradation products in which more is discussed by the following articles [1,8,42]. In Fig. 3.6, the peaks monitored were m/z 613, 656, and 700 which concluded a 25.20%, 24.63%, and 55.93% decrease of PEG in the waterproof ink, respectively; however, the

non-waterproof ink shows a 74.39%, 78.64%, and 80.64% reduction. Fig. 3.6 illustrates the different rate of oxidation caused by the waterproof and non-waterproof characteristic of the ink. Han et al. [43] investigated the mechanism of thermal degradation of PEG in air at 80˚ C and reported that PEG and linear polymers undergo molecular weight reduction and diminution of chain length during the process of degradation caused by a random chain scission oxidation mechanism, resulting from the bond scission in the backbone of the macromolecules. Upon application, inks begin to age and oxidize once deposited on the paper surface due to solvent loss, resin polymerization and dye degradation [44]. As proof of concept, DAPNe-NSI-MS has the capability to detect the oxidation products of PEG.

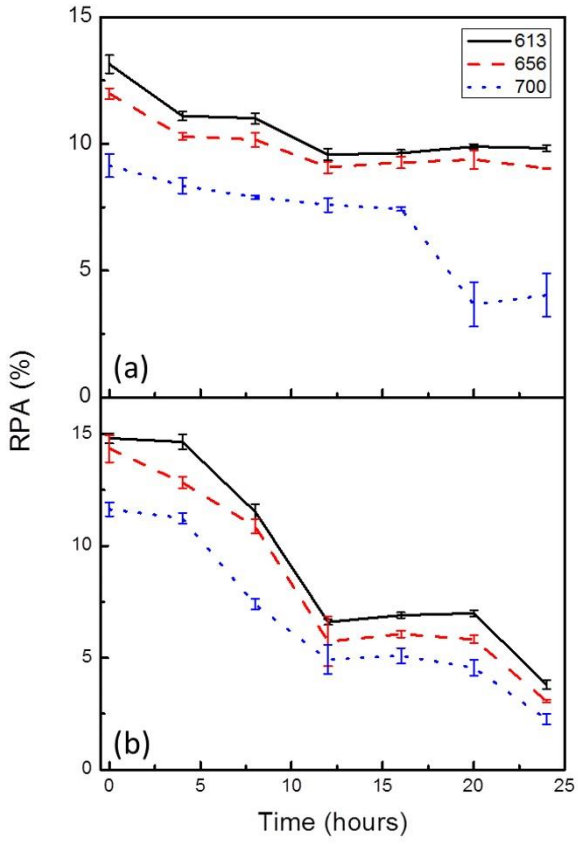

Figure 3.6. Percent RPA of (a) waterproof (4415) and (b) non-waterproof (4425) drawing ink.

3.5 Conclusion

A new technique for the extraction and analyses of ink and its components from documents has been developed and its diverse application illustrated. Using microscopy with direct analyte probe nanoextraction coupled to nanospray mass spectrometry for localized chemical analysis of document inks provide the advantages of analysis with small sample volume, high resolution, low limits of detection, and direct analysis, eliminating further sample preparation and saving analysis time. The procedure does not leave any visible footprint on the surface of the document, at most a water mark as indicated in Fig. 3.7(c). This is advantageous for the analysis of historical, governmental, and/or other documents where maintaining the integrity is crucial. Furthermore, microscopy with DAPNe-NSI- MS technique provided reproducible results with imperceptible damage.

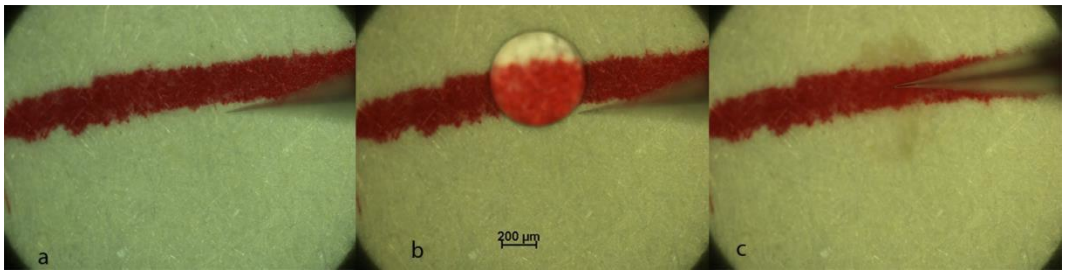

Fig. 3.7. (a) Microscope view of the ink line with nanospray tip set up for extraction. (b) A drop of water placed on the surface of the document where diffusion of ink into the droplet will occur. (c) View after extraction has been completed.

3.6 References

[1] M. Ezcurra, J.M.G. Go´ ngora, I. Maguregui, R. Alonso, Analytical methods for dating modern writing instrument inks on paper, Forensic Sci. Int. 197 (2010) 1–20.

[2] R.L. Brunelle, K.R. Crawford, Advances in the Forensic Analysis and Dating of Writing Ink, Charles C. Thomas Publisher, Springfield, IL, 2003.

[3] G. Reed, K. Savage, D. Edwards, N.N. Daeid, Hyperspectral imaging of gel pen inks: an emerging tool in document analysis, Sci. Justice 54 (2014) 71–80.

[4] S. Bell, A Dictionary of Forensic Science, Oxford University Press, Oxford, 2012.

[5] D. Djozan, T. Baheri, G. Karimian, M. Shahidi, Forensic discrimination of blue ballpoint pen inks based on thin layer chromatography and image analysis, Forensic Sci. Int. 179 (2008) 199–205.

[6] O.P. Jasuja, A.K. Singla, B.L. Seema, Thin-layer chromatographic analysis of Indian stamp pad inks, Forensic Sci. Int. 42 (1989) 255–262.

[7] C.D. Adams, S.L. Sherratt, V.L. Zholobenko, Classification and individualisation of black ballpoint pen inks using principle component analysis of UV–vis absorption spectra, Forensic Sci. Int. 174 (2008) 16–25.

[8] M. Gallidabino, C. Weyermann, R. Marquis, Differentiation of blue ballpoint pen inks by positive and negative mode LDI-MS, Forensic Sci. Int. 204 (2011) 169–178.

[9] B. Matthews, G.S. Walker, H. Kobus, P. Pigou, C. Bird, G. Smith, The analysis of dyes in ball point pen inks on single paper fibres using laser desorption ionisation time of flight mass spectrometry (LDI-TOFMS), Forensic Sci. Int. 209 (2011) e26–e30.

[10] L. Ng, P. Lafontaine, L. Brazeau, Ballpoint pen inks: characterization by positive and negative ion-electrospray ionization mass spectrometry for the forensic examination of writing inks, J. Forensic Sci. 47 (2002) 1238–1247.

[11] M.R. Williams, C. Moody, L. Arceneaux, C. Rinke, K. White, M.E. Sigman, Analysis of black writing ink by electrospray ionization mass spectrometry, Forensic Sci. Int. 191 (2009) 97–103.

[12] Y. Liu, J. Yu, M. Xie, Y. Liu, J. Han, T. Jing, Classification and dating of black gel pen ink by ion-pairing high-performance liquid chromatography, J. Chromatogr. A 1135 (2006) 57–64.

[13] Y. Wu, C. Zhou, J. Yu, H. Liu, M. Xie, Differentiation and dating of gel pen ink entries on paper by laser desorption ionization- and quadruple-time of flight mass spectrometry, Dyes Pigm. 94 (2012) 525–532.

[15] Y. Liu, J. Yu, M. Xie, Y. Chen, G. Jiang, Y. Gao, Studies on the degradation of blue gel pen dyes by ion-pairing high performance liquid chromatography and electro-spray tandem mass spectrometry, J. Chromatogr. A 1125 (2006) 95–103.

[16] L.M. Petrick, T.A. Wilson, W.R. Fawcett, High-performance liquid chromatogra-phy–ultraviolet–visible spectroscopy–electrospray ionization mass spectrometry method for acrylic and polyester forensic fiber dye analysis, J. Forensic Sci. 51 (2006) 771–779.

[17] C. Vogt, J. Vogt, A. Becker, E. Rohde, Separation, comparison and identification of fountain pen inks by capillary electrophoresis with UV–visible and fluorescence detection and by proton-induced X-ray emission, J. Chromatogr. A 781 (1997) 391–405.

[18] C. Cruces-Blanco, L. Ga´ miz-Gracia, A.M. Garcı´a-Campana, Applications of capillary electrophoresis in forensic analytical chemistry, Trends Anal. Chem. 26 (2007) 215–226.

[19] R.B. Cole, Electrospray Ionization Mass Spectrometry: Fundamentals, Instrumen-tation, and Applications, Wiley, New York, NY, 1997.

[20] L.D. Maquille` , L. Renaudin, F. Goutelard, A. Jardy, J. Vial, D. Thie` baut, Determina-tion of ethylenediaminetetraacetic acid in nuclear waste by high-performance liquid chromatography coupled with electrospray mass spectrometry, J. Chro-matogr. A 1276 (2013) 20–25.

[21] J. Coumbaros, K.P. Kirkbride, G. Klass, W. Skinner, Application of time of flight secondary ion mass spectrometry to the in situ analysis of ballpoint pen inks on paper, Forensic Sci. Int. 193 (2009) 42–46.

[22] J.M. Brown, W.D. Hoffmann, C.M. Alvey, A.R. Wood, G.F. Verbeck, R.A. Petros, One-bead, one compound peptide library sequencing via high-pressure ammonia cleavage coupled to nanomanipulation/nanoelectrospray ionization mass spec-trometry, Anal. Biochem. 398 (2010) 7–14.

[23] N.L. Ledbetter, B.L. Walton, P. Davila, W.D. Hoffmann, R.N. Ernest, G.F. Verbeck IV, Nanomanipulation-coupled nanospray mass spectrometry applied to the extrac-tion and analysis of trace analytes found on fibers, J. Forensic Sci. 55 (2010) 1218–1221.

[24] N.M. Wallace, E.E. Hueske, G.F. Verbeck, Electrostatic lifting-coupled with nano-manipulation nanospray ionization for the analysis of illicit drugs, Sci. Justice 51 (2011) 196–203.

[25] P.J. Horn, U. Joshi, A.K. Behrendt, K.D. Chapman, G.F. Verbeck, On-stage liquid-phase lipid microextraction coupled to nanospray mass spectrometry for de-tailed, nano-scale lipid analysis, Rapid Commun. Mass Spectrom. 26 (2012) 957–962.

[26] J.A. Amato, Surfaces: A History, University of California Press, London, England, 2013.

[27] W.E. Deal, Handbook to Life in Medieval and Early Modern Japan, Facts on File Inc., New York, NY, 2006.

[28] J.A. Siegel, P.J. Saukko, Encyclopedia of Forensic Sciences, second ed., Academic, San Diego, CA, 2000, pp. 375–379.

[29] G. Chiavari, S. Montalbani, S. Prati, Y. Keheyan, S. Baroni, Application of analytical pyrolysis for the characterisation of old inks, J. Anal. Appl. Pyrolysis 80 (2007) 400–405.

[30] R. D'Agata, G. Grasso, S. Parlato, S. Simone, G. Spoto, The use of atmospheric pressure laser desorption mass spectrometry for the study of iron-gall ink, Appl. Phys. A 89 (2007) 91–95.

[31] O. Hahn, W. Malzer, B. Kanngiesser, B. Beckhoff, Characterization of iron-gall inks in historical manuscripts and music compositions using x-ray fluorescence spectrometry, X-Ray Spectrom. 33 (2004) 234–239.

[32] V. Rouchon, E. Pellizzi, M. Duranton, F. Vanmeert, K. Janssens, Combining XANES, ICP-AES, and SEM/EDS for the study of phytate chelating treatments used on iron gall ink damaged manuscripts, J. Anal. At. Spectrom. 26 (2011) 2434–2441.

[33] Y. Yao, J. Song, J. Yu, X. Wang, F. Hou, A. Zhang, Y. Liu, J. Han, M. Xie, Differentiation and dating of red ink entries of seals on documents by HPLC and GC/MS, J. Sep. Sci. 32 (2009) 2919–2927.

[34] C. Weyermann, D. Kirsch, C.C. Vera, B. Spengler, A GC/MS study of the drying of ballpoint pen ink on paper, Forensic Sci. Int. 168 (2007) 119–127.

[35] G.M. LaPorte, J.D. Wilson, A.A. Cantu, S.A. Mancke, S.L. Fortunato, The identifica-tion of 2-phenoxyethanol in ballpoint inks using gas chromatography/mass spectrometry—relevance to ink dating, J. Forensic Sci. 49 (2004) 1–5.

[36] B. Li, P. Xie, Y. Guo, Q. Fei, GC analysis of black gel pen ink stored under different conditions, J. Forensic Sci. 59 (2014) 543–549.

[37] L. Giurato, A. Candura, G. Grasso, G. Spoto, In situ identification of organic components of ink used in books from the 1900s by atmospheric pressure matrix assisted laser desorption ionization mass spectrometry, Appl. Phys. A 97 (2009) 263–269.

[38] Z. Chen, Q. Sun, Y. Xi, G. Owens, Speciation of metal-EDTA complexes by flow injection analysis with electrospray ionization mass spectrometry and ion chro-matography with inductively coupled plasma mass spectrometry, J. Sep. Sci. 31 (2008) 3796–3802.

[39] B. Wagner, E. Bulska, On the use of laser ablation inductively coupled plasma mass spectrometry for the investigation of the written heritage, J. Anal. At. Spectrom. 19 (2004) 1325–1329.

[40] J. Siegel, J. Allison, D. Mohr, J. Dunn, The use of laser desorption/ionization mass spectrometry in the analysis of inks in questioned documents, Talanta 67 (2005) 425–429.

[41] L.J. Soltzberg, A. Hagar, S. Kridaratikorn, A. Mattson, R. Newman, MALDI-TOF mass spectrometric identification of dyes and pigments, J. Am. Soc. Mass Spectrom. 18 (2007) 2001–2006.

[42] C. Weyermann, D. Kirsch, C. Costa-Vera, B. Spengler, Photofading of ballpoint dyes studied on paper byLDIandMALDIMS,J. Am.Soc.MassSpectrom.17 (2006)297–306.

[43] S. Han, C. Kim, D. Kwon, Thermal/oxidative degradation and stabilization of polyethylene glycol, Polymer 38 (1997) 317–323.

[44] C. Weyermann, B. Spengler, The potential of artificial aging for modelling of natural aging processes of ballpoint ink, Forensic Sci. Int. 180 (2008) 23–31.

CHAPTER 4

INVESTIGATION OF FALSIFIED DOCUMENTS VIA DIRECT ANALYTE-PROBED NANOEXTRACTION COUPLED TO NANOSPRAY MASS SPECTROMETRY, FLUORESCENCE MICROSCOPY, AND RAMAN SPECTROSCOPY[5]

4.1 Abstract

Microscopy with direct analyte-probed nanoextraction coupled to nanospray ionization mass spectrometry (DAPNe-NSI-MS) is a direct extraction technique that extracts ultra-trace amounts of analyte. It has been proven to extract ink from documents with little to no physical or chemical footprint. In this study, DAPNe has been coupled to Raman spectroscopy, fluorescence microscopy, and NSI-MS to determine if an ink entry from a document was falsified. A handwritten number was altered using a different ink pen to test if the aforementioned techniques could discriminate the original number from the altered number, qualitatively and/or quantitatively. Chemical species from part of the original number, altered number, and a point at which both inks intersect were successfully differentiated by all techniques when using different pens. DAPNe coupled to fluorescence microscopy and Raman spectroscopy was not able to discriminate the forged ink entry when the exact same pen was used to modify the text (due to the same ink formula). However, DAPNe-NSI-MS successfully discerned that the pen was dispensed on different days by quantitating the oxidation process.

[5]Contents of this chapter have been previously published from V. Huynh, K. C. Williams, T. D. Golden, and G.F. Verbeck *Analyst* 140 (2015) 6553-6562. Reproduced with permission from The Royal Society of Chemistry.

4.2 Introduction

The field of questioned document analysis is an important area in forensic science, particularly fraud and forgery of handwritten ink entries. The analyses of ink entries on these falsified documents include looking for added ink to the original written ink entry, thus, changing the meaning of the text (e.g., changing the number four into a nine). Discrimination and dating of inks can provide sufficient information, aiding scientific evidences and clues for determining the authenticity of the manuscript [1]. Material evidence found at crime scenes must be kept in its pristine state in order to preserve its evidentiary value. However, a nondestructive method is difficult to achieve when analyzing ink markings. Useful but destructive techniques have been previously applied to forged documents, include mass spectrometry methods such as laser desorption ionization mass spectrometry (LDI-MS), matrix-assisted laser desorption ionization (MALDI), and secondary ion mass spectrometry (SIMS). Utilizing MS techniques instead of chromatographic separation reduces both time and solvent needs [2-6]. Weyermann et al. [7] analyzed 30 black gel pen inks using LDI-MS, where the sample was fixed to a solid steel plate with glue. Even though the samples were directly analyzed without the addition of a matrix, reducing preparation time, the samples were cut in order to fit the plate. Similarly, Wu et al.[1] cut 5 cm ink entries into small pieces and extracted the ink by 1.0 mL of dimethyl formamide (DMF) for 12 h and then filtered through a 0.22 μm Millipore film prior to LDI-MS analysis, both destructive and time-consuming. LDI and MALDI techniques are limited to the size of the sample plate and can have an extended sample preparation time. Denman et al. [8] analyzed 24 blue ballpoint pens using time-of-flight (ToF)-SIMS and prepared the samples by drawing a 3 cm line on paper with each spectral analysis performed over a 100 × 100 μm raster area. Although surface analysis by ToF-SIMS provides ballpoint pen ink discrimination and is nondestructive, like the

previous techniques, it is also limited to the size of the sample holder. Other common procedures such as micropunch [9], removal of ink-bearing fibers from the paper [10], and cutting a small strip from the document [1,2,11] have been used for the extraction of ink from manuscripts. A less destructive approach is needed among ink analysts in order to extract and analyze the ink chemistry of documents while still preserving their original forms.

Direct analyte-probed nanoextraction coupled to nanospray ionization mass spectrometry (DAPNe-NSI-MS) is a technique that extracts ultra-trace amounts of analyte and has already proven to extract ink from documents with minimal to no destruction in addition to providing a quantitative and qualitative advantage with increased sensitivity and resolution [12]. DAPNe uses a device comprised of a nanomanipulator mounted on the stage of a high-powered microscope. Nanomanipulation has been used for many forensic and biological applications including ultra-trace drug identification [13], extraction of a peptide from an individual library of beads [14], extraction of lipid content directly from organelle, preparations of plant tissues [15], and ultra-trace molecular analysis [16].

The advantage of DAPNe-NSI-MS for the analyses of ink and document examination is that it keeps the document in its pristine form. Through coupling a piezoelectric-controlled positioner of the nanomanipulator to a pressure injector, extractions of ultra-trace analytes (as low as 300 attograms) can be achieved [17]. As shown in Fig. 4.1, a solvent droplet is placed on the ink of interest, diffusing components of the ink into the droplet. The ink-infused droplet is then extracted into the nanospray tip for further MS analysis, leaving a water mark at most [12]. The high surface tension of the water droplet holds until the extraction is complete. This is because the ink creates a barrier between the paper and the droplet, increasing the time it takes for the droplet to soak into the paper and allowing enough time for extraction. The nanomanipulator can

effectively be coupled to NSI-MS, achieving picomolar sensitivity. The sample can be analyzed using MS directly after extraction, reducing sample preparation and time. This technique is minimally destructive and the working space is capable of examining full documents, including books. In a previous study [12], DAPNe-NSI-MS was able to extract inorganic and organic components from iron gall ink and carbon-based inks, respectively, as well as utilizing the data for an age determination mechanism for the oxidation of polyethylene glycol (PEG), a stabilizer found in inks. By changing the chemistry of the extraction solvent, the DAPNe technique can target specific components in the ink. For example, a chelator was added to the extraction solvent in order to target metal ions (Fe and Mn) within iron gall ink.

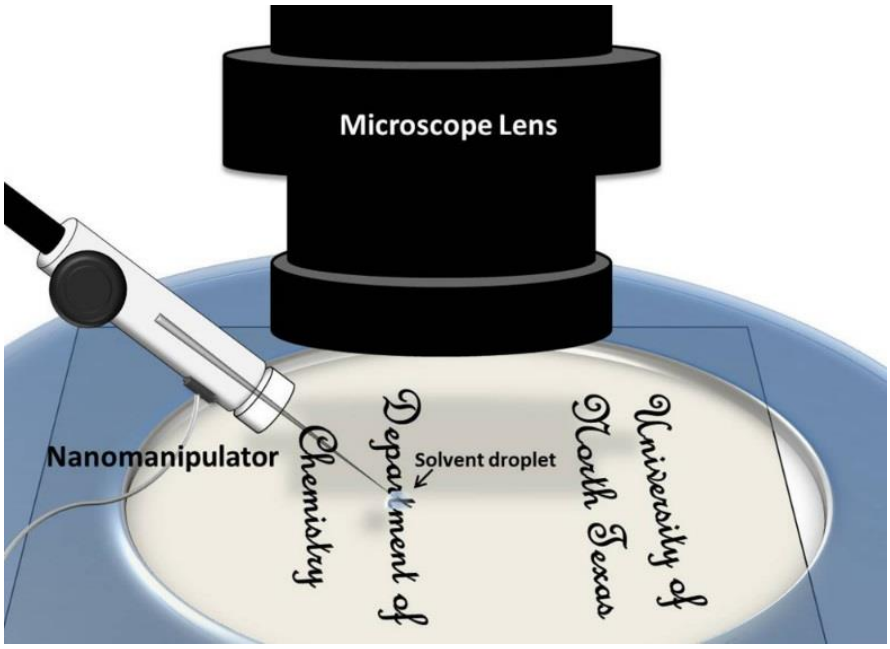

Figure 4.1. A schematic of the DAPNe technique extracting ink from a document. Ink diffuses into a solvent droplet placed on the paper. A nanospray tip then extracts the solvent and ink.

Although DAPNe-NSI-MS can identify whether different ink pens or the same ink pen was used in a particular handwritten document, initially locating where in the text the modification has

occurred may be difficult. Therefore, other techniques need to be implemented to locate the falsified ink entries. Other nondestructive techniques such as Raman spectroscopy [18–20] and fluorescence microscopy [20] can be applied prior to ink extractions in order to image where the alterations have been made. Raman spectroscopy has become increasingly popular in analyzing inks from forensic cases because it is chemically selective, nondestructive, and no sample preparation is required [18]. Braz et al. [21] examined blue crossing ink lines via Raman imaging and determined that the longer the time separating the application of the inks, the easier it was to discriminate the order of the ink lines drawn. Mazzella et al. [22] demonstrated Raman spectroscopy as a general technique for gel pen ink analysis. Different brands and models of 55 blue gel pen inks were examined and identified two main pigments, pigment blue 15 and pigment violet 23. A Video Spectral Comparator (VSC) is a nondestructive way to analyze ink through various energy sources (tungsten, halogen, and fluorescent lamps). da Silva et al. [23] analyzed different types and brands of blue pen inks in cursive handwriting using a VSC ranging from 400–1000 nm. The authors were able to distinguish between the different types and brands of blue pens. Reed et al. [24] also utilized a VSC to discriminate 42 different gel inks (blue, red, and black). Raman imaging and fluorescence are useful techniques that provide a chemical footprint of inks which is crucial circumstantial evidence in cases of counterfeit documents. These methods are able to discriminate between the original ink and the added ink of fraudulent documents.

As technology and direct ionization progress, new direct analysis techniques are coming to light. These include desorption electrospray ionization (DESI), direct analysis in real time (DART), and liquid extraction surface analysis (LESA). DESI provides a rapid and direct approach to ultra-trace analysis by releasing charged droplets onto the surface for ionization of analytes [25]. DART is another high throughput surface method that releases excited state gas molecules for

ionization of the analytes on the surface [26]. LESA uses an automated sampling probe for direct analysis [27]. LESA is the most similar technique to DAPNe in that they both interact directly with the surface at the liquid junction. DESI and DART requires a large amount of surface area for analyte ionization and in turn are more destructive. LESA currently has an enclosed workstation with limited workspace which confines document size. The other major weakness with LESA is that it uses pipette tips with a diameter of 800 μm, producing a surface area wetted with extraction solvent of 1–3 mm [28]. DAPNe uses tips with an inner diameter of 1 μm, minimizing the surface area wetted to 5 μm or less. DAPNe's platform strength comes from the coupling to high magnification microscopy and imaging spectroscopy to aid in chemical find, and reduce document destruction.

In this study, DAPNe has been coupled to Raman spectroscopy, fluorescence microscopy, and NSI-MS for the examination of counterfeit or forged manuscripts. These techniques have shown the capability to characterize and differentiate between different pens of the same color. Unfortunately, when the exact same pen is used to alter a document the same chemical species are present, making spectroscopic discrimination more difficult. By using DAPNe-NSI-MS, the oxidation process of the same ink dispensed at different times can be quantified.

4.3 Experimental methods

4.3.1 Reagents and solvent preparation

Millipore water was obtained from Milli-Q Plus (Millipore; Billerica, MA) with 18 MΩ resistivity. The glacial acetic acid was purchased from Mallinckrodt Baker Inc. (Phillisburg, NJ). Optima LC/MS methanol, toluene, chloroform, ammonium hydroxide, and analytical grade ammonium acetate were acquired from Fischer Scientific (Fair Lawn, NJ). BIC® cristal, Xtra

BOLD (1.6 mm), pens were obtained by the pack, with 10 assorted inks (Shelton, CT). Pilot G2, Bold 1.0 mm, pens (premium gel rollers, item #G21C4001) are manufactured from ©Pilot Corporation of America (Jacksonville, Fl). Uni-ball vision, fine 0.7 mm, assorted pens (item #1823944) and black waterproof (item #1824106) pens are made from ©2013 Newell Rubbermaid office products (Oak Brook, IL). A black Pigma Micron archival pen (0.20 mm, Sakura Color Products of America) was also used. All pens are commercially available.

The extraction solvents that were used are methanol : water (1 : 1, v/v) with 1% acetic acid, toluene : methanol (1 : 10, v/v) with 0.1% ammonium acetate, methanol : chloroform (1 : 1, v/v) with 0.1% ammonium hydroxide, and methanol : chloroform (1 : 1, v/v) with 0.1% ammonium acetate.

4.3.2 Modified ink analysis

Several replicates of the number four was written on A4 type grid paper (ensuring reproducibility), denoted as ink pen 1, and altered to a number nine two days later with a different pen, known as ink pen 2 (Fig. 4.2). A few hours after alteration, DAPNe-NSI-MS, fluorescence microscopy, and Raman spectroscopy were all used to analyze the alteration.

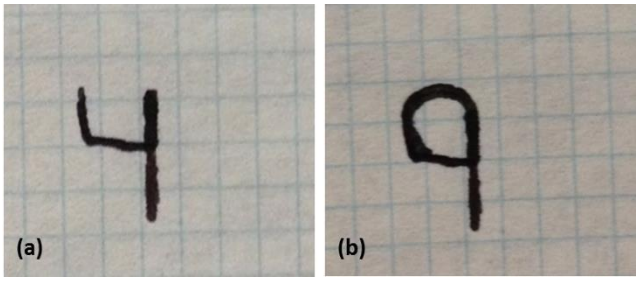

Figure 4.2. An illustration of a number being altered: (a) a number four was modified into a (b) nine.

4.3.3 Instrumentation

A Nikon AZ 100 (Nikon Instruments Inc.; Melville, NY) microscope was equipped with an L200 nanomanipulator (Zyvex; Richardson, TX), mounted on the microscope stage. The nanospray tip is maneuvered by a joystick controller, with a fine spatial resolution up to 5 nm. The injection and extraction of the nanospray tip is controlled by a PE2000b four channel pressure injector (MicroData Instruments Inc.; S.Plainfield, NJ). The nanomanipulator has been previously detailed [12–14,17] and the direct analytical scheme used for the extraction of ink from documents is described thoroughly by Huynh et al. [12] The mass spectrometric analysis was conducted on a LCQ DECA XP Plus equipped with a nanospray ionization source (Proxeon Biosystems; Odense, Denmark). The Nikon AZ 100 microscope is also equipped with an Intensilight fiber illuminator, utilizing a mercury light source, suitable for fluorescence observation (Nikon Intensilight C-HGFI). Filter cubes (or optical blocks) are used to selectively isolate fluorescence emission of certain wavelengths. The Nikon fluorescence filter cubes (Nikon Instruments, Inc. Melville, NY) include epi-fluorescence interference and absorption filter combinations. These filter cubes include an excitation filter, dichcromatic beamsplitter, and a barrier filter to satisfy the excitation and emission requirements of the fluorescent compounds. The filter cubes are easily interchanged to match the spectral excitation and emission characteristics of chromophores in the ink. Raman measurements were performed using an Almega XR Raman spectrometer equipped with an Olympus BX51 microscope and mapping capabilities controlled by Omnic for Almega 7 software (Thermo Fisher Scientific Inc., Madison, USA).

4.3.4 Raman imaging

Raman mapping was conducted on two different samples: (i) a black Micron pen was used to write the four (ink pen 1) and a black pilot pen (ink pen 2) was used to modify the four into a nine. (ii) A black pilot pen was used to write the four and then used again to alter into a nine. An Almega XR Raman spectrometer equipped with Olympus BX51 microscope with mapping capabilities and spatial resolution down to 1 μm was used. An excitation source of 780 nm (30% of 40 mW), single transverse mode, high brightness diode laser was used. The laser power was not high enough to visibly damage the paper. The Raman signal was collected over the range of 4000–100 cm^{-1} using a 10x microscope objective (0.25 NA).

4.3.5 DAPNe-NSI-MS

The nanospray tip was filled with the desired extraction solvent prior to inserting into the nanopositioner. A 2 μL droplet of Millipore water is dispensed onto the ink. The nanospray tip is then positioned into the solvent droplet and injected with a tiny amount of extraction solvent using an injection pressure of 15 psi and allowed to sit for 15–20 s, letting the ink diffuse into the droplet. It is important to note that propelling the extraction solvent into the water droplet encourages the components of ink to dissolve into the droplet. The droplet is finally extracted with a fill pressure of 35 psi. The analyte contained in the nanospray tip is directly analyzed through NSI-MS without further modification. Extractions were conducted on three different locations of the fraudulent ink entries (Fig. 4.2(b)): (i) ink pen 1 (part of the four), (ii) ink pen 2 (part of the nine), and (iii) where the ink from the four and nine intersect. The extractions were accomplished using methanol : H_2O (1 : 1) with 1% acetic acid and mass spectra were scanned from a range of m/z 50–1500 in positive mode with a spray voltage of 2.5 kV.

4.3.6 Oxidation of altered text

A black Uni-ball (waterproof) pen was used to write the number four and then set to dry for 24 hours. Using the exact same pen, the four was then changed to a number nine and extractions were conducted 1–2 hours later using methanol : H_2O (1 : 1) with 1% acetic acid. After the first extraction, another extraction was completed subsequently every 24 hours for a total of 5 days. Oxidation was then quantified by calculating the percent relative peak area (RPA) [12, 29–33] with three repetitions, defined as

$$RPA_i = \frac{A_i}{A_{tot}} \, x \, 100\% \tag{4.1}$$

where A_i is the area of peaks of interest at m/z = i and A_{tot} is the summation of all the significant signals above a certain intensity threshold. The overall concentration cannot be controlled, but relative amounts of extracted analytes are consistent within a given extraction solvent. Mass spectra were scanned from a range of m/z 50–1500 in positive mode.

4.3.7 Nanospray solvent chemistry

The solvent chemistry was evaluated by using different extraction solvents in the nanospray tip. Depending on the extraction solvent, glycols or dyes could be extracted separately. Several combinations of extraction solvents were used to change the selectivity of which component is being extracted from the ink as well as optimizing the intensities. This was conducted by drawing several lines of ink on A4 type grid paper and then set to dry for 1–2 hours before extraction. The extraction solvents discussed in section 4.3.1 were used.

4.4 Data and discussion

4.4.1 Fluorescence microscopy

The emission of inks is shown in Fig. 4.3. Noticeable alterations can be observed from Fig. 4.3(a and b). Fig. 4.3(b) shows three different red shades of emission from the paper, ink 1, and ink 2. This is because two different pens of the same color were used to modify the number; dissimilar components from each pen fluoresce differently. Fig. 4.3(c and d) show no discrimination, indicating time does not have a significant effect on fluorescence intensities of the same pen. Fluorescence microscopy was unable to observe a fluorescent difference when the text is altered using the same pen.

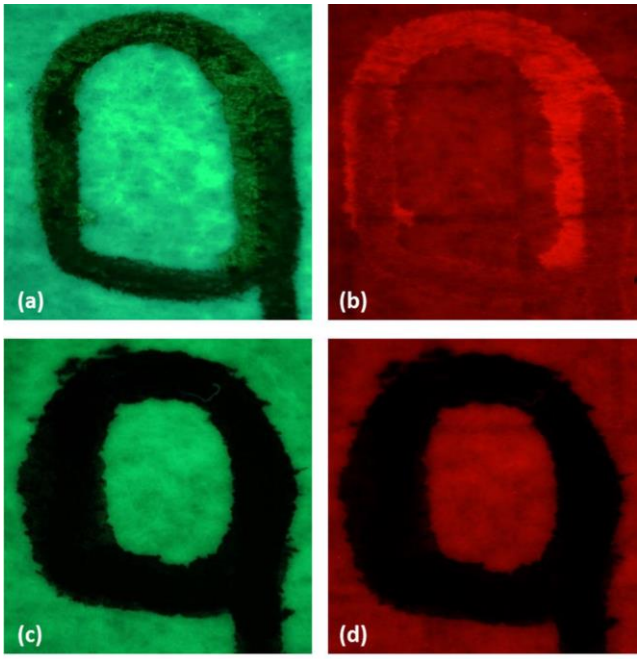

Figure 4.3. Fluorescent images of the altered text where (a) and (b) was modified with two different black pens, and (c) and (d) was modified with the same black pen. (a) and (c) used a blue excitation filter (420–495 nm) and (b) and (d) used a green excitation filter (510–560 nm).

4.4.2 Raman imaging

Raman spectroscopy is a valuable technique utilized in the detection of document falsification because it is highly specific for chemical identification that can discriminate

molecular species in inks [18, 34]. Although a valuable technique, the fluorescence interference from both the ink and paper make distinguishing peaks difficult. Paper contains approximately 33% of fluorescent whitening agents (FWAs) or also known as optical brightening agents (OBAs), approximately 80% of which are based on stilbene compounds [35]. Stilbene compounds are chemically similar to anionic direct dyes due to their planar/linear structures containing delocalized π electron systems and one or more sulphonic acid groups ($–SO_3H$), indicating emission at short visible wavelengths (400–500 nm) [35]. Inks contain dyes, pigments, resins, and binding agents that absorb light strongly in the visible region [36]. They contain structural characteristics that are present in the chromophore, such as electron donating groups (e.g., –OH, $–NH_2$, $–OCH_3$) that may increase the quantum yield. The fluorescence interference is an issue because it can cover the anticipated chemical footprints of the sample. Using a 780 nm laser greatly reduced the fluorescence interference compared to a 532 nm laser. Therefore, a 780 nm laser was used throughout all experiments [37].

Fig. 4.4 shows the result of the altered four where the sample in Fig. 4.4(a and b) was altered using different pens and the sample in Fig. 4.4(c and d) was modified using the same pen. The images in Fig. 4.4(b and d) are overlaying the actual written sample. Human error in making these samples cause variations in the scale. The Raman mapping analysis was conducted at 10× magnification. A magnification at 10× was preferred because the spectral variances due to the paper's irregular topography were minimized and the resulting spot size covered a more representative area of ink [21]. The contour map is represented on a color scale from red to blue, where red represents very high intensities of a chemical species at a wavenumber and blue represents very low intensities of a different chemical species at the same wavenumber. At 283 cm^{-1} (Fig. 4.4(a and b)), high intensities from the compounds in the pilot pen (ink pen 2) are similar

to the compounds found in paper; hence, ink pen 2 blends in with the paper. This is because both the paper and ink pen 2 contain a type of C–C aliphatic chain. Ink pen 1 contains dissimilar components in its ink formula than ink pen 2, creating the image of only the four. Thus, successfully discriminating the two different pens used in forging written ink entries. Raman mapping was not successful in identifying fraudulent ink entries when using the same pen to modify the text (Fig. 4.4(c and d)). There were also peaks at 3610, 1625, 1428, 769, and 721 cm^{-1} (not shown) with Raman images that looked similar to the Raman image at 497 cm^{-1}.

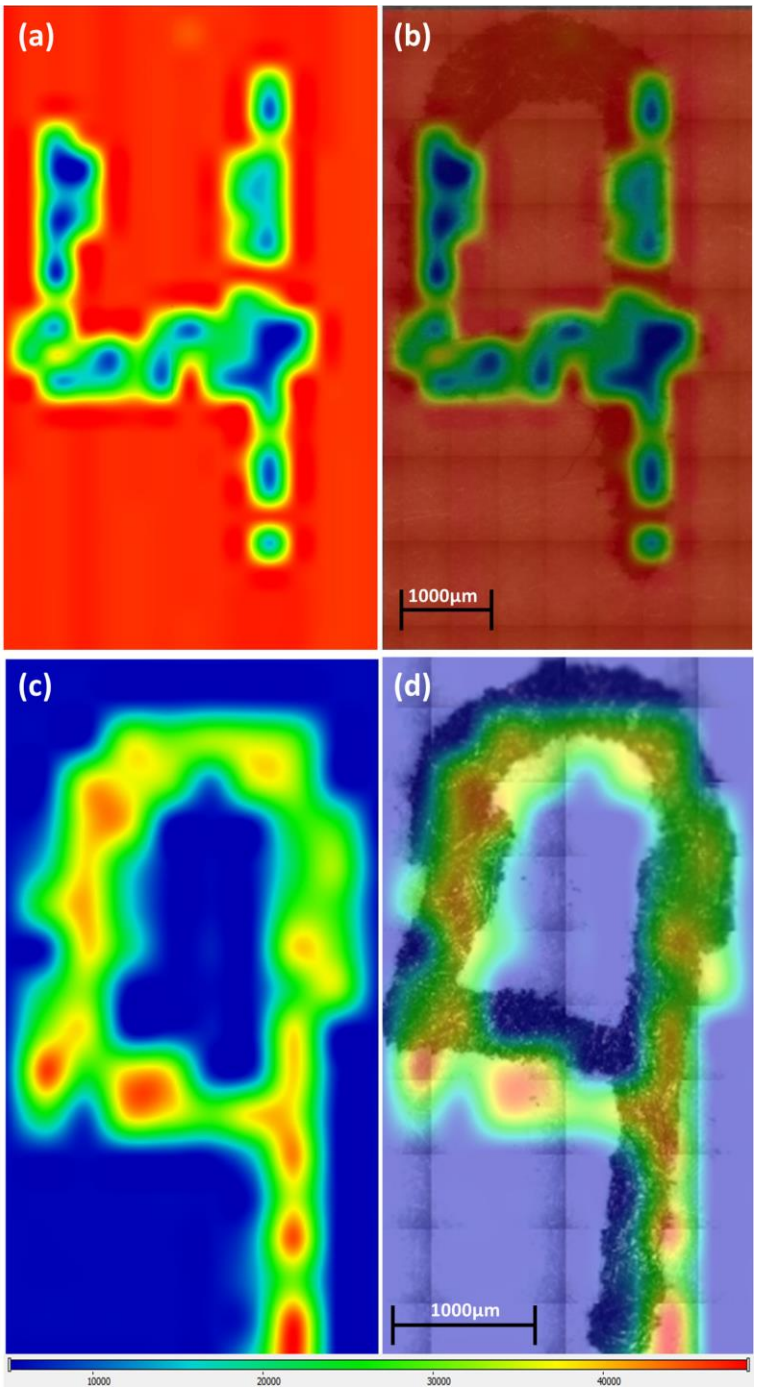

Figure 4.4. Raman mapping of the number four altered into a nine where (a, b) was modified using different pens (displayed at wavenumber 283 cm^{-1}) and (c, d) was modified using the same pen (displayed at wavenumber 497 cm^{-1}). (b) and (d) are the Raman images overlaying the actual sample. The map intensity scale bar ranges from 5,181 to 48,426.

4.4.3 DAPNe-NSI-MS

DAPNe-NSI-MS successfully identified the original ink, ink used to alter the number, and the point at where both inks intersect. In Fig. 4.5, successful extractions indicate that black ink pen 1 (Black BIC pen) contains Crystal Violet and black ink pen 2 (Black Uni-ball pen) contains PEG, a binding agent and stabilizer. Stabilizing polymers prevent dyes or pigment particles from clumping together and give inks a smoother flow [31]. Components from both black ink pens are shown in Fig. 4.5(c), where the extraction was conducted at the intersection of ink pen 1 and 2. Similar results were observed when two different red pens were used. Components from both red pens were successfully extracted at the intersection (Fig. 4.6(c)). Red ink pen 1 (Red Pilot pen) consist of triethanolamine (m/z 150.13 ($[M + H^+]$) and 172.20 ($[M + Na]^+$)) and New Fuschin or also known as Basic Violet 2 (m/z 329.50, $[M - Cl]^+$), where M is the molecular species. Dunn et al. characterized red dyes found in ballpoint pens using laser desorption mass spectrometry, including New Fuschin found at m/z 330 [38]. Ink pens can become too acidic; therefore, triethanolamine is often used to regulate the pH of the ink preventing damage to the pen [39]. Red ink pen 2 (Red BIC pen) contains Rhodamine 6G dye, corresponding to peaks at m/z 443.53 ($[M - Cl]^+$) and 415.46 ($[M - C_2H_5]^+$).

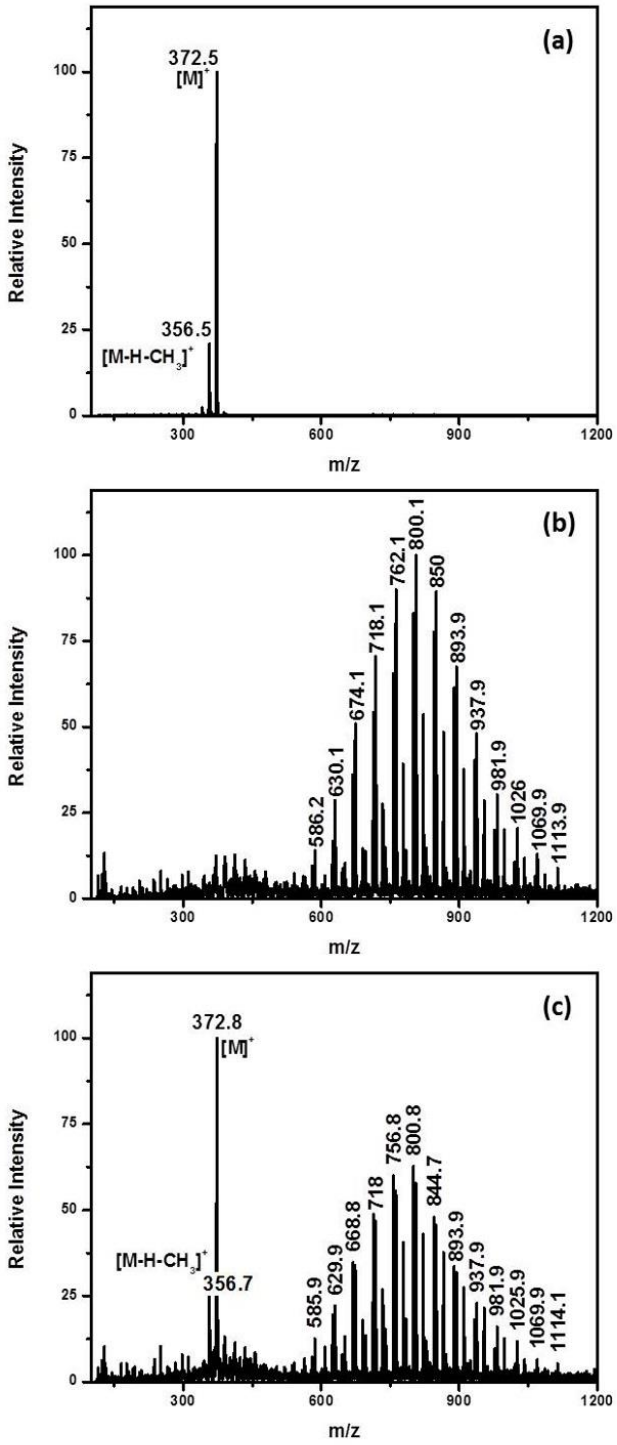

Figure 4.5. Spectra of (a) black ink pen 1, (b) black ink pen 2, and (c) the intersection of black ink pen 1 and 2 using DAPNe-NSI-MS.

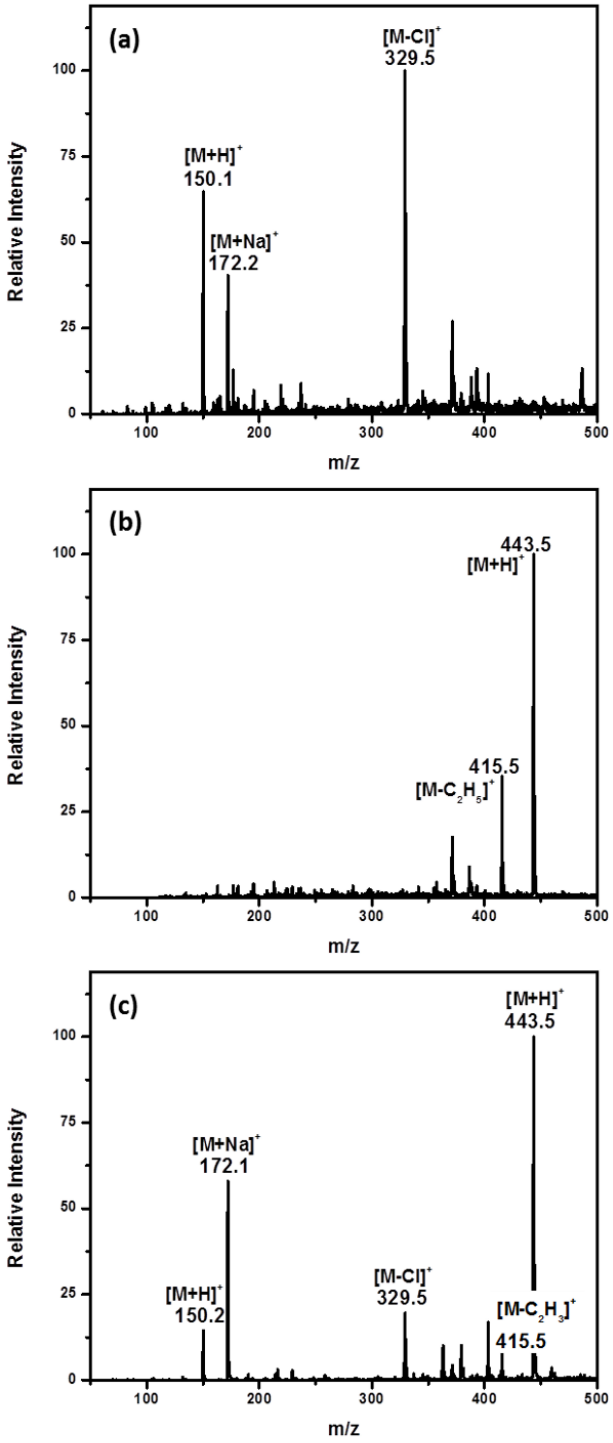

Figure 4.6. Spectra of (a) red ink pen 1, (b) red ink pen 2, and (c) the intersection of red ink pen 1 and 2 using DAPNe-NSI-MS.

4.4.4 Oxidation of altered text

Fig. 4.7 illustrates the distribution change of PEG from the same black pen dispensed on different days. PEG has a melting point of 13 °C and can be severely degraded by air through thermal degradation, inducing a random chain scission oxidation mechanism [40]. In excess air, PEG and oxygen react to form PEG peroxide (random chain scission process), leading to the formation of several low-molecular-weight oxygenated products (e.g., formic esters). Han et al. compared fresh PEG with PEG aged in a vacuum and almost no degradation occurred [41]. It was found that the oxidation reaction caused by air can effectively be suppressed by adding antioxidants. PEG ions have a distinct distribution with a 44 u separation between each signal and can be detected as protonated or sodiated species, $[M + H]^+$ or $[M + Na]^+$ respectively. The 44 u separation is denoted by a repeating monomeric unit, $(–OCH_2CH_2–)_n$ where n represents the number of monomeric ions.

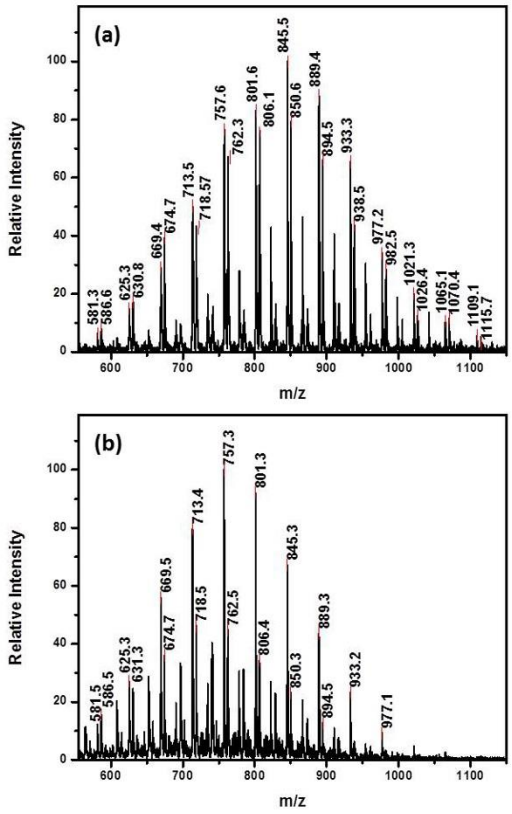

Figure 4.7. Spectra comparison of the modified number where (a) is the ink from the number four (24 hours old ink) (b) is the ink from the nine (fresh ink) using the same black pen. Extractions were conducted using DAPNe-NSI-MS.

The m/z peaks are labeled in pairs, having a 5 u difference from each other. The 5 u difference results from the removal of water (18 u) and a sodium adduct (23 u). The ratio of the m/z peak pairs asymptotically approaches one after four to five days (Fig. 4.7(a)). The more intense peaks of these pairs oxidize into smaller peaks, increasing the intensity of the less intense peaks. For example, m/z 757 and 801 will degrade in to m/z 762 and 806 respectively. Thus, the intensity of m/z 762 and 806 will increase over time. This observation was quantitated by calculating the percent RPA values of the monitored peaks, m/z 757, 762, 801, and 806 shown in Fig. 8.

There is a 3.01 ± 0.14% and 3.33 ± 0.16% difference from day 1 to day 2 for m/z 757 and 762, respectively. For peaks m/z 801 and 806, there is a 0.39 ± 0.04% and 3.41 ± 0.20% change from day one to day two separately. The oxidation process generally has the largest difference after the first day. For m/z 801, the largest difference occurred from day two to three, 2.57 ± 0.17%. The oxidation processes for inks can occur for several reasons: (i) resin polymerization, (ii) dye degradation, and (iii) solvent loss [41, 42]. In this case, PEG is thermally degrading, leading to chain length reduction and lower molecular weight [40, 41, 43]. Upon application, the inks used to modify the number similarly follow the oxidation trend seen in Fig. 4.8 [12].

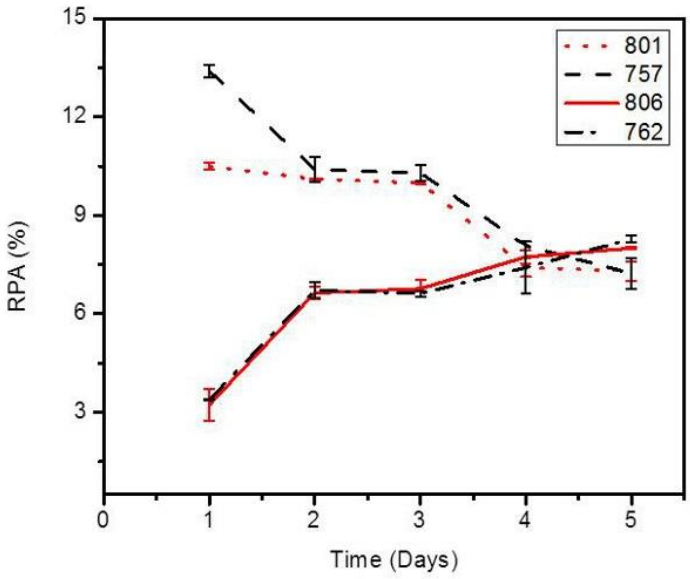

Figure 4.8. The percent RPA of monitored PEG peaks (m/z 757, 762, 801, and 806) from a black pen over a 5 day period (n = 3).

This oxidation process allows the analyst to determine which ink was placed last because it will have a higher RPA value. After examining the modified four, the ink from part of the nine had a higher RPA value. The four has an RPA value of 9.12 ± 0.52% and the nine has an RPA

value of 13.40 ± 0.18% for m/z 757 on day 1, indicating the nine was forged. Calculating the RPA value is not limited to the peaks chosen in this paper; any peaks may be used as long as the RPA_i equation is correctly used. Furthermore, modified text using the same pen can be distinguished because the ink was placed on different days.

4.4.5 Nanospray solvent chemistry

The extraction solvent used to fill the nanospray tip influences which component of the ink is being extracted and the intensities of the molecular ion peaks in a mass spectrum. For example, PEG and Crystal Violet was extracted from Uni-Ball black (waterproof) ink separately. The extraction of Crystal Violet and PEG is achieved when using methanol : chloroform (1 : 1) with 0.1% ammonium acetate and methanol : H_2O (1:1) with 1% acetic acid as the extraction solvent, respectively (Fig. 4.9). In a previous study, EDTA was incorporated into the extraction solvent in order to chelate Fe and Mn ions from iron gall ink [12]. Being able to extract different components from the same ink entry is very important, especially when the same ink pen has been used to forge documents. Once deposited on paper, dyes are more stable than vehicles, taking longer to oxidize than PEG. Upon application to document forgeries, selectively extracting PEG gives analysts the opportunity to track its oxidation process which aids in differentiating if ink from the same kind of pen was placed at different times.

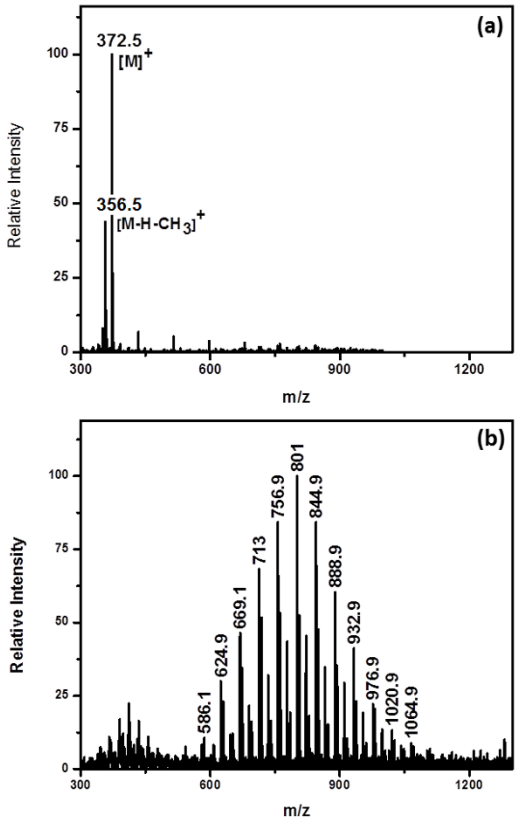

Figure 4.9. Spectra of Uni-ball black (waterproof) pen using two different extraction solvents, (a) methanol : chloroform (1 : 1) with 0.1% ammonium acetate and (b) methanol : H_2O (1 : 1) with 1% acetic acid.

In many cases, the same component from the ink sample is extracted by using different extraction solvents. Although the spectrum looks similar, the intensities of certain peaks will differ. The variation of peak intensities is compared by converting the relative peak intensities into points via a rating scale, as shown in Table 4.1. The peak intensities are first normalized and then assigned points based on the rating scale. The rating scale is based on normalization to 100 but this can relatively be altered. For example, in Fig. 4.7(b) the peak at m/z 801.3 has a relative intensity of 92.1 which converts to 9 points.

Relative peak intensities	Points
<10	0
11-19	1
20-29	2
30-39	3
40-49	4
50-59	5
60-69	6
70-79	7
80-89	8
90-100	9

Table 4.1. A rating scale used to convert relative peak intensities into points.

Three different solvents were used on eleven different pens to illustrate how the intensities are affected by the extraction solvents. Table 4.2 shows the intensities converted into points for each ion obtained from the ink of a blue BIC pen. The Crystal Violet ions were validated by J. Siegel et al. [44] when analyzing a blue BIC pen. The three degradation ions that belong to Crystal Violet in Table 4.2 have resulted from natural aging. The natural aging of Crystal Violet successively losses methyl groups which are then replaced by solvent protons, losing 14 mass units each time [44]. Basic Yellow 2 was also confirmed by J. A. Denman et al. [8] when analyzing a blue BIC pen. After the intensities were converted into points for the ions, they were then totaled together to determine which solvent gave the highest amount of points, indicating which solvent is optimal for that ink. For blue BIC pen, methanol : H_2O (1 : 1) with 1% acetic acid and toluene : methanol (1 : 10) with 0.1% ammonium acetate received a total of 18 and 19 points, respectively, which is 6–7 points higher than extracting with chloroform : methanol (1 : 1), with 0.1% NH_4OH. In this case, two of three solvents would be suitable for blue BIC pen. Table 4.3 lists only the total points for each pen. All three solvents, in Table 4.3, extracted PEG from Uni-Ball black (waterproof) pen, but each solvent enhanced different peaks For example, m/z 800 could equal 9 points and m/z 844 could equal 2 points for methanol : H_2O (1 : 1) with 1% acetic acid. However,

they'd equal 4 points and 9 points, respectively, when using methanol : chloroform (1 : 1) with 0.1% ammonium hydroxide. Depending on which PEG peaks are being monitored, the total points can vary for this ink. Black BIC pen received 11 points for all three solvents, indicating all three solvents are suitable. Red pilot pen received 23 points when using toluene : methanol (1 : 10) with 0.1% ammonium acetate compared to the other two solvents which both totaled to 16 points. Selectivity for the analytes being extracted can easily be controlled by solvent alteration.

			Solvent		
m/z	Ions	Component	Methanol:H_2O (1:1), with 1% CH_3O_2H	Toluene:Methanol (1:10), with 0.1% $NH_4C_2H_3O_2$	Chloroform:Methanol (1:1), with 0.1% NH_4OH
268.3	$[M\text{-}Cl]^+$	Basic Yellow 2	9	9	9
344.0	$[M+2H\text{-}(CH_3)_2]^+$	Crystal Violet	0	1	0
358.4	$[M+H\text{-}CH_3]^+$		3	4	1
372.5	$[M]^+$		6	5	2
		Total	18	19	12

Table 4.2. A comparison of mass spectrometric intensities from a blue BIC pen using three different solvents, based on a rating scale.

Pen Color	Brand	Solvent		
		Methanol:H_2O (1:1), with 1% CH_3O_2H	Toluene:Methanol (1:10), with 0.1% $NH_4C_2H_3O_2$	Chloroform:Methanol (1:1), with 0.1% NH_4OH
Pink	BIC	11	10	11
Blue		18	19	12
Red		12	14	12
Green		12	9	9
Black		11	11	11
Black	Uni-ball	49	61	66
Green		19	21	18
Light Blue		11	16	15
Red	Pilot	16	23	16
Black		25	16	15
Blue		43	9	24

Table 4.3. A comparison of a variety of mass spectrometric intensities from several different pens, using three different solvents, based on a rating scale.

4.5 Conclusions

The nanomanipulator is a versatile tool, especially in the field of forensic document examination. Its ability to couple with other document examination techniques, jobs of document analysts may be made simpler. DAPNe with NSI-MS, fluorescence microscopy, and Raman spectroscopy are advantageous couplings because these techniques do not leave destructive chemical or physical foot prints, keeping the document intact. Fluorescence microscopy and Raman spectroscopy demonstrate direct characterization without sample preparation and initially identify areas of different inks or areas of altered text. Upon extraction by nanomanipulation, mass spectrometry can be employed to detect the presence of a dissimilar ink and prove if alteration occurred. Raman spectroscopy detects chemically-active components of ink, fluorescence microscopy offers detection of emission profiles for colorants and additives, and NSI-MS is able

to characterize different components of ink with a simple solvent preparation. Oxidation can be effectively quantitated using the RPA equation, especially if the overall concentration cannot be controlled, but relative amounts of extracted analytes are consistent within a given extraction solvent. Due to the nondestructive nature of these techniques and their ability to confirm if a text has been modified, the forensic community will be able to further their studies in chemical composition of fraudulent documents.

Acknowledgements

This project is funded by the National Institute of Justice grant no. NIJ-2013-3361.

4.6 References

[1] Y. Wu, C. Zhou, J. Yu, H. Liu and M. Xie, Dyes Pigm., 2012, 94, 525–532.

[2] M. Gallidabino, C. Weyermann and R. Marquis, Forensic Sci. Int., 2011, 204, 169–178.

[3] R. B. Cole, Electrospray Ionization Mass Spectrometry: Fundamentals, Instrumentation, and Applications, Wiley, New York, NY, 1997.

[4] L. D. Maquillè, L. Renaudin, F. Goutelard, A. Jardy, J. Vial and D. Thièbaut, J. Chromatogr., A, 2013, 1276, 20–25.

[5] J. Coumbaros, K. P. Kirkbride, G. Klass and W. Skinner, Forensic Sci. Int., 2009, 193, 42–46.

[6] O. P. Jasuja, A. K. Singla and B. L. Seema, Forensic Sci. Int., 1989, 42, 255–262.

[7] C. Weyermann, L. Bucher, P. Majcherczyk, W. Mazzella, C. Roux and P. Esseiva, Forensic Sci. Int., 2012, 217, 127–133.

[8] J. A. Denman, W. M. Skinner, K. P. Kirkbride and I. M. Kempson, Appl. Surf. Sci., 2010, 256, 2155–2163.

[9] L. Ng, P. Lafontaine and L. Brazeau, J. Forensic Sci., 2002, 47, 1238–1247.

[10] M. R. Williams, C. Moody, L. Arceneaux, C. Rinke, K. White and M. E. Sigman, Forensic Sci. Int., 2009, 191, 97–103.

[11] Y. Liu, J. Yu, M. Xie, Y. Liu, J. Han and T. Jing, J. Chromatogr., A, 2006, 1135, 57–64.

[12] V. Huynh, U. Joshi, J. M. Leveille, T. D. Golden and G. F. Verbeck, Forensic Sci. Int., 2014, 242, 150–156.

[13] N. Wallace, E. Hueske and G. F. Verbeck, Sci. Justice, 2011, 51, 196–203.

[14] J. M. Brown, W. D. Hoffman, C. M. Alvey, A. R. Wood, G. F. Verbeck and R. A. Petros, Anal. Biochem., 2010, 398, 7–14.

[15] P. J. Horn, U. Joshi, A. K. Behrendt, K. D. Chapman and G. F. Verbeck, Rapid Commun. Mass Spectrom., 2012, 26, 957–962.

[16] M. Phelps, J. Hamilton and G. F. Verbeck, Rev. Sci. Instrum., 2014, 85, 1–5.

[17] K. Clemons, J. Dake, E. Sisco and G. F. Verbeck, Forensic Sci. Int., 2013, 232, 98–101.

[18] A. Braz, M. López-López and C. García-Ruiz, Forensic Sci. Int., 2013, 232, 206–212.

[19] A. Braz, M. López-López and C. García-Ruiz, Forensic Sci. Int., 2014, 245, 38–44.

[20] J. Zięba-Palus and M. Kunicki, Forensic Sci. Int., 2006, 158, 164–172.

[21] A. Braz, M. López-López and C. García-Ruiz, Forensic Sci. Int., 2015, 249, 92–100.

[22] W. D. Mazzella and P. Buzzini, Forensic Sci Int., 2005, 152, 241–247.

[23] V. A. G. da Silva, M. Talhavini, I. C. F. Peixoto, J. J. Zacca, A. O. Maldaner and J. W. B. Braga, Microchem. J., 2014, 116, 235–243.

[24] G. Reed, K. Savage, D. Edwards and N. Nic Daeid, Sci. Justice, 2014, 54, 71–80.

[25] Z. Takáts, J. M. Wiseman and R. G. Cooks, J. Mass Spectrom., 2005, 40, 1261–1275.

[26] R. B. Cody, J. A. Laramée and H. D. Durst, Anal. Chem., 2005, 77, 2297–2302.

[27] M. R. L. Paine, P. J. Barker and S. J. Blanksby, Anal. Chim. Acta, 2014, 808, 190–198.

[28] D. Eikel and J. Henion, Rapid Commun. Mass Spectrom., 2011, 25, 2345–2354.

[29] X. Wang, Y. Zhang, Y. Wu, J. Yu and M. Xie, Forensic Sci. 30 C. Weyermann, L. Bucher and P. Majcherczyk, Sci. Justice,2011, 51, 122–130.

[31] M. Ezcurra, J. M. G. Góngora, I. Maguregui and R. Alonso, Forensic Sci. Int., 2010, 197, 1–20.

[32] M. Gallidabino, C. Weyermann and R. Marquis, Forensic Sci. Int., 2011, 204, 169–178.

[33] C. Weyermann, D. Kirsch, C. Costa-Vera and B. Spengler, J. Am. Soc. Mass Spectrom., 2006, 17, 297–306.

[34] A. Raza and B. Saha, Sci. Justice, 2013, 53, 332–338.

[35] J. C. Roberts, Paper Chemistry, Blackie, Glasgow, 2nd edn, 1996.

[36] C. Poole, Instrumental-Thin-Layer Chromatography, Elsevier, Amsterdam, 2015.

[37] C. Claybourn and M. Ansell, Sci. Justice, 2004, 40, 261– 271.

[38] J. D. Dunn, J. A. Siegel and J. Allision, J. Forensic. Sci., 2003, 48, 1–6.

[39] J. K. Fink, Hydraulic Fracturing Chemicals and Fluids Technology, Elsevier, Waltham, 1st edn, 2013.

[40] S. Han, C. Kim and D. Kwon, Polym. Degrad. Stab., 1995, 47, 203–208.

[41] S. Han, C. Kim and D. Kwon, Polym., 1997, 38, 317– 323.

[42] C. Weyermann and B. Spengler, Forensic Sci. Int., 2008, 180, 23–31.

[43] D. Bagal, H. Zhang and P. D. Schnier, Anal. Chem., 2008, 80, 2408–2418.

[44] J. Siegel, J. Allison, D. Mohr and J. Dunn, Talanta, 2005, 67, 425–429.

CHAPTER 5

LASER ABLATION COUPLED WITH DAPNE-NSI-MS APPLIED TO REDACTED DOCUMENTS[6]

5.1 Abstract

Laser ablation has been applied to redacted documents, where the text has been concealed by other ink. This technique strips the redacting ink revealing the text that was once redacted. Once removed, a nanomanipulation technique is used to extract the ink of the underlying text where mass spectrometry is then implemented to analyze its ink chemistry. In order to facilitate microscopy with direct analyte-probed nanoextraction coupled to nanospray ionization mass spectrometry (DAPNe-NSI-MS), laser ablation must be executed prior to ink extraction. Laser ablation has a nondestructive approach of stripping the ink used to redact the document. Not only does this reveal the text, it clears an area for DAPNe to directly extract ink, in miniscule amounts, from the document without inducing destruction. The redacting ink was concluded to affect the aging process of the concealed handwritten ink more than the printed text. The redacted handwritten sample obtained higher relative peak area (%) values than the control samples (text that was not redacted) and the control for the printed text produced higher amounts of low molecular weight products than the sample. Implementing laser ablation on these samples could also affect the chemical properties of the underlying ink due to the additional UV radiation and plasma heating. Results indicate by using laser ablation to remove the redacting ink, the relative peak area of the underlying ink deviates by 1.25%. The thermal degradation of binding agents such

[6]Contents of this chapter have been submitted to Science and Justice, on January 15 2016, with the authors V. Huynh, Z. J. Sasiene, P. M. Mach, T. D. Golden, and G.F. Verbeck. The publisher is Chartered Society of Forensic Sciences by Elsevier Inc.

as polymethylene, polyethylene glycol, and diethylene glycol was monitored by calculating the relative peak area for five days which, in turn, tracks the oxidation process. The relative peak are values were also used to determine the chemical kinetics of polyethylene glycol, where degradation and polymerization occur.

5.2 Introduction

Redacted documents have become a prominent issue when analyzing due to the concealed text. This method is normally done with a marker or pen that deposits ink over the document, which hides the information. The importance of analyzing redacted documents is to expose information that a subject attempted to hide. This could occur within the private sector, such as in the business division both for lawful and unlawful practices. Therefore, it is important to remove the ink used to conceal the written/printed text with the aim of revealing the passage and analyzing the ink underneath.

Ink analysis continues to play a significant role in questioned and authentic documents. The courts prefer nondestructive methods so most forensic approaches focus on nondestructive means of analysis, preventing undue alteration or introducing any aberrations. The most common nondestructive methods make use of visual microscopy [1] and video spectral comparisons (VSC) [1]. However, these methods can be defeated by the redaction process (i.e., specifically black-on-black or ink obliterations). With the help of a laser ablation (LA) method, visual microscopy and VSC can be used once the redacting ink is removed. The LA process is a nondestructive method which preserves the original text while providing a method to uncover the text that was once redacted. Other visual and chemical analyses can be performed due to the preservation of the remaining chemistry on the text [2]. Currently, research continues to investigate analysis of ink in combination with other nondestructive methods [2].

The use of diverse instruments to examine inks has been successful in identifying markers and unique characteristics of inks. Many manufacturers also include dopants into ink which make them easily identifiable; unfortunately these are proprietary to the company and are not made known to the public. Various methods utilizing separations and mass spectrometric techniques have yielded great results in analyzing different components of inks, dyes, and pigments [3–6]. Employing mass spectrometric procedures instead of chromatographic methods reduces sample preparation, time, and solvent needs. Separation techniques such as gas chromatography (GC) [7–9], high performance liquid chromatography (HPLC) [10–12], thin-layer chromatography (TLC) [13], and capillary electrophoresis [14] require destruction to the document when analyzing the ink. This includes removing a small portion of the document via cutting strips [12, 15, 16], micropunching holes [17], or extracting ink coated fibers [6] and then soaking those pieces into a solvent in order to remove the ink. These preconcentration techniques require longer sample preparation and analysis time. Mass spectrometric techniques such as matrix-assisted laser desorption ionization (MALDI) [18, 19, 20], secondary ion mass spectrometry (SIMS) [21], direct analysis in real time mass spectrometry (DART-MS) [22, 23, 24], desorption electrospray ionization (DESI) [25, 26], and liquid extraction surface analysis (LESA) [27], laser ablation inductively coupled mass spectrometry (LA-ICP-MS) [28, 29, 30], SEM-EDS [31], and LIBS [15, 29, 30, 32, 33, 34] are all direct analysis techniques with minimal to no sample preparation needed, saving time. One main issue arises when using these techniques, full document analysis without destruction cannot be achieved. MALDI, SIMS, LA-ICP-MS, and SEM-EDS can analyze documents without added destruction, but are confined to the limited size of the sample holder which eliminates full document analysis. DART-MS, DESI, and LIBS can directly analyze full documents but require a large amount of surface area for analyte ionization, making these

techniques more destructive. Analyzing at trace levels is difficult for LIBS to achieve [29]. LESA has an enclosed workstation, constricting full document investigation, and utilizes a pipette tip with a diameter of 800 μm for sample extraction. This size pipette tip creates a wetted area of 1-3 mm which aids unnecessary harm to the document [35]. An assortment of methods so far has been used to distinguish between legal and counterfeit currency, but researching on a technique that preserves the integrity of the articles while conducting analyses is much needed.

Microscopy with direct analyte-probed nanoextraction coupled to nanospray ionization mass spectrometry (DAPNe-NSI-MS) is a direct extraction technique for analyzing ultra-trace amounts of material (as low as 300 attograms). This is made possible by equipping a nanomanipulator to the stage of a high-powered microscope. The nanomanipulator contains a piezoelectric-controlled nanopositioner with a removable nanospray tip (i.d of 1 μm) to aspirate/extract via pressure injector shown in Figure 5.1. DAPNe-NSI-MS has been used for the extraction of trace cocaine particles directly from a single rayon fiber [36], ultra-trace residues retrieved from electrostatic lifting process [37], the cleavage and extraction of peptides from resin beads [38], analyzing trace analysis of energetic materials [39], and the extraction of lipid contents directly from organelle preparations of plant tissues [40]. Recently, the DAPNe technique has proven its, direct extraction, analytical scheme for document and ink analysis by extracting ancient and modern inks from documents [41] and proving a document was falsified by identifying ink forgery [42]. DAPNe was coupled to fluorescence microscopy and Raman spectroscopy to identify where the forgery occurred within the text. The direct extraction scheme is conducted by placing a 2 μL solvent droplet onto the ink of interest, minimizing the surface area wetted to 5 μm or less post-extraction. The pre-filled nanospray tip is then positioned into the droplet, propelling a miniscule amount of solvent, inducing liquid phase microextraction. After the ink components

diffuse into the droplet (15-20 s), it is then extracted into the tip for mass spectrometric analysis without further modification. By coupling NSI-MS with DAPNe, the resolution is increased and picomolar sensitivity is achieved. Coupling other techniques with DAPNe-NSI-MS opens the window for many opportunities beneficial for the scientific community. In this study, DAPNe-NSI-MS is coupled with laser ablation to analyze redacted documents.

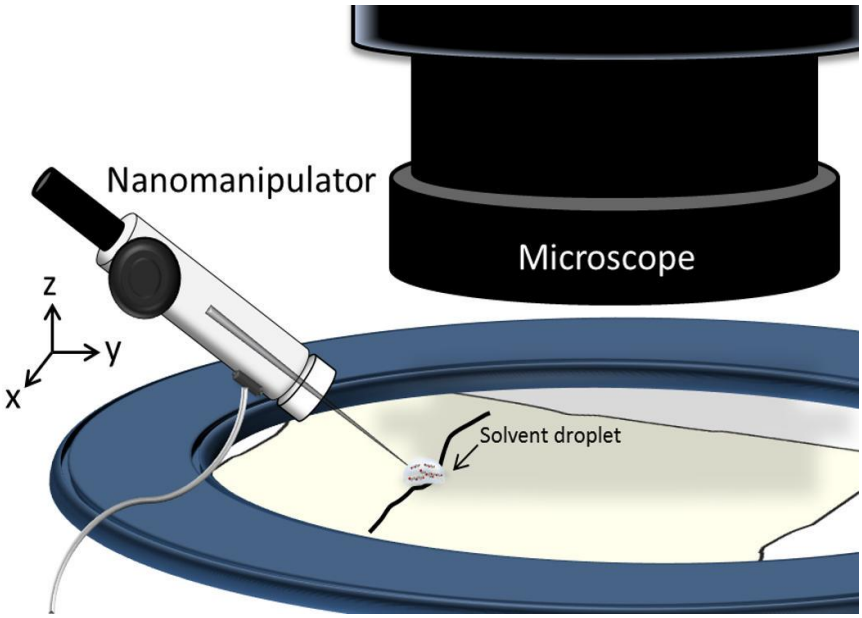

Figure 5.1. Schematic of the nanomanipulator extracting ink from a document, movable in xyz-planes.

Laser ablation is a technique that requires an infinitesimal or miniscule amount of sample preparation and is easy to learn and perform. Laser ablation has the ability to thwart attempts at redacting a document. This process is nondestructive and has fine control so that the settings can be changed for different media and inks. The application of laser ablation would be to strip the ink used to redact the document from the handwritten/typed text. This is possible due to the effects of multi-pass laser ablation over large areas and single lines of multiple layered inks which have been printed or written on paper. Steward et al. [43] multi-layered colored inks on white wood pulp

paper to generate a full colored image with a tactile quality (creating features for anti-counterfeiting color copying). LA was used to effectively remove selective layers subsequently, revealing the different colored inks. The same technique was also efficiently applied when layering ink samples consisting of white/cyan/white/black layers [44]. LA is simple, rapid, with good precision, and almost harmless to the sample and is very suitable for the demand of pen analysis in forensic chemistry. Ma et al. [45] laser ablated 95 different blue ballpoint pens and almost no damage was done to the sample. The laser power and parameters were adjusted to remove just enough ink for metal analysis with no visible destruction. LA is a necessity when analyzing disguised or covered-up inks, exposing a small area for ink extractions. Furthermore, it is questionable whether the ink used to redact the text suppresses the oxidation of the handwritten/printed ink underneath. By tracking the oxidation process, this question can be elucidated. This paper will demonstrate that the laser ablation process is successful for inkjet printed and handwritten documents; in combination with the proven techniques of nanomanipulation extraction for further analysis. With this, the oxidation process of the handwritten/typed text concealed can be determined.

5.3 Materials and methods

5.3.1 Reagents and solvent preparation

All solutions were made with Millipore water, obtained from Aqua Solutions Inc. (Deer Park, TX) having 18 MΩ resistivity. The glacial acetic acid was purchased from Mallinckrodt Baker Inc. (Phillipsburg, NJ). Optima LC/MS methanol, acetonitrile, toluene, chloroform, ammonium hydroxide, and analytical grade ammonium acetate were acquired from Fischer Scientific (Fair Lawn, NJ). A deskjet ink cartridge (HP 60 Black Noir) and laserjet cartridge (HP 43X black toner) was obtained from Hewlett-Packard Company (Palo Alto, CA). Uni-Ball black

ballpoint pen, a black Sharpie permanent marker, BIC pens, Pilot pens, Expo markers, and Casemate permanent marker were commercially purchased.

Several solvents were used to optimize the extraction of inks, including chloroform, acetonitrile, methanol, and toluene. Acetonitrile and methanol were optimal for ballpoint pen ink extraction and acetonitrile was optimal for deskjet printed ink extraction. It is important to note that none of the listed solvents were able to extract any compounds from laser printed paper (data not shown). This may be because the laser printer uses toner-based cartridges instead of ink-based cartridges.

The extraction solvent for the ballpoint pen ink consisted of methanol:water (1:1, v/v) with 1% acetic acid and acetonitrile:water (1:1, v/v) with 0.1% ammonium acetate, separately. The inkjet printer ink extraction solvent used was made up of acetonitrile:water with 0.1% ammonium acetate. These solvents were used in conjunction with Millipore water (the solvent droplet) during the liquid phase microextraction.

5.3.2 Instrumentation

A L200 nanomanipulator (Zyvex; Richardson, TX), fixed onto the stage of a Nikon AZ 100 microscope (Nikon Instruments Inc.; Melville, NY), is controlled by maneuvering the removable nanospray tip via joystick controller (fine spatial resolution up to 5 nm). A PE2000b four channel pressure injector (MicroData Instruments Inc.; S. Plainfield, NJ) controls the aspiration/extraction of the nanospray tip. All mass spectrometric analyses were conducted on a LCQ DECA XP Plus equipped with a nanospray ionization source (Proxeon Biosystems; Odense, Denmark). After the sample extraction is complete, the nanospray tip is removed from the nanomanipulator and transferred directly to the

nanospray ionization source with no further alteration. The nanomanipulator has been previously detailed [40–42,44,46,47] and the direct analytical scheme used for the extraction of ink from documents is described thoroughly by Huynh et al. [41,42].

A UP-213 laser ablation instrument (New Wave; Freemont, CA) with a 213 nm Nd:YAG laser source was used to perform the ablation of the redacted handwritten and printed documents. The samples were written/printed on generic multipurpose computer paper. Five samples of each (handwritten and printed text) were created and redacted with a Sharpie permanent marker at the same time, labeled day 0 to day 4. Figure 5.2 shows examples of the different samples that were redacted post laser ablation. Figure 5.2a shows an example of a sample that was poorly laser ablated. Figure 5.2(b-h) are variations of different redacted inks laser ablated with optimized settings. A redacted sample and a control sample were examined. The control sample was not redacted. The prepared sample text was marked over until the paper was highly saturated with the redacting marker ink. Day 0 redacted sample was then placed into the ablation chamber with 50 mL/min of argon gas to provide an inert and dry environment, and additionally clearing away any ablated material. Methods were developed for various materials with minor differences exhibited between sample types, Table 5.1. Figure 5.2(d) and (h) used different markers to redact the underlying text, using 85% laser power instead of 60% with one pass. The ablation process was repeated every 24 hours for 5 consecutive days.

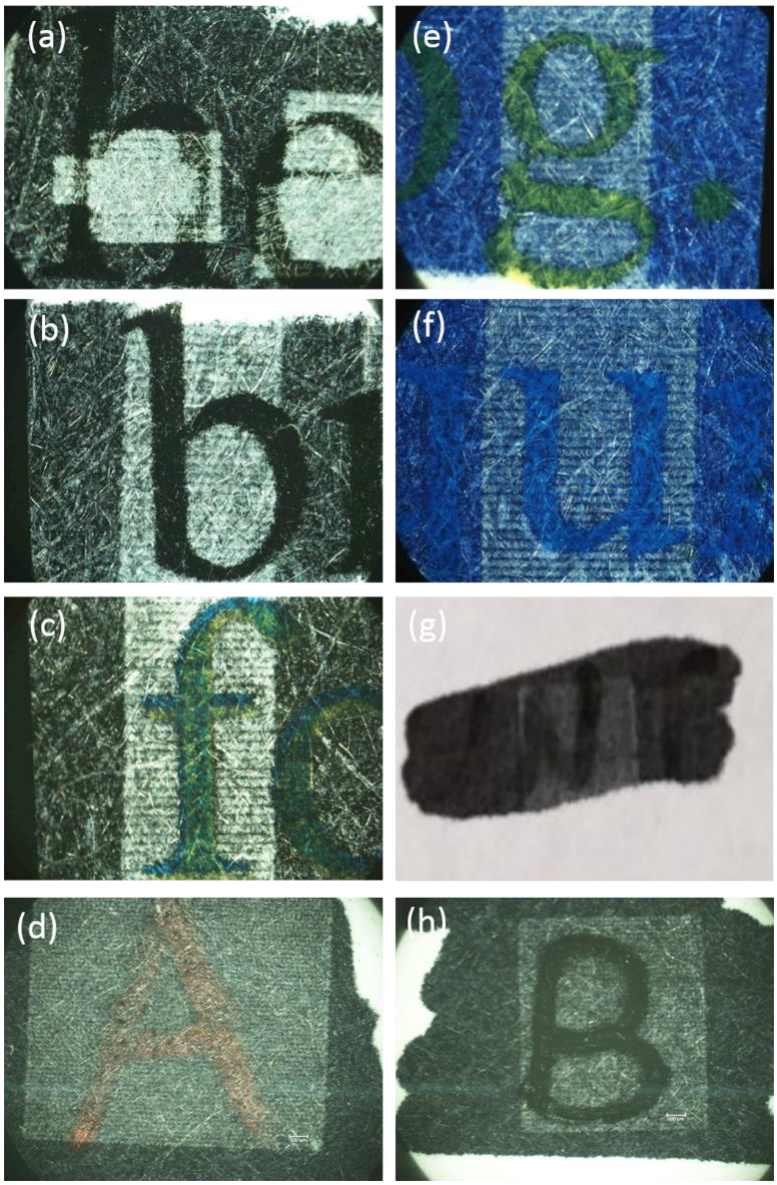

Figure 5.2. An illustration of redacted ink, post-laser ablation where (a) shows what the sample would look like with poor LA settings of black printed text redacted with a black Sharpie, (b) is black printed text redacted with black Sharpie, (c) is green printed text redacted with black Sharpie, (d) is handwritten red (BIC) ink redacted with permanent marker (Casemate), (e) is yellow printed text redacted with blue Sharpie, (f) is blue printed text with blue Sharpie, (g) is handwritten black ink (Uni-ball) redacted with black Sharpie, and (h) is handwritten black (Pilot) ink redacted with black marker (Expo).

Parameters	Handwritten Text	Printed Text
Raster Spacing	100 µm	100 µm
Raster Speed	100 µm/s	100 µm/s
Spot Size	100 µm	100 µm
Output	60%	60%
Repetition Rate	1 Hz	4 Hz
Argon Flow Rate	50 mL/min	50 mL/min
Number of Passes	2	1

Table 5.1. Laser setting differences between handwritten and printed texts for redacted documents.

5.3.3 Direct extraction analytical scheme

The nanospray tip is filled with the desired extraction solvent prior to insertion into the nanopositioner. A 2 µL droplet of Millipore water is dispensed onto the ink. The nanospray tip is then positioned into the solvent droplet and aspirated with a miniscule amount of extraction solvent using an injection pressure of 15 psi and allowed to sit for 15-20 s, letting the ink diffuse into the droplet. It is important to note that propelling the extraction solvent into the water droplet encourages liquid phase microextraction, allowing the components of ink to dissolve into the droplet. The droplet is finally extracted from the page with a fill pressure of 35 psi. The analyte contained in the nanospray tip is directly analyzed through NSI-MS without further modification.

5.3.4 Oxidation of redacted inks

The inkjet printed text, laser printed text, and handwritten ink was redacted as soon as the ink was dried (30 min—1 h). Five replicates of each sample were made, kept in a case, and stored in a desk drawer throughout the experiments. Each sample was laser ablated and then the ink was extracted for spectrometric analysis for five consecutive days. The first sample was completed directly after it was redacted, known as day 0. Oxidation was then quantified by calculating the percent relative peak area (RPA) with three repetitions. Mass spectra were scanned from a range of *m/z* 50-1500 in positive mode at 2.5 kV.

5.3.5 Oxidation effects of laser ablation on inks

The effect of laser ablation on written ink, that has not been redacted, has been investigated. The ultraviolet (UV) radiation and plasma heating of the laser could potentially oxidize the hidden text underneath further while removing the Sharpie layer. A Uni-ball black pen was used to draw several lines. Each line of ink was laser ablated at different laser powers ranging from 0 to 100% at 1 Hz. Once the ink line was laser ablated at a set power, DAPNe-NSI-MS was used to extract the ink and monitor the oxidation of PEG peaks by calculating the RPA.

5.4. Results and discussion

5.4.1 Oxidation of Polyethylene glycol

Ballpoint pens with oil-based inks were first introduced in the 1940s, presenting a new kind of writing apparatus and ink. Before this time, water-based inks were used with fountain and dip pens [47]. Polyethylene glycol (PEG)-based inks began replacing the oil-based ink formulas in 1952. Advancing through history, many different pen apparatuses and ink formulas were

introduced; but PEG has managed to remain constant in many ink formulations today. The polar nature of PEG has allowed a wider range of dyes to be used and were found to adhere firmly to cellulose fibers where inks can neither be smudged nor transferred [48]. It also helps pigments to stay dispersed in solution. The molecular structure of PEG contains a repeating oxyethylene unit ($-C_2H_4O-$), making the oligomer distribution spaced 44 u apart [49]. The structural formula of PEG is $H(C_2H_4O)_nOH$, where n represents the number of repeating units. For mass spectral analysis, PEG ions are observed to have proton, sodium, or potassium adducts, $[HO(C_2H_4O)_nH + H]^+$, $[HO(C_2H_4O)_nH + Na]^+$, or $[HO(C_2H_4O)_nH + K]^+$, respectively [7].

Unfortunately, PEG is susceptible to radical oxidative attack. This leads to the thermal degradation of PEG producing low molecular weight products. As thermal degradation continues, the amount of low molecular weight products increase [50]. L. Boughen et al. [51] determined that after a few years of PEG in a capped bottle, the degraded PEG had a strong aldehyde/ketone odor and it had become a paste (like toothpaste). J. Glastrup et al. [52] heated PEG 4000 for 2-4 h which has in some cases led to the formation of a liquid that would not solidify after cooling. They have shown that this liquid more resembled PEG 600 than the original PEG 4000. For those valuable reasons, the relative peak area (RPA) equation may be implemented to track the oxidative process of polyethylene glycol, and is defined as:

$$RPA_i = \frac{A_i}{A_{tot}} \, x \, 100\% \tag{5.1}$$

where A_i is the area of peaks of interest at m/z=i and A_{tot} is the summation of all the significant signals above a certain intensity threshold [8,15,41,42,53]. The overall concentration cannot be controlled, but relative amounts of extracted analytes are consistent within a given extraction solvent.

5.4.2 Oxidation of printer inks

Shown in Figure 5.3, three polymeric distributions have been extracted from a deskjet printed text simultaneously. The low molecular weight distribution, including peaks *m/z* 415.9, 430.5, 445.2, 460.1, 474.6, 489.3, 504.4, 518.8, and 533.3, are derived from a polymer known as polymethylene. Each of those peaks are spaced 14 u with the structural formula of $(\text{-}CH_2\text{-})_n$ [54]. The high molecular weight distribution, including peaks *m/z* 526.5, 548.6, 570.5, 592.5, 614.5, 636.5, 658.4, 680.4, 702.4, 724.4, 746.4, and 768.5, are separated by 22 u between each peak and 44 u between every other peak. This contains two homologous PEG distributions within itself.

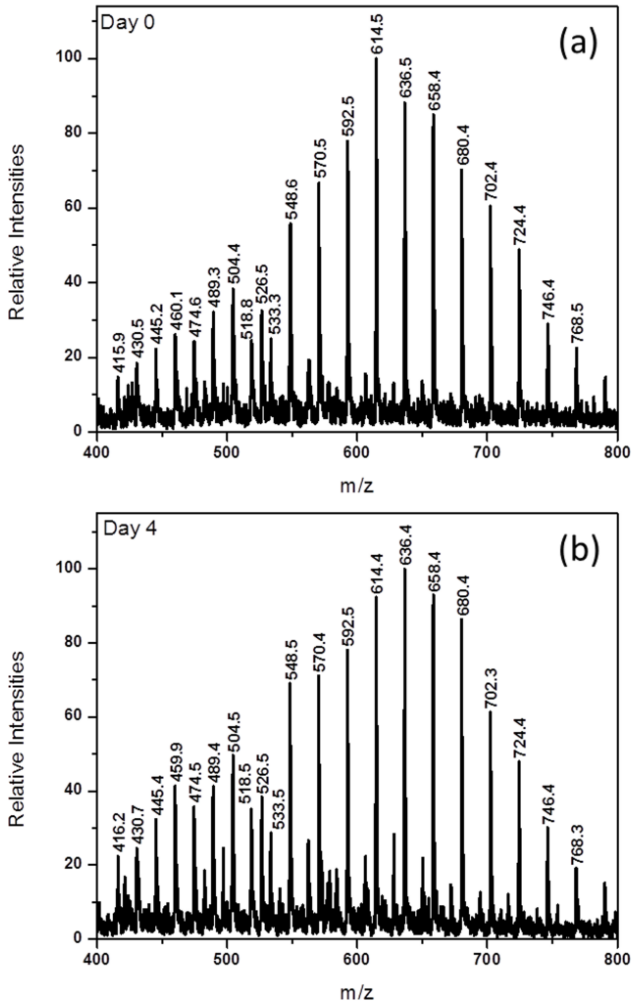

Figure 5.3. The spectrum obtained when extracting printer ink with acetonitrile:H_2O (1:1) with 0.1% ammonium acetate where (a) was characterized on day 0 and (b) was characterized on day 4.

The oxidation trend, after five days, correlates with the degradation studies of PEG [50–52]. As thermal degradation progresses after each day, the amount of low molecular weight products increase, causing the melting point and heat of fusion to be lowered [50]. A shift in peak intensities is observed after five days (day 0 to day 4), shown in Figure 5.3. For example, peak *m/z* 614.5 is no longer the most abundant peak; over time, peak *m/z* 636.4 becomes the most abundant

peak. The oxidation progress of peaks *m/z* 460, 489, 636, and 658 was quantitated by calculating the RPA (%) values shown in Figure 5.4. It is imperative to acknowledge any peak may be observed and that there is no significance in the specific peaks that were chosen. The general trend for the larger peaks, *m/z* 614 and 636, progressively decreases. The high molecular weight peaks are thermally degrading, increasing the intensities of the low molecular weight peaks. This is proven by the increase in RPA (%) when monitoring the following low molecular weight peaks, *m/z* 460 and 489, and the decrease in high molecular weight peaks, *m/z* 614 and 636. The controls in Figure 5.4(a, b) begin at higher RPA (%) values than the samples. This is because the controls for the high molecular weight peaks are oxidizing at a faster rate than the once redacted samples. The faster oxidation rate produces more low molecular weight products. This difference may be due to the masking effect of the Sharpie permanent marker.

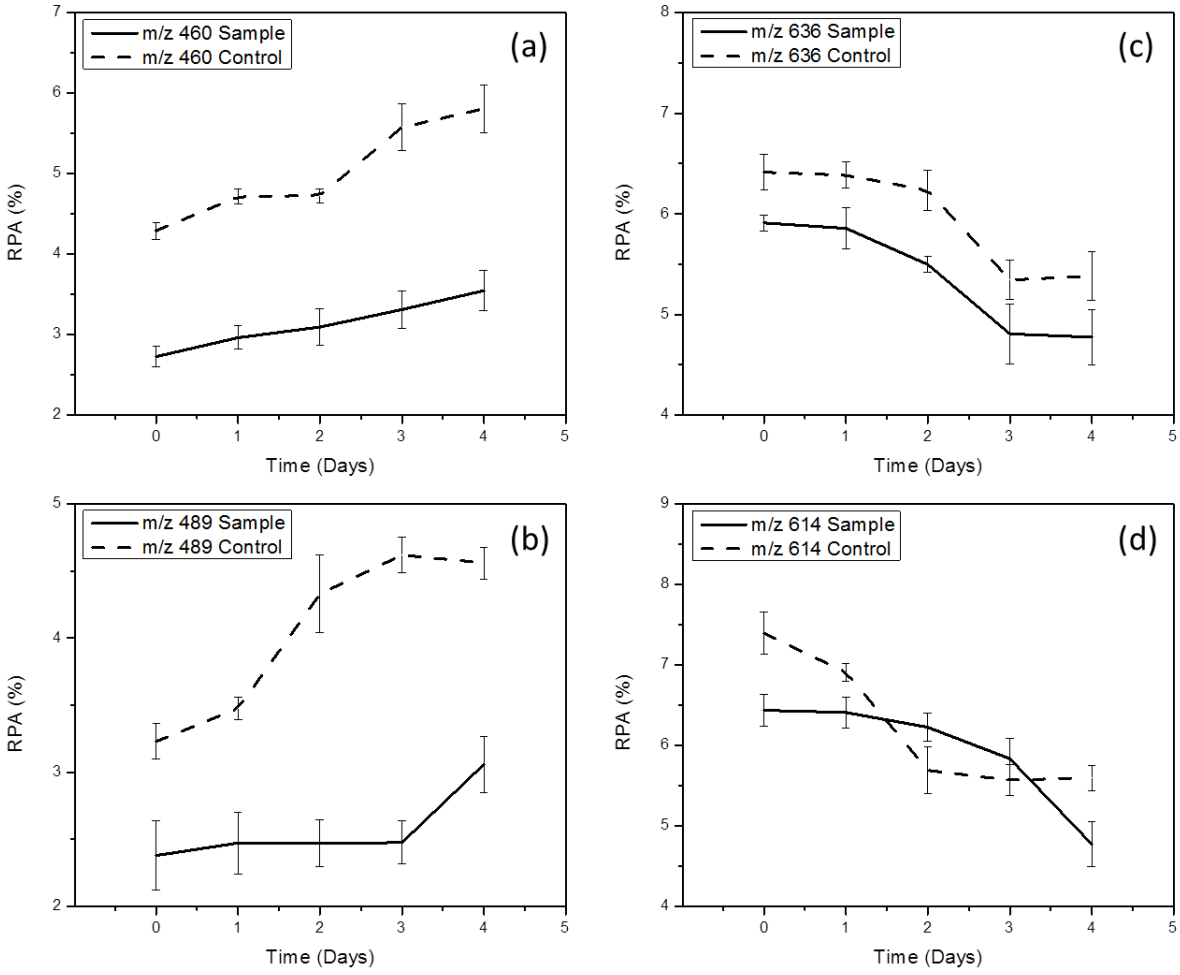

Figure 5.4. RPA (%) curves depicting the oxidation of deskjet printer ink over five days.

5.4.3 Oxidation of ballpoint pen

The DAPNe technique can facilitate the chemical variations of ink by changing the extraction solvent. Figure 5.5 illustrates the different spectra obtained when extracting with two different solvents. The extraction solvent used in Figure 5.5(a, b) was methanol:H_2O (1: 1) with 1% acetic acid, where polyethylene glycol was the main component removed. Two distributions were observed. The outer distribution, including peaks *m/z* 585.9, 629.9, 673.9, 717.9, 761.9, 805.7, 849.7, 893.7, 937.7, 981.6, 1025.6, and 1069.7, are PEG ions with sodium adducts

($[M+Na]^+$, where M represents the molecular species). The inner distribution, including peaks *m/z* 601.7, 645.7, 689.7, 733.7, 777.7, 821.6, 865.5, 909.5, 953.5, 997.5, 1041.4, and 1084.4, are PEG ions with potassium adducts ($[M+K]^+$). The difference between the adjacent peaks are 16 u (e.g., *m/z* 805.7 and 821.6), which correlates with the difference between sodium and potassium mass units. A. Anne et al. [55] observed the same phenomenon when analyzing modified PEG using a MALDI-TOF spectrometer where the potassium adducts were part of the inner distribution and the sodium adducts were part of the outer distribution. The spectra shown in Figure 5.5(c, d) was obtained by extracting the Uni-ball black pen using acetonitrile:H_2O (1:1) with 0.1% ammonium acetate. Three different polymer distributions were obtained as well as diethylene glycol (DEG). DEG is a moist-keeping agent and also a volatile vehicle component that is anticipated to carry the dye or pigment onto the writing surface, increasing the bond strength between the ink and writing surface [2]. The peak at *m/z* 124 represents DEG with an ammonium ion adduct, $[DEG+NH_4]^+$. The same peak was observed when J. Ding et al. [56] analyzed diethylene glycol in toothpaste products using neutral desorption reactive extractive electrospray ionization tandem mass spectrometry. The affinity of the cation adduct was studied, concluding that the DEG molecules have a higher affinity towards forming a complex with an ammonium cation than with a sodium cation. For this reason, $[DEG+Na]^+$ complex does not form a significant amount when extracting the Uni-ball pen with methanol:H_2O (1: 1) with 1% acetic acid. The peaks in the first polymeric distribution are spaced 22 u apart, including peaks at *m/z* 341.6, 365.4, 387.5, 409.5, 431.5, 453.5, 475.4, 497.5, and 519.5. Once again, this is due to two homologous PEG distributions, where every other peak is separated by 44 u. The two remaining distributions, overlapping, are PEG. These peaks are separated by 44 u and the adjacent peaks have a difference of 16 u, concluding PEG complexes with sodium and potassium adducts are present [7].

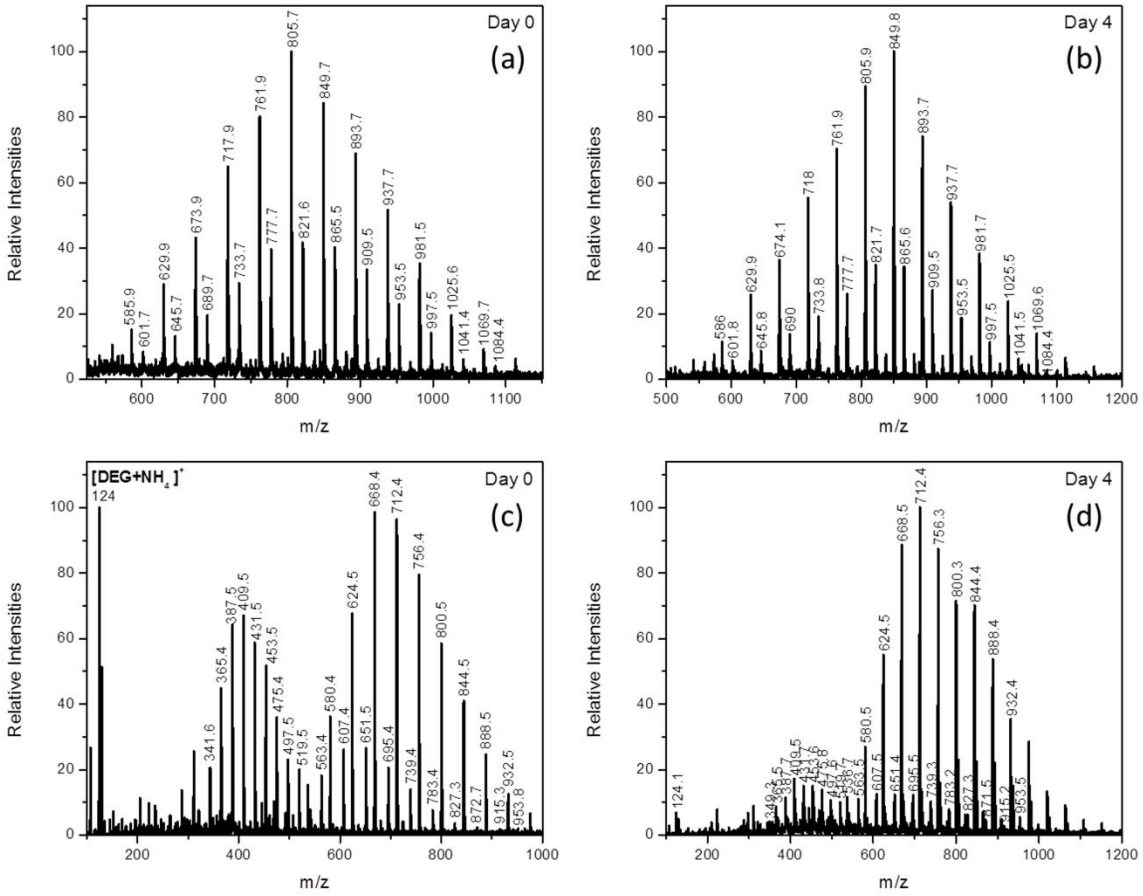

Figure 5.5. The spectra of Uni-ball black pen where (a, b) were extracted with methanol:H_2O with 1% acetic acid on day 0 and day 4 and (c, d) were extracted with acetonitrile:H_2O with 0.1% ammonium acetate on day 0 and day 4 using DAPNe-NSI-MS.

Oxidation can be observed through the peak shifts just after five days and by the obvious change in ratios between the DEG complex and the polymeric distributions (Figure 5.5(c, d)). DEG is a volatile organic component where a majority of its disappearance occur as soon as the ink is deposited on the writing surface. The RPA (%) curves shown in Figure 5.6, shows that redacting the text was effective. The control starts at a lower RPA (%) value because most of the DEG had already volatized compared to the sample. There is a 4.47±0.01% difference between the control

and sample on day 0. The time it took to write the text to the time it took to implement the first extraction, 1-2 hours, most of the volatiles had already disappeared. Redacting the text caused the sample to have a higher RPA (%) value compared to the control. The volatiles in the masked ink were temporarily suppressed, especially between day 0 and day 1. All the RPA (%) curves in Figure 5.7 are decreasing. The sample RPA (%) curves begin at a higher value, signifying that the redaction process was also effective. The RPA (%) curves for peaks *m/z* 387, 409, 668, and 712 are all thermally degrading, explaining the decreasing trend seen in Figure 5.8. Redacting the document has also shown to be effective due to the sample peaks having higher RPA (%) values.

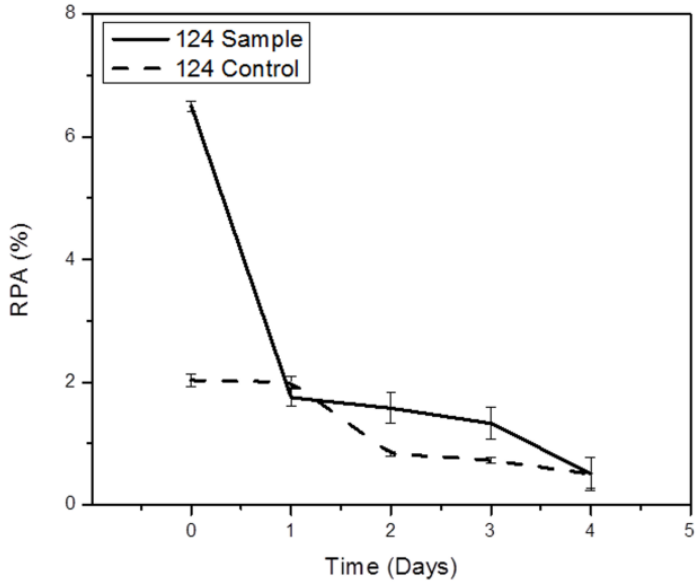

Figure 5.6. RPA (%) curve depicting the oxidation of DEG within Uni-ball black pen over five days when extracting with acetonitrile:H_2O with 0.1% ammonium acetate.

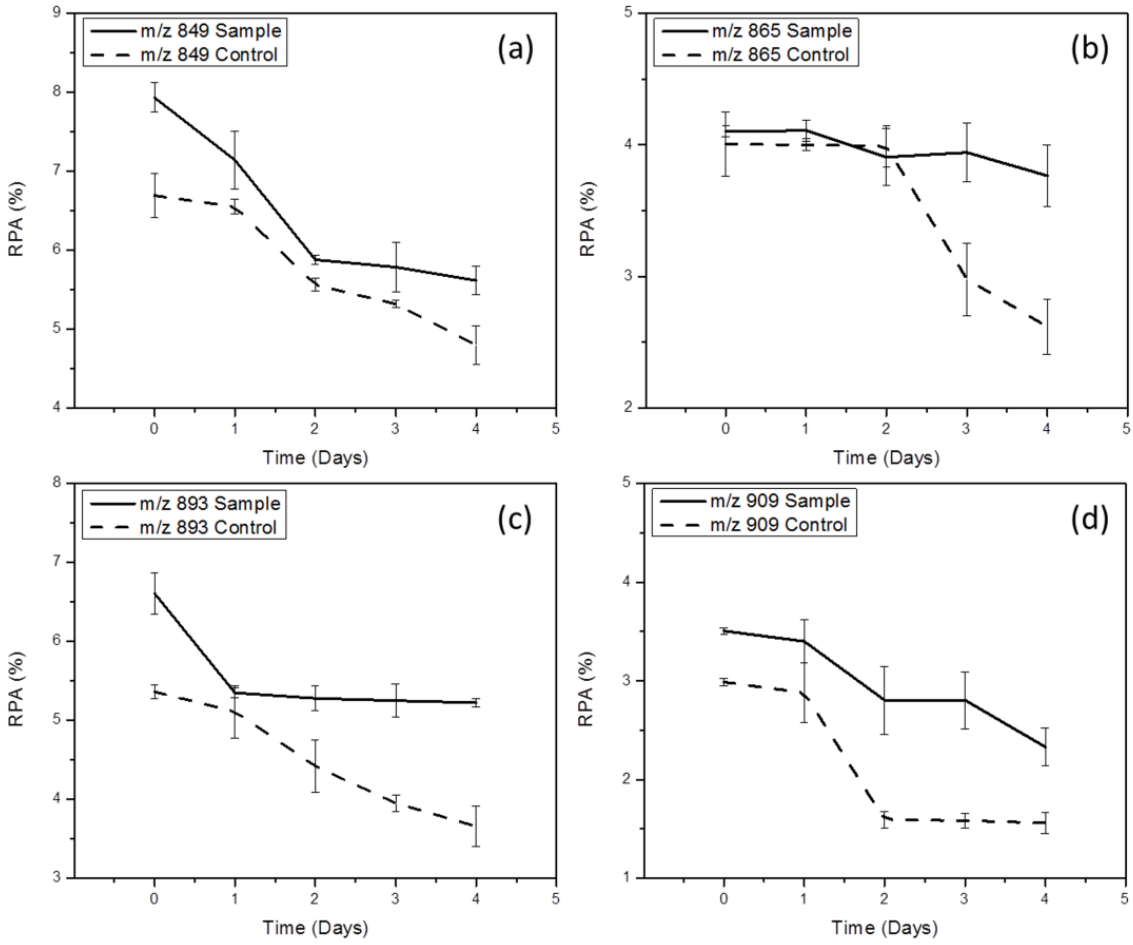

Figure 5.7. RPA (%) curves depicting the oxidation of Uni-ball black pen over five days when extracting with methanol:H_2O with 1% acetic acid.

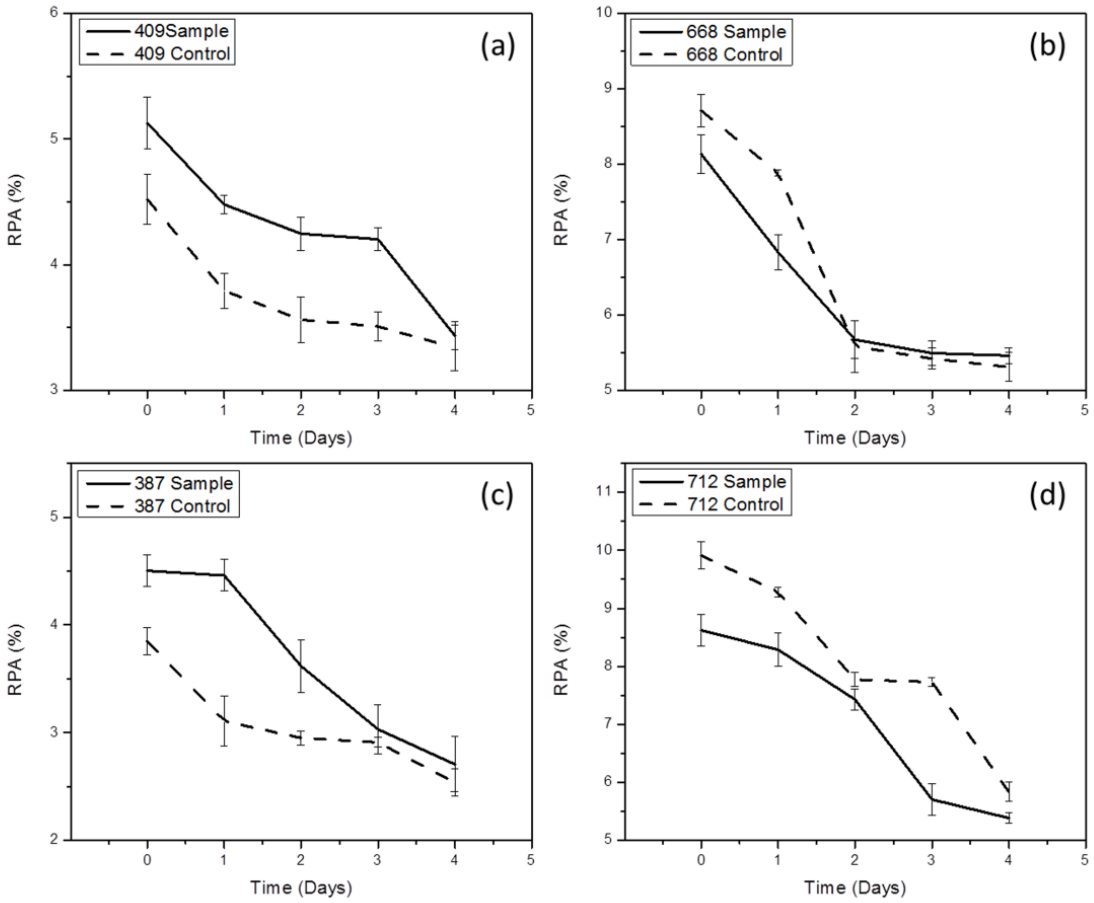

Figure 5.8. RPA (%) curves depicting the oxidation of Uni-ball black pen over five days when extracting with acetonitrile:H_2O with 0.1% ammonium acetate.

5.4.4 Kinetics

For inks, the environment has a huge impact on how the ink in the pens oxidize. By calculating the kinetics at which these reactions occur, we can determine the reaction rates and overall order with respect to the changing environment (i.e., heating with an incandescent bulb and redacting the text). The different chemistry that occurs during the oxidation of inks leads to some components degrading into products while some of those products simultaneously polymerize to form larger products.

The low molecular weight products during oxidation include formaldehyde, acetaldehyde, formic acid, acetic acid, diethylene glycol, triethylene glycol, tetraethylene glycol, and ethylene glycols. The major products formed are formic acid and ethylene glycol. Due to radical oxidative attack, glycol oxides are also formed. These products also polymerize into PEG chains [57].

$$[PEG]_n + O_2 \rightarrow \text{low molecular weight products [aldehydes + organic acids]}$$

Moreover, ethylene oxide can polymerize with glycol derivatives, via radical and ionic mechanisms, and form PEG. This produces smaller chains from the initial PEG structure shown in Figure 5.9.

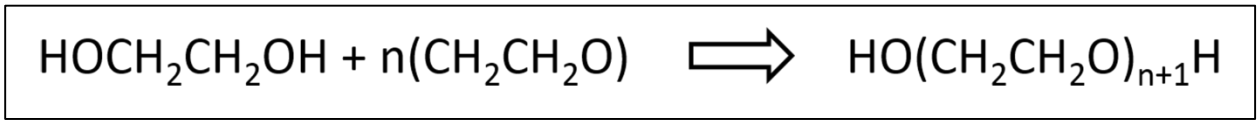

Figure 5.9. Polymerization of ethylene oxide with ethylene glycol forming PEG.

PEG is produced by the interaction of ethylene oxide with water, ethylene glycol, or ethylene glycol oligomers. The condensation of PEG is not limited to the interaction of ethylene oxide, but to other glycol oxides as well. The reaction rate of the degradation and formation of PEG can be determined through kinetics as well as the reaction order. For simplicity variables are used, as follows:

Degradation: $[A]^a + [B]^b \underset{k_2}{\overset{k_1}{\rightleftarrows}} [C]^c$

Formation: $[C]^c \xrightarrow{k_3} [D]^d$

A represents PEG, B represents excess oxygen, C signifies one of the low molecular weight products formed which are glycol oxides, and D refers to the polymerization product from glycol

oxides. The concentration of PEG is the only reactant that changes over time. This is because the concentration of O_2 is in excess and does not change to any appreciable amount. Thus, using the method of flooding or method of isolation is implicated on the final rate law in order to derive the final equation:

$$Rate_D = k'[A]^a \tag{5.1}$$

where $k' = \frac{k_3 k_1 [B]^b}{k_2 + k_3}$ and $[B]^b$ has been included as a constant in the reaction. In order to determine the reaction order, values from Table 5.2 must be plugged into the $Rate_D$ equation. The values were obtained by calculating the $\frac{\Delta[\ ]}{\Delta t}$ per day from the RPA (%) curve (Figure 5.10). The RPA (%) represents the reactants decreasing over time when exposed to air as well as products polymerizing and forming new peaks. By inserting the values from Table 5.2 into equation (5.1), first order kinetics is obtained for all values. For example,

$$\frac{Rate_{D2}}{Rate_{D1}} = \frac{[k'[A]^a]_2}{[k'[A]^a]_1}$$

$$\frac{2.78x10^{-8}}{2.43x10^{-8}} = \frac{0.0024^a}{0.0021^a}$$

$$1.14 = [\frac{0.0024}{0.0021}]^a$$

$$1.14 = 1.14^a$$

Therefore, "a" must equal 1 concluding first order kinetics. In the application of redacted documents, the reaction rate does not differ more than one order of magnitude. In the case where the ink is exposed to incandescent heat exposure, the initial rate of reaction occurs more than one

order of magnitude faster compared to ink exposed to air. Although the reaction rate is faster, the order stays consistent.

Experiment	Concentration (RPA)	Initial rate (RPA/s)
Peak *m/z* 614, Control, degradation		
Day 0-1	0.0738-0.0691=0.0047	$5.44x10^{-8}$
Day 1-2	0.0691-0.0573=0.0118	$1.37x10^{-7}$
Day 2-3	0.0573-0.0571=0.0002	$2.31x10^{-9}$
Day 3-4	0.0571-0.0560=0.0011	$1.27x10^{-8}$
Peak *m/z* 614, Sample, degradation		
Day 0-1	0.0644-0.0643=0.0001	$1.16x10^{-9}$
Day 1-2	0.0643-0.0622=0.0021	$2.43x10^{-8}$
Day 2-3	0.0622-0.0583=0.0039	$4.51x10^{-8}$
Day 3-4	0.0583-0.0476=0.0107	$1.24x10^{-7}$
Peak *m/z* 636 Control, degradation		
Day 0 -1	0.0641-0.0637=0.0004	$4.63x10^{-9}$
Day 1-2	0.0637-0.0623=0.0014	$1.62x10^{-8}$
Day 2-3	0.0623-0.0538=0.0085	$9.84x10^{-8}$
Day 3-4	0.0538-0.0536=0.0002	$2.32x10^{-9}$
Peak *m/z* 636 Sample, degradation		
Day 0-1	0.0591-0.0586=0.0005	$5.79x10^{-9}$
Day 1-2	0.0586-0.0550=0.0036	$4.17x10^{-8}$
Day 2-3	0.0550-0.0480=0.0070	$8.10x10^{-8}$
Day 3-4	0.0480-0.0477=0.0003	$3.47x10^{-9}$
Peak *m/z* 658 Control, degradation		
Day 0-1	0.0570-0.0570=0.0000	0
Day 1-2	0.0570-0.0562=0.0008	$9.26x10^{-9}$
Day 2-3	0.0562-0.0462=0.0100	$1.16x10^{-7}$
Day 3-4	0.0462-0.0458=0.0004	$4.63x10^{-9}$
Peak *m/z* 658 Sample, degradation		
Day 0-1	0.0565-0.0554=0.0011	$1.27x10^{-8}$
Day 1-2	0.0554-0.0541=0.0013	$1.50x10^{-8}$
Day 2-3	0.0541-0.0537=0.0004	$4.63x10^{-9}$
Day 3-4	0.0537-0.0493=0.0044	$5.09x10^{-8}$
Peak *m/z* 460 Control, formation		
Day 0-1	0.0472-0.0429=0.0043	$4.98x10^{-8}$
Day 1-2	0.0473-0.0472=0.0001	$1.16x10^{-9}$
Day 2-3	0.0557-0.0473=0.0084	$9.72x10^{-8}$
Day 3-4	0.0578-0.0557=0.0021	$2.43x10^{-8}$
Peak *m/z* 460 Sample, formation		
Day 0-1	0.0295-0.0273=0.0022	$2.54x10^{-8}$
Day 1-2	0.0310-0.0295=0.0015	$1.74x10^{-8}$
Day 2-3	0.0331-0.0310=0.0021	$2.43x10^{-8}$

Day 3-4	0.0354-0.0331=0.0023	2.66×10^{-8}
Peak *m/z* 474 Control, formation		
Day 0-1	0.0404-0.0368=0.0036	4.17×10^{-8}
Day 1-2	0.0469-0.0404=0.0065	7.52×10^{-8}
Day 2-3	0.0507-0.0469=0.0038	4.40×10^{-8}
Day 3-4	0.0511-0.0507=0.0004	4.63×10^{-9}
Peak *m/z* 474 Sample, formation		
Day 0-1	0.0277-0.0222=0.0055	6.37×10^{-8}
Day 1-2	0.0288-0.0277=0.0011	1.27×10^{-8}
Day 2-3	0.0290-0.0288=0.0002	2.31×10^{-9}
Day 3-4	0.0332-0.0290=0.0042	4.86×10^{-8}
Peak *m/z* 489 Control, formation		
Day 0-1	0.0348-0.0324=0.0024	2.78×10^{-8}
Day 1-2	0.0434-0.0348=0.0086	9.95×10^{-8}
Day 2-3	0.0462-0.0434=0.0028	3.24×10^{-8}
Day 3-4	0.0462-0.0459=0.0003	3.47×10^{-9}
Peak *m/z* 489 Sample, formation		
Day 0-1	0.0247-0.0238=0.0009	1.04×10^{-8}
Day 1-2	0.0247-0.0247=0.0000	0
Day 2-3	0.0247-0.0247=0.0000	0
Day 3-4	0.0306-0.0247=0.0059	6.83×10^{-8}
Incandescent light, peak *m/z* 801		
0 - 4 hours	0.1477-0.1463=0.0014	1.62×10^{-8}
4 - 8 hours	0.1463-0.1146=0.0317	3.67×10^{-7}
8 - 12 hours	0.1146-0.0668=0.0478	5.53×10^{-7}
12 - 16 hours	0.0668-0.0691=0.0023	2.66×10^{-8}
16 - 20 hours	0.0691-0.0700=0.0009	1.04×10^{-8}
20 - 24 hours	0.0700-0.0372=0.0328	3.80×10^{-7}

Table 5.2. The calculations for the $\Delta[\ ]/\Delta t$ from the RPA (%) curves.

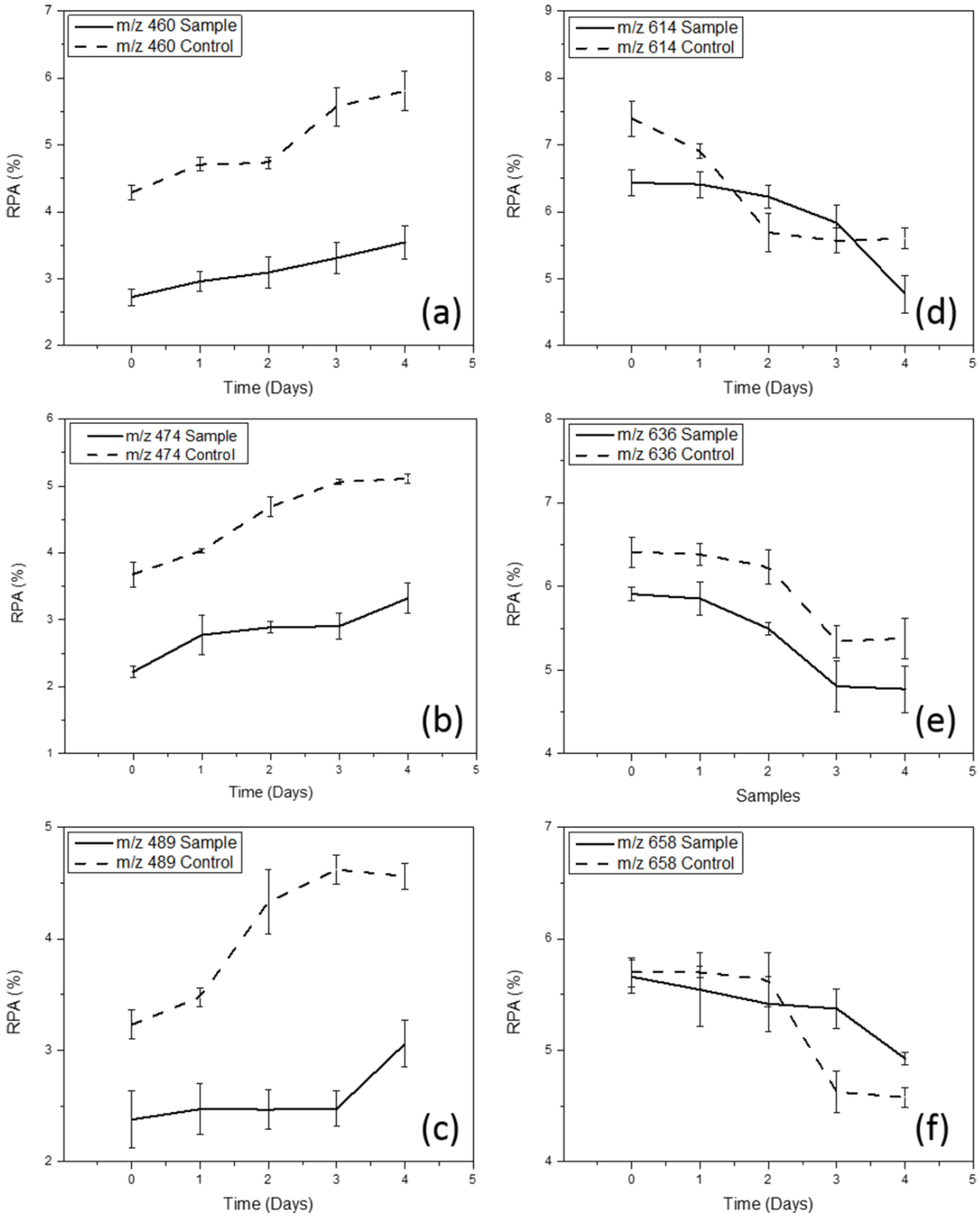

Figure 5.10. RPA (%) curves monitoring the oxidation of PEG of individual peaks where (a-c) are the low molecular weight peaks and (d-f) are the high molecular weight peaks.

5.4.5 Oxidation effects of laser ablation on inks

The high plasma temperature and plasma expansion induced from laser ablation could potentially have an effect on the underlying text. It is important to note the possible chemical changes and degradation of the ink caused by the interaction of the laser during the removal of the redacted layer. In order to show this effect, the written text itself (not redacted) was laser ablated at different energies to see how its profile oxidizes with increasing power. Figure 5.11 shows this effect by laser ablating a drawn ink line at different laser powers ranging from 0 to 100%. The high molecular weight peaks from PEG such as *m/z* 849, 894, and 1069 are decreasing as the low molecular weight peak such as *m/z* 411 is increasing. The largest oxidation change was observed between 0% laser power (fresh ink) and 20% laser power where peaks *m/z* 411, 849, 893, and 1069 showed a 5.48±0.06%, 5.08±0.03%, 6.123±0.09%, and 1.94±0.02% difference respectively. A significant change was not detected after 20% laser power was used. The largest alteration distinguished between 20 and 40% was 0.52±0.05% for *m/z* 849. Between 40% and 60% laser power, the RPA values had a difference of 1.72±0.05%, 2.32±0.07%, 2.48±0.07%, 0.64±0.01% for peaks *m/z* 411, 849, 893, and 1069. The fourth highest molecular weight peak, *m/z* 1069, almost disappeared after implementing 60% laser power on the ink (0.94±0.16% remaining). When laser ablating the inks with 80 and 100% power, there was not enough ink left for extraction. Thus, PEG was not seen in the spectra.

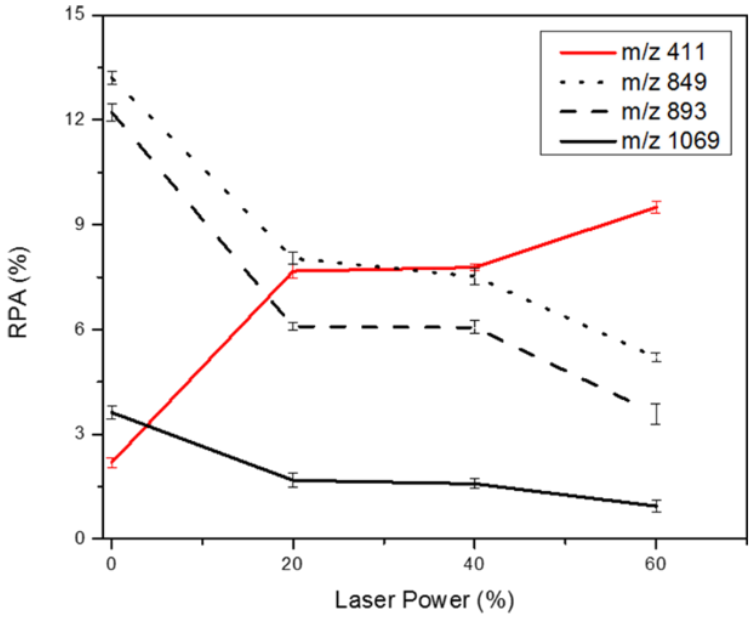

Figure 5.11. RPA (%) curves of individual peaks from PEG obtained from the extraction of ink laser ablated at different powers.

A laser power of 60% was used to remove the redacting ink layer from the text. As shown in Figure 5.2, the Sharpie was not completely removed but enough was removed to clearly reveal the text that was once redacted and extract the underlying ink. Figure 5.7 shows the effect of the laser on day 0 between the control and the sample. These samples were created at the same time where the control was not redacted and the sample was redacted with a Sharpie. After laser ablating and analyzing the sample, peaks *m/z* 849 and 893 has a 1.24±0.06% and 1.25±0.12% difference, respectively, between the sample and the control on day 0. This indicates that redacting the text and using laser ablation to remove the redacting ink affects the oxidation of the underlying ink by the aforementioned percentages. From this data, the Sharpie absorbs a majority of the UV radiation and plasma heating from the interaction of the laser but the underlying ink is still mildly affected.

5.5 Conclusion

Redacting documents or concealing text with another ink has been proven to influence the aging process of ink. Once ink is deposited on the writing surface, it will immediately start to age and oxidize. The aging process of ink can be altered in several ways. The "freshness" of the ink may differ depending on the surrounding levels of humidity and temperature. Ink may appear aged if heat was applied, such as setting the document in the sun or applying incandescent heat. Unfortunately, the drawback for applying laser ablation to full documents is time. In order to ablate an area of 1 cm^2 with 100 µm spot size would take 2.78 hours. Although effective, time would be an issue. Another issue to consider is the exposure of UV radiation and heat created between the laser and the ink, especially when monitoring the oxidation process of the ink. When the written text itself was laser ablated at 60% laser power, the RPA of the ink oxidized between 5-6%. The written text oxidized significantly less when redacted, the RPA changed about 1.25%. This deviation in RPA values could be compensated by using a correction factor (e.g, 1.25%) for a more accurate value. One last subject to consider when analyzing redacted documents is the chamber. The laser ablation chamber needs to be large enough to analyze full documents. This can be done by modifying the chamber to the desired size, which has been discussed in previous articles for different applications [58, 59, 60, 61].

For future applications, the laser ablation method can also be used to distinguish between legitimate and counterfeit breeder documents such as a driver's licenses. Breeder documents, such as birth certificates with limited or poor security features, are used to acquire other forms of identification and if a criminal obtains a breeder document then they can assume another person's identity and participate in illicit activities while going undetected [62]. A plastic polymer is applied over printed identification cards and licenses. The plastic polymer interferes and prevents

spectroscopy techniques from being utilized. By utilizing the laser ablation method the plastic polymer layer is ablated away and techniques such as Raman spectroscopy and DAPNe can be performed without opposition from the plastic polymer. Once a small section of the plastic is removed the laser will continue to ablate until the ink is exposed. Nanomanipulative techniques allow further chemical analysis and determining whether the original ink is being used on a falsified document. It can also be used to determine the ratio components in different inks, where the formulation is proprietary to the company. Overall, DAPNe-NSI-MS is very adaptable especially when coupled with other techniques which extends the window for many possibilities beneficial for forensic investigations. Furthermore, analyzing redacted documents from the federal government or documents from businesses are made easier with these techniques. By utilizing DAPNe-NSI-MS, the oxidation process can be monitored as well as characterizing the ink itself. Most importantly, the application of laser ablation and DAPNe is not harmful to the document, specifically the ink of interest.

Acknowledgements

This research is funded by the National Institute of Justice grant, award NIJ-2013-3361. We would also like to thank Gabriel D. Watts for his expertise, forensic document examiner with the U.S. Government.

5.6 References

[1] S. Bell, A Dictionary of Forensic Science, Oxford University Press, Oxford, 2012. doi:10.1093/acref/9780199594009.001.0001.

[2] K.R. Brunelle, Richard L.; Crawford, Advances in the Forensic Analysis and Dating of Writing ink, Charlies C. Thomas Publisher, LTD., Springfield, 2003.

[3] J. Coumbaros, K.P. Kirkbride, G. Klass, W. Skinner, Application of time of flight secondary ion mass spectrometry to the in situ analysis of ballpoint pen inks on paper, Forensic Sci. Int. 193 (2009) 42–46. doi:10.1016/j.forsciint.2009.08.020.

[4] B. Matthews, G.S. Walker, H. Kobus, P. Pigou, C. Bird, G. Smith, The analysis of dyes in ball point pen inks on single paper fibres using laser desorption ionisation time of flight mass spectrometry (LDI-TOFMS), Forensic Sci. Int. 209 (2011) e26–e30. doi:10.1016/j.forsciint.2011.03.033.

[5] L.J. Soltzberg, A. Hagar, S. Kridaratikorn, A. Mattson, R. Newman, MALDI-TOF Mass Spectrometric Identification, J. Am. Soc. Mass Spectrom. 18 (2007) 2001–2006. doi:10.1016/j.jasms.2007.08.008.

[6] M.R. Williams, C. Moody, L.-A. Arceneaux, C. Rinke, K. White, M.E. Sigman, Analysis of black writing ink by electrospray ionization mass spectrometry., Forensic Sci. Int. 191 (2009) 97–103. doi:10.1016/j.forsciint.2009.07.003.

[7] R.W. Jones, J.F. McClelland, Analysis of writing inks on paper using direct analysis in real time mass spectrometry, Forensic Sci. Int. 231 (2013) 73–81. doi:10.1016/j.forsciint.2013.04.016.

[8] M. Ezcurra, J.M.G. Góngora, I. Maguregui, R. Alonso, Analytical methods for dating modern writing instrument inks on paper, Forensic Sci. Int. 197 (2010) 1–20. doi:10.1016/j.forsciint.2009.11.013.

[9] C. Weyermann, D. Kirsch, C.C. Vera, B. Spengler, A GC/MS study of the drying of ballpoint pen ink on paper, Forensic Sci. Int. 168 (2007) 119–127. doi:10.1016/j.forsciint.2006.06.076.

[10] G. Chiavari, S. Montalbani, S. Prati, Y. Keheyan, S. Baroni, Application of analytical pyrolysis for the characterisation of old inks, J. Anal. Appl. Pyrolysis. 80 (2007) 400–405. doi:10.1016/j.jaap.2007.04.011.

[11] Y.-Z. Liu, J. Yu, M.-X. Xie, Y. Chen, G.-Y. Jiang, Y. Gao, Studies on the Degradation of Blue Gel Pen Dyes by Ion-Pairing High Performance Liquid Chromatography and Electrospray Tandem Mass Spectrometry., J. Chromatogr. A. 1125 (2006) 95–103. doi:10.1016/j.chroma.2006.05.034.

[12] Y.-Z. Liu, J. Yu, M.-X. Xie, Y. Liu, J. Han, T.-T. Jing, Classification and dating of black gel pen ink by ion-pairing high-performance liquid chromatography, J. Chromatogr. A. 1135 (2006) 57–64. doi:10.1016/j.chroma.2006.09.031.

[13] C. Neumann, R. Ramotowski, T. Genessay, Forensic examination of ink by high-performance thin layer chromatography-The United States Secret Service Digital Ink Library, J. Chromatogr. A. 1218 (2011) 2793–2811. doi:10.1016/j.chroma.2010.12.070.

[14] C. Vogt, J. Vogt, a. Becker, E. Rohde, Separation, comparison and identification of fountain pen inks by capillary electrophoresis with UV-visible and fluorescence detection and by proton-induced X-ray emission, J. Chromatogr. A. 781 (1997) 391–405. doi:10.1016/S0021-9673(97)00621-3.

[15] M. Gallidabino, C. Weyermann, R. Marquis, Differentiation of blue ballpoint pen inks by positive and negative mode LDI-MS, Forensic Sci. Int. 204 (2011) 169–178. doi:10.1016/j.forsciint.2010.05.027.

[16] Y. Wu, C.X. Zhou, J. Yu, H.L. Liu, M.X. Xie, Differentiation and dating of gel pen ink entries on paper by laser desorption ionization- and quadruple-time of flight mass spectrometry, Dye. Pigment. 94 (2012) 525–532. doi:10.1016/j.dyepig.2012.03.005.

[17] L. Ng, L.K.; Lafontaine, P.; Brazeau, Ballpoint pen inks: characterization by positive and negative ion-electrospray ionization mass spectrometry for the forensic examination of writing inks, J. Forensic Sci. 47 (2002) 1238–1247.

[18] C. Weyermann, L. Bucher, P. Majcherczyk, W. Mazzella, C. Roux, P. Esseiva, Statistical discrimination of black gel pen inks analysed by laser desorption/ionization mass spectrometry, Forensic Sci. Int. 217 (2012) 127–133. doi:10.1016/j.forsciint.2011.10.040.

[19] L. Heudt, D. Debois, T.A. Zimmerman, L. Köhler, F. Bano, F. Partouche, et al., Raman spectroscopy and laser desorption mass spectrometry for minimal destructive forensic analysis of black and color inkjet printed documents, Forensic Sci. Int. 219 (2012) 64–75. doi:10.1016/j.forsciint.2011.12.001.

[20] J. Donnelly, Shawn; Marrero, Josette E.; Cornell, Trevor; Fowler, Kevin; Allison, Analysis of Pigmented Inkjet Printer Inks and Printed Documents by Laser Desorption ⁄ Mass Spectrometry * , J. Forensic Sci. 55 (2010) 129–135. doi:10.1111/j.1556-4029.2009.01244.x.

[21] J.A. Denman, W.M. Skinner, K.P. Kirkbride, I.M. Kempson, Organic and inorganic discrimination of ballpoint pen inks by ToF-SIMS and multivariate statistics, Appl. Surf. Sci. 256 (2010) 2155–2163. doi:10.1016/j.apsusc.2009.09.066.

[22] R.B. Cody, J.A. Laramee, H.D. Durst, Versatile New Ion Source for the Analysis of Materials in Open Air under Ambient Conditions, Anal. Chem. 77 (2005) 2297–2302. doi:10.1021/ac050162j.

[23] J. Adams, Analysis of printing and writing papers by using direct analysis in real time mass spectrometry, Int. J. Mass Spectrom. 301 (2011) 109–126. doi:10.1016/j.ijms.2010.07.025.

[24] S. Houlgrave, G.M. Laporte, J.C. Stephens, J.L. Wilson, The Classification of Inkjet Inks Using AccuTOF DART (Direct Analysis in Real Time) Mass Spectrometry-A Preliminary Study, J. Forensic Sci. 58 (2013) 813–821. doi:10.1111/1556-4029.12048.

[25] R.G. Takats, Z.; Wiseman, J.M.; Cooks, Ambient mass spectrometry using desorption electrospray ionization (DESI): instrumentation, mechanisms and applications in forensics, chemistry, and biology, J. Mass Spectrom. 40 (2005) 1261–1275.

[26] L.S. Eberlin, R. Haddad, R.C. Sarabia Neto, R.G. Cosso, D.R.J. Maia, A.O. Maldaner, et al., Instantaneous chemical profiles of banknotes by ambient mass spectrometry, Analyst. 135 (2010) 2533–2539. doi:10.1039/c0an00243g.

[27] M.R.L. Paine, P.J. Barker, S.J. Blanksby, Characterising in situ activation and degradation of hindered amine light stabilisers using liquid extraction surface analysis-mass spectrometry., Anal. Chim. Acta. 808 (2014) 190–8. doi:10.1016/j.aca.2013.09.039.

[28] A. van Es, J. de Koeijer, G. van der Peijl, Discrimination of document paper by XRF, LA-ICP-MS and IRMS using multivariate statistical techniques, Sci. Justice. 49 (2009) 120–126. doi:10.1016/j.scijus.2009.03.006.

[29] K. Subedi, T. Trejos, J. Almirall, Forensic analysis of printing inks using tandem Laser Induced Breakdown Spectroscopy and Laser Ablation Inductively Coupled Plasma Mass Spectrometry, Spectrochim. Acta Part B At. Spectrosc. 103-104 (2015) 76–83. doi:10.1016/j.sab.2014.11.011.

[30] T. Trejos, A. Flores, J.R. Almirall, Micro-spectrochemical analysis of document paper and gel inks by laser ablation inductively coupled plasma mass spectrometry and laser induced breakdown spectroscopy, Spectrochim. Acta Part B At. Spectrosc. 65 (2010) 884–895. doi:10.1016/j.sab.2010.08.004.

[31] T. Trejos, R. Corzo, K. Subedi, J. Almirall, Characterization of toners and inkjets by laser ablation spectrochemical methods and Scanning Electron Microscopy-Energy Dispersive X-ray Spectroscopy, Spectrochim. Acta Part B At. Spectrosc. 92 (2014) 9–22. doi:10.1016/j.sab.2013.11.004.

[32] F.B. Gonzaga, W.F.D.C. Rocha, D.N. Correa, Discrimination between authentic and false tax stamps from liquor bottles using laser-induced breakdown spectroscopy and chemometrics, Spectrochim. Acta Part B At. Spectrosc. 109 (2015) 24–30. doi:10.1016/j.sab.2015.04.011.

[33] M. Hoehse, A. Paul, I. Gornushkin, U. Panne, Multivariate classification of pigments and inks using combined Raman spectroscopy and LIBS, Anal. Bioanal. Chem. 402 (2012) 1443–1450. doi:10.1007/s00216-011-5287-6.

[34] A. Kula, R. Wietecha-Posłuszny, K. Pasionek, M. Król, M. Woźniakiewicz, P. Kościelniak, Application of laser induced breakdown spectroscopy to examination of writing inks for forensic purposes, Sci. Justice. 54 (2014) 118–125. doi:10.1016/j.scijus.2013.09.008.

[35] D. Eikel, J. Henion, Liquid extraction surface analysis (LESA) of food surfaces employing chip-based nano-electrospray mass spectrometry, Rapid Commun. Mass Spectrom. 25 (2011) 2345–2354. doi:10.1002/rcm.5107.

[36] N.L. Ledbetter, B.L. Walton, P. Davila, W.D. Hoffmann, R.N. Ernest, G.F.V. Iv, et al., Nanomanipulation-Coupled Nanospray Mass Spectrometry Applied to the Extraction and Analysis of Trace Analytes Found on Fibers *, J. Forensic Sci. 55 (2010) 1218–1221. doi:10.1111/j.1556-4029.2010.01406.x.

[37] N. Wallace, E. Hueske, G.F. Verbeck, Science and Justice Ultra-trace analysis of illicit drugs from transfer of an electrostatic lift, Sci. Justice. 51 (2011) 196–203. doi:10.1016/j.scijus.2010.11.004.

[38] J.M. Brown, W.D. Hoffmann, C.M. Alvey, A.R. Wood, G.F. Verbeck, R.A. Petros, One-bead , one-compound peptide library sequencing via high-pressure ammonia cleavage coupled to nanomanipulation / nanoelectrospray ionization mass spectrometry, Anal.

Biochem. 398 (2010) 7–14. doi:10.1016/j.ab.2009.10.044.

[39] K. Clemons, J. Dake, E. Sisco, G.F. Verbeck, Trace analysis of energetic materials via direct analyte-probed nanoextraction coupled to direct analysis in real time mass spectrometry, Forensic Sci. Int. 231 (2013) 98–101. doi:10.1016/j.forsciint.2013.04.022.

[40] P.J. Horn, U. Joshi, A.K. Behrendt, K.D. Chapman, G.F. Verbeck, On-stage liquid-phase lipid microextraction coupled to nanospray mass spectrometry for detailed , nano-scale lipid analysis, Rapid Commun. Mass Spectrom. 26 (2012) 957–962. doi:10.1002/rcm.6194.

[41] V. Huynh, U. Joshi, J.M. Leveille, T.D. Golden, G.F. Verbeck, Nanomanipulation-coupled to nanospray mass spectrometry applied to document and ink analysis, Forensic Sci. Int. 242 (2014) 150–156. doi:10.1016/j.forsciint.2014.06.037.

[42] V. Huynh, K.C. Williams, T.D. Golden, G.F. Verbeck, Investigation of falsified documents via direct analyte-probed nanoextraction coupled to nanospray mass spectrometry, fluorescence microscopy, and Raman spectroscopy, Analyst. 140 (2015) 6553–6562. doi:10.1039/c5an01026h.

[43] R. Stewart, L. Li, D. Thomas, Multipass laser ablation of three coloured ink from a paper substrate, J. Mater. Process. Technol. 114 (2001) 161–167. doi:10.1016/S0924-0136(01)00728-2.

[44] R. Stewart, L. Li, D. Thomas, Laser ablation of multilayers of ink from a paper substrate for tactile printing, 32 (2000) 301–305.

[45] X.Y. Ma, D.; Shen, M.; Luo, Y.W.; Bo, J.; Xu, C.; Zhuo, Determination of blue ballpoint pen ink by laser ablation inductively coupled plasma mass spectrometry, Spectrosc. Spectr. 30 (2010) 2816–2819.

[46] R. Stewart, L. Li, D. Thomas, Multipass laser ablation of three coloured ink from a paper substrate, 114 (2001).

[47] B.S. Kelly, J.S.; Lindblom, ed., Scientific Examination of Questioned Documents, CRC Press, Boca Raton, 2006.

[48] S. Thompson, Tim; Black, ed., Forensic Human Identification, CRC Press, Boca Raton, 2006.

[49] J.L. Koenig, Spectroscopy of Polymers, Second, Elsevier, New York, 1999.

[50] S. Han, C. Kim, D. Kwon, Thermal/oxidative degradation and stabilization of polyethylene glycol, Polymer (Guildf). 38 (1997) 317–323. doi:10.1016/S0032-3861(97)88175-X.

[51] L. Boughen, J. Liggat, G. Ellis, Thermal degradation of polyethylene glycol 6000 and its effect on the assay of macroprolactin., Clin. Biochem. 43 (2010) 750–3. doi:10.1016/j.clinbiochem.2010.02.012.

[52] J. Glastrup, Degradation of polyethylene glycol. A study of the reaction mechanism in a model molecule: Tetraethylene glycol, Polym. Degrad. Stab. 52 (1996) 217–222. doi:10.1016/0141-3910(95)00225-1.

[53] C. Weyermann, D. Kirsch, C. Costa-vera, B. Spengler, Photofading of Ballpoint Dyes Studied on Paper by LDI and MALDI MS, Am. Soc. Mass Spectrom. 17 (2006) 297–306. doi:10.1016/j.jasms.2005.11.010.

[54] J.L. Campbell, M.N. Fiddler, K.E. Crawford, P.P. Gqamana, H.I. Kenttämaa, Analysis of polyethylene by using cyclopentadienyl cobalt chemical ionization combined with laser-induced acoustic desorption/fourier transform ion cyclotron resonance mass spectrometry., Anal. Chem. 77 (2005) 4020–4026. doi:10.1021/ac048409k.

[55] A. Anne, M.A. Bahri, A. Chovin, C. Demaille, C. Taofifenua, Probing the conformation and 2D-distribution of pyrene-terminated redox-labeled poly(ethylene glycol) chains end-adsorbed on HOPG using cyclic voltammetry and atomic force electrochemical microscopy, Phys. Chem. Chem. Phys. 16 (2014) 4642–4652. doi:10.1039/C3CP54720E.

[56] J. Ding, H. Gu, S. Yang, M. Li, J. Li, H. Chen, Selective detection of diethylene glycol in toothpaste products using neutral desorption reactive extractive electrospray ionization tandem mass spectrometry, Anal. Chem. 81 (2009) 8632–8638. doi:10.1021/ac9013594.

[57] S.A. Hemenway, Jeffrey N.; Carvalho, Thiago C.; Rao, Venkatramana M.; Wu, Yongmei; Levons, Jaquan K.; Narang, Ajit S.; Paruchuri, Srinivasa R.; Stamato, Howard J.; Varia, Formation of Reactive Impurities in Aqueous and Neat Polyethylene Glycol 400 Effects of Antioxidants and Oxidation Inducers, J. Pharm. Sci. 101 (2010) 3305–3318. doi:10.1002/jps.

[58] J.S. Becker, M. V. Zoriy, C. Pickhardt, N. Palomero-Gallagher, K. Zilles, Imaging of copper, zinc, and other elements in thin section of human brain samples (hippocampus) by laser ablation inductively coupled plasma mass spectrometry, Anal. Chem. 77 (2005) 3208–

3216. doi:10.1021/ac040184q.

[59] J. Feldmann, A. Kindness, P. Ek, Laser ablation of soft tissue using a cryogenically cooled ablation cell, J. Anal. At. Spectrom. 17 (2002) 813–818. doi:10.1039/b201960d.

[60] M.B. Fricker, D. Kutscher, B. Aeschlimann, J. Frommer, R. Dietiker, J. Bettmer, et al., High spatial resolution trace element analysis by LA-ICP-MS using a novel ablation cell for multiple or large samples, Int. J. Mass Spectrom. 307 (2011) 39–45. doi:10.1016/j.ijms.2011.01.008.

[61] I. Konz, B. Fernández, M.L. Fernández, R. Pereiro, A. Sanz-Medel, Design and evaluation of a new Peltier-cooled laser ablation cell with on-sample temperature control, Anal. Chim. Acta. 809 (2014) 88–96. doi:10.1016/j.aca.2013.11.040.

[62] B.P. Davies, S.J.; Hertig, C.A.; Gilbride, Security Supervision and Management, fourth, Butterworth-Heinemann:Elsevier, Waltham, 2015.

CHAPTER 6

DIRECT ANALYTE-PROBED NANOEXTRACTION (DAPNe) COUPLED TO MATRIX ASSITED LASER DESORPTION IONIZATION (MALDI) FOR INK ON DOCUMENT ANALYSIS[7]

6.1 Abstract

Matrix-assisted laser desorption/ionization mass spectrometry (MALDI-MS) has been coupled to direct analyte-probed nanoextraction (DAPNe) through use of nanomanipulation for ink on document analysis. Utilizing only MALDI-MS for this application is destructive to the document due to its plate size limitation. The document must be cut in order to be fitted to the sample plate. To solve this problem, DAPNe is first used to extract ink from the document and then deposits the sample on the MALDI plate. Through this method, cutting the document for MALDI-MS analysis is avoided. DAPNe extracts ink from documents with minimal to no visible destruction. This research shows the advantages of using MALDI-MS coupled to DAPNe by characterizing Crystal Violet, Basic Yellow 2, Rhodamine B, and polyethylene glycol from red and blue BIC pens, Uni-ball black pen, and black HP inkjet printer cartridge.

6.2 Introduction

Laser desorption has proven to be a powerful tool for colorant analysis in art and ballpoint pens in addition to colorant and pigment analysis of ink jet printer inks.[1,2] Coupling the technique to mass spectrometry yields a large amount of structural information.[3] This has led to the use of matrix-assisted laser desorption ionization mass spectrometry (MALDI-MS) for analyzing ink

[7] Contents of this chapter have been submitted to the *Journal of Forensic Science*, on January 28, 2016, from the authors V. Huynh, M. S. Phelps, T. D. Golden, and G.F. Verbeck, on January. The publisher is John Wiley & Sons, Inc.

from documents and identifying specific dyes. [1,4,5, 6, 7, 8, 9] No visible damage, from the interaction of the laser, has been reported when analyzing ink directly from the document.[5, 9] Although this technique saves time and is efficient, the size of the sample plate is constricted and limits document size, analyzing full documents requires cutting and fixing an area of the document to the sample plate. Thus, there is some destructive limitation of MALDI-MS in analyzing full documents.

Recent articles have shown success in coupling direct analyte-probed nanoextraction (DAPNe) with nanospray ionization mass spectrometry (NSI-MS) for ink on document analysis.[10, 11] This technique has also been used for biological [12, 13] and drug residue [14, 15] applications. DAPNe is a nanomanipulation technique that directly extracts minute amount of analytes from a variety of surfaces with minimal to no visible damage.[10,11] The nanomanipulator is fixed on the stage of a high-powered microscope and contains a removable, tip emitter that is pre-filled with an extraction solvent. There are however a few drawbacks in using NSI-MS with DAPNe. NSI-MS requires a coated tip in order to transfer ions from solution into the gas phase for mass analysis.[16] The tip emitter is typically coated (e.g., AuPd) which is more expensive when analyzing many samples. NSI-MS also requires accurate positioning to the MS source leading to longer preparation time. The major disadvantage of utilizing NSI is sample consumption. The continuous flow of NSI means that the sample is constantly being consumed.[17, 18, 19] Therefore, a large amount of sample is wasted. There are no mass spectrometers that can constantly analyze ions. For example, quadrupole ion trap (QIT) cannot accept any more ions once it reaches ion volume capacity. Coupling DAPNe with MALDI-MS instead can lead to several advantages. Since the tip emitters do not need to be coated for MALDI-MS analysis, they can be pulled in the lab for quick use instead of ordering them commercially pre-coated, thus reducing cost. Since MALDI-MS uses a pulsed laser, it ablates ions as needed and no sample is wasted.[19] It is important to not "throw

away" ions, especially for ultra-trace analyses. MALDI-MS can often provide data from sub-femtomole amounts of sampling loading, achieving high levels of sensitivity.[2, 19] MALDI-MS is also advantageous due to its high tolerance to salts and buffers (physiological levels of salts), unlike NSI.

By coupling MALDI-MS with direct analyte-probed nanoextraction (DAPNe), analyzing full documents can be made possible. The aim of this research is to demonstrate the ease of analyzing ink on documents from different pens and printed documents with DAPNe coupled to MALDI-MS. Different matrices will also be used to compare absolute intensities of ink components such as dyes and binding agents. These matrices include 1, 5-diaminonapthalene (DAN), 2, 5-dihydroxybenzoic acid (DHB), and silver nanoparticles. The absolute intensities of these matrices will be compared to the absolute intensity of samples with no matrix. For the first time, MALDI-MS has been transformed into a nondestructive technique for ink on document analysis.

6.3 Experimental Section

6.3.1 Reagents and solvent preparation

The solvents used are 18 Ω Millipore water (Milli-Q Plus; Billerica, MA) and optima LC/MS methanol (Fischer Scientific; Fair Lawn, NJ). The matrices used are 1,5-diaminonaphthalene (Sigma Aldrich; St. Louis, MO) and 2,5 dihydroxybenzoic acid (Sigma Aldrich; St. Louis, MO), and silver nanoparticles (99.999% purity, SPI Supplies; West Chester, PA). Blue and red pens (BIC; Shelton, CT), Uni-ball black pen (Newell Rubbermaid; Downers Grove, IL), deskjet (Black 60) ink cartridge (HP; Alto, CA), and A4 type copy paper were commercially obtained.

The extraction solvent used for all samples was methanol:water (1:1, v/v). Matrix spotting (0.5 µL per sample spot) was completed with 20 mg/mL of 2,5 dihydroxybenzoic acid (DHB) and 1,5-diaminonaphthalene (DAN), separately, solution in 70:30 mixture of acetonitrile: water (v/v). The matrix, silver nanoparticles, was landed on the sample using soft-landing ion mobility (SLIM).[20, 21, 22, 23]

6.3.2 Instrumentation and Sampling Technique

The nanomanipulator is fixed on the stage of a high-powered microscope, illustrated in Figure 6.1. It contains a removable, borosilicate glass, tip emitter that is pre-filled with an extraction solvent. The tip emitters were pulled in the lab using a P-2000 laser-based micropipette puller (Sutter Instrument; Novato, CA). This system integrates a CO_2 laser-based heat source to create different inner diameter (i.d.) tip sizes. Borosilicate glass (with filament) were used to create these tips with an outer diameter (o.d.) of 1.2 mm, i.d. 0.69 mm, and length of 10 cm (item #: BF120-69-10). Two tip emitters are created from one borosilicate glass capillary. Once made, the capillary was then cut to 2.5-3 cm for nanopositioner. A program with a heat setting of 280, velocity setting of 30, a pull setting of 0, and a delay setting of 200 was used to create these tip emitters. With this program, the average i.d. of the tip emitters was 42 µm. The i.d. of the tip emitters was determined using an Environmental FEI Quanta 200 scanning electron microscope (SEM).

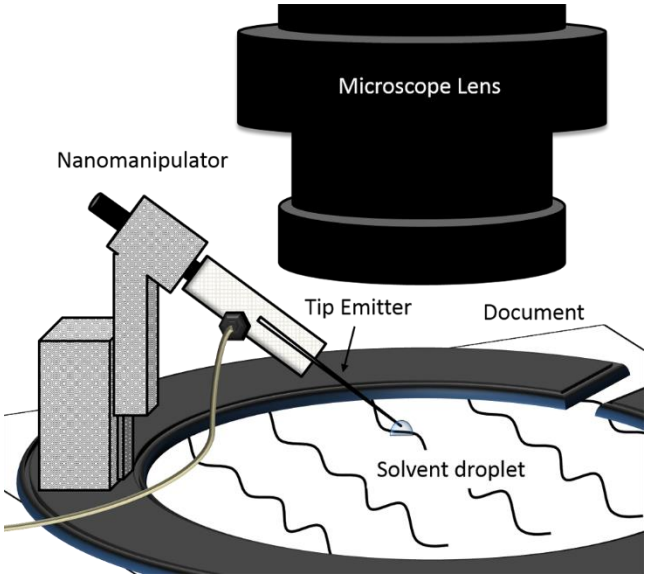

Figure 6.1. Schematic of nanomanipulator extracting ink from a document.

The piezoelectric-controlled nanomanipulator consists of an L200 nanomanipulator (DCG Systems; Richardson, TX) mounted on a Nikon AZ 100 (Nikon Instruments Inc.; Melville, NY) microscope stage. The range of motion for the joystick controlled nanomanipulator is 12 mm in the x- and z-direction and 28 mm in the y-coordinates. The translational resolution for fine and course mode are 5 nm and 100 nm, respectively. A PE2000b four-channel pressure injector (MicroData Instrument Inc.; S. Plainfield, NJ) was used to perform injection and aspiration.

The samples were made by drawing a line with different pens and printing text on copy paper. Figure 6.2 show micrographs that illustrate the process used for ink extraction. The tip emitter was first filled with 10 µL of extraction solvent. A 5 µL solvent droplet of Millipore water was then placed on the ink (Figure 6.2(b)). The tip emitter was positioned, using a joystick controller, where a miniscule amount of extraction solvent was injected via pressure injector (5 psi) into the droplet. While the droplet was still holding its tension, the extraction solvent induces liquid phase microextraction where components from the ink diffuse into the solvent. After 15-20

s the solvent droplet is then extracted (at 10 psi) back into the tip. As shown in Figure 6.2(c), this extraction method has a low impact on the document and ink where a watermark is left at most. The sample in the tip is then dispensed on a glass slide or MALDI plate (at 35 psi) where a matrix may be added or analyzed as is with laser desorption ionization exploration. The technique of extracting from a sample and depositing onto a glass slide for MALDI-MS analysis, with the nanomanipulator, was first conducted by Phelps et al.[24] for the analysis of single organelles. The direct extraction technique has also been previously discussed in other articles.[10, 11, 24]

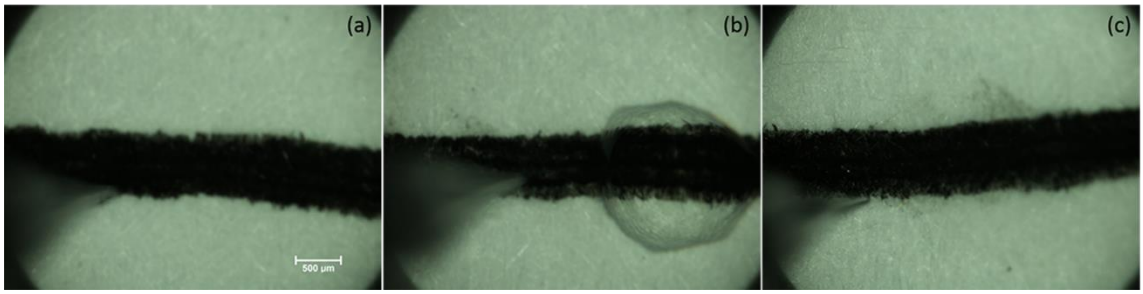

Figure 6.2. Micrographs of ink extraction from a black Uni-ball pen where (a) is before, (b) is during, and (c) is after extraction.

After spotting the samples with a matrix, the slides were analyzed by MALDI-LTQ-XL-Orbitrap (Thermo Scientific; San Jose, CA). This instrument is equipped with an intermediate pressure MALDI source (75 mTorr) using a 337 nm N_2 laser (MNL 100; Lasertechnik; Berlin, Germany). Automatic gain control (ACG) was on for all samples. Each sample was scanned from a *m/*z range of 100-2000 in positive mode. The laser power used for irradiating samples using DHB and DAN was 10 µJ. Laser energies ranging from 10 to 80 µJ was conducted on printer ink with no matrix. The spectra obtained for blue BIC pen, red BIC pen, and black Uni-ball pen (with no matrix) was conducted using a laser energy of 25 µJ, 35 µJ, and 15 µJ respectively. The data was processed using Xcalibur v 2.2 (Thermo Scientific; San Jose, CA) and image processing was performed with ImageQuest v 1.01 (Thermo Scientific; San Jose, CA).

For silver matrix studies, a soft-landing ion mobility chamber was used to deposit silver nanoparticles on top of the samples. SLIM uses a combination of cluster formation via laser ablation to soft land silver nanoparticles on a substrate.[21] The average sizes of one or more metal nanoparticles landed ranges from 10-500 nm.[20] A silver rod (99.999% purity; SPI Supplies; West Chester, PA) was laser ablated for silver nanoparticle deposition via 532 nm Nd:YAG laser (Minilite; Continuum; Santa Clara, CA) at 1 and 2 Torr He buffer gas for a deposition time of 60 minutes. Soft landing silver nanoparticles with the SLIM system has been previously discussed in more detail in a patent by Verbeck et al.[20] and in a most recent publication by Walton et al.[21]

6.4 Results and Discussion

6.4.1 Ink pens

The first ink sample analyzed was a blue BIC pen, which contains two dyes. After extraction, the ink sample was first imaged with no matrix and then analyzed with different matrices using MALDI-MS. Crystal Violet and Basic Yellow 2 were the dyes observed for the blue BIC pen. The mass spectrometric species for Crystal Violet dye and its degradation products include $[M\text{-}Cl]^+$, $[M\text{-}CH_3+H]^+$, and $[M\text{-}2CH_3+2H]^+$ [25, 26, 27] corresponding to *m/z* 372.244±0.003, 358.400±0.003, 344.953±0.003, respectively, and for Basic Yellow 2 is $[M\text{-}Cl]^+$ representing *m/z* 268.14±0.003.[25] Figure 6.3 shows the image of blue BIC pen, with no matrix, where *m/z* 372.244±0.003 is isolated. The red spots indicate high intensities of that peak where the blue areas indicate lower intensities. Figure 6.4(a) shows the spectrum obtained from a red region. Not using a matrix gave the highest intensity peaks for Crystal Violet due to its strong UV absorption characteristic. The most matrix assisting effect was observed when using DAN. Even though Crystal Violet was able to undergo absorption without a matrix, Basic Yellow 2 was not. Figure 6.4(a), inset, shows that Basic Yellow 2 does appear but at very low intensity compared to Crystal

Violet. The ratio difference of Basic Yellow 2 to Crystal Violet when not using a matrix and using DAN as a matrix is 0.0182 and 1.3319, respectively. This may be due to the low molar absorptivity of Basic Yellow 2 at the wavelength of the laser compared to Crystal Violet.[16] Therefore a matrix must be used to enhance its signal. According to Table 6.1, DHB has the most reduced matrix assisting effect and highest absolute intensity for *m/z* 268.181±0.003.

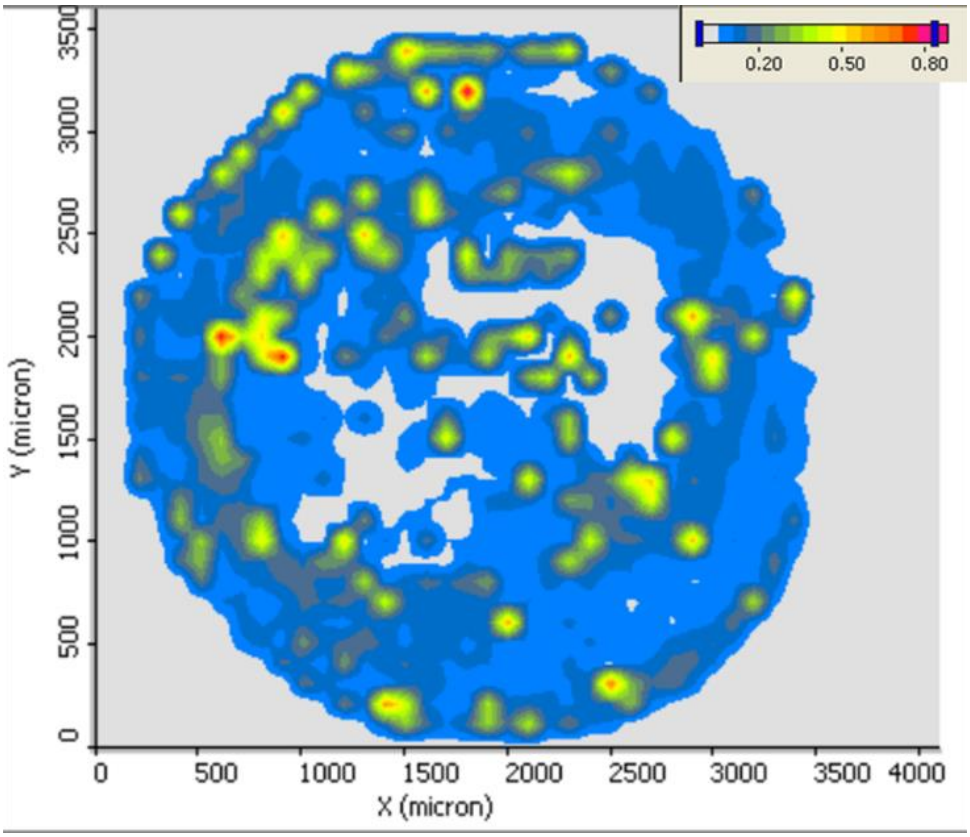

Figure 6.3. A MALDI-MS image of a blue BIC pen sample with no matrix, scale bar indicated (top right).

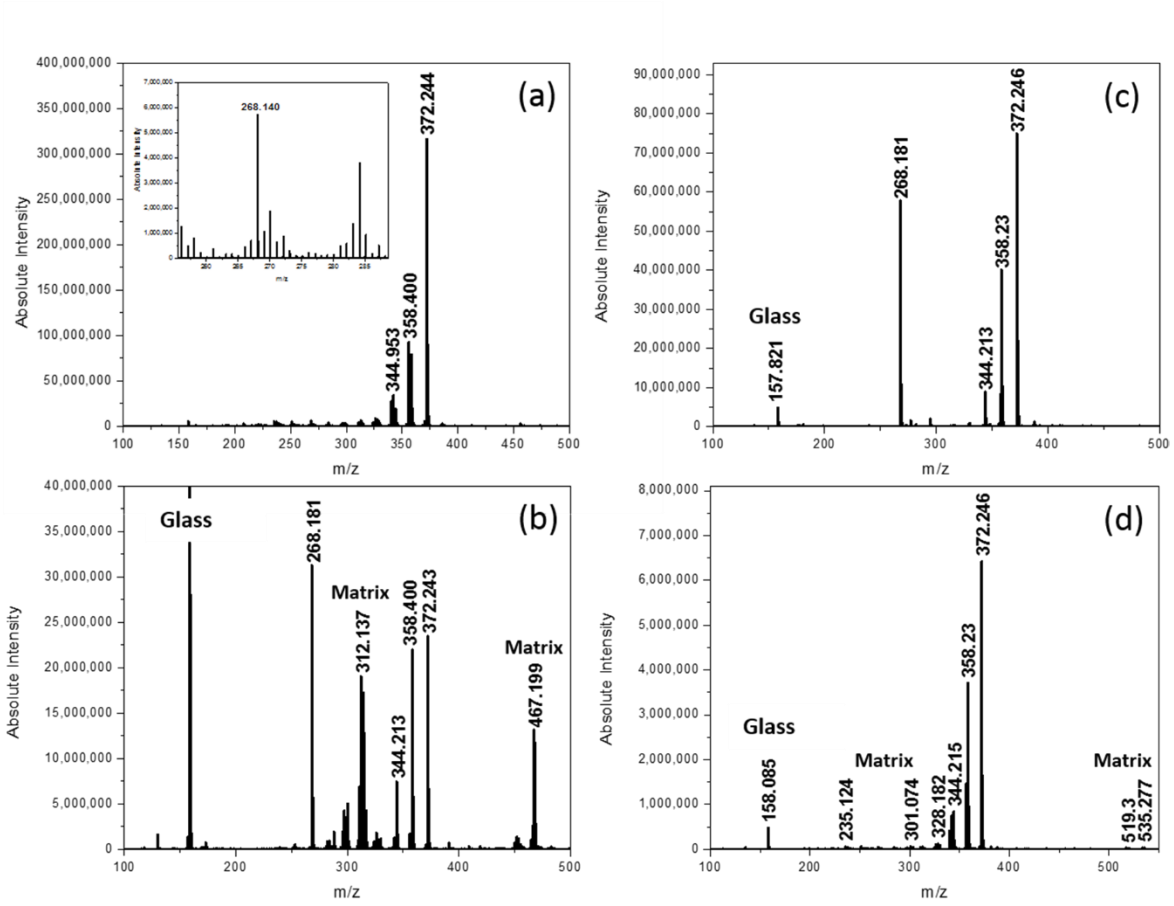

Figure 6.4. Spectra of Blue BIC pen using (a) no matrix, (b) DAN, (c) DHB, and (d) silver nanoparticles.

Sample	Matrix	Peaks	*m/z* (±0.003)	Absolute Intensity
Blue BIC	DAN	Crystal Violet	372.243	23,409,836
			358.400	21,868,852
			344.213	7,442,623
		Basic Yellow 2	268.181	31,180,328
		Glass	158.933	112,295,082
	DHB	Crystal Violet	372.246	74,745,290
			358.230	39,934,480
			344.213	8,891,072
		Basic Yellow 2	268.181	57,641,278
		Glass	158.821	4,596,232
	Ag	Crystal Violet	372.246	6,261,736
			358.230	3,574,888
			344.215	834,033
		Basic Yellow 2	268.130	43,683
		Glass	158.085	430,615
	None	Crystal Violet	372.244	315,163,934
			358.400	79,098,360
			344.953	33,606,557
		Basic Yellow 2	268.140	5,743,443
		Glass	158.152	4,746,701

Table 6.1. Different matrices used compared to no matrix for blue BIC pen.

Red BIC pen was analyzed with no matrix and different matrices. Figure 6.5 shows the spectra obtain from using no matrix and different matrices. Table 6.2 consists of compiled absolute intensity values from the substrate and dyes found in a red BIC pen. Three different components from Rhodamine B were observed. These peaks were *m/z* 443.235±0.003, 415.204±0.003, and 399.12±0.003 corresponding to $[M\text{-}Cl]^-$, $[M\text{-}CH_3+H]^+$, and $[M\text{-}CO_2]^+$ respectively (M represents

the parent ion).[26]. Although Rhodamine B was characterized adequately with no matrix, DHB greatly enhanced the signal by one order of magnitude. Matrix effects of DHB and the substrate did not suppress the dye signal. The spectra from Figure 6.5(b) and 6.5(d) show that using DAN and silver nanoparticles, correspondingly, greatly suppress the signals of interest.

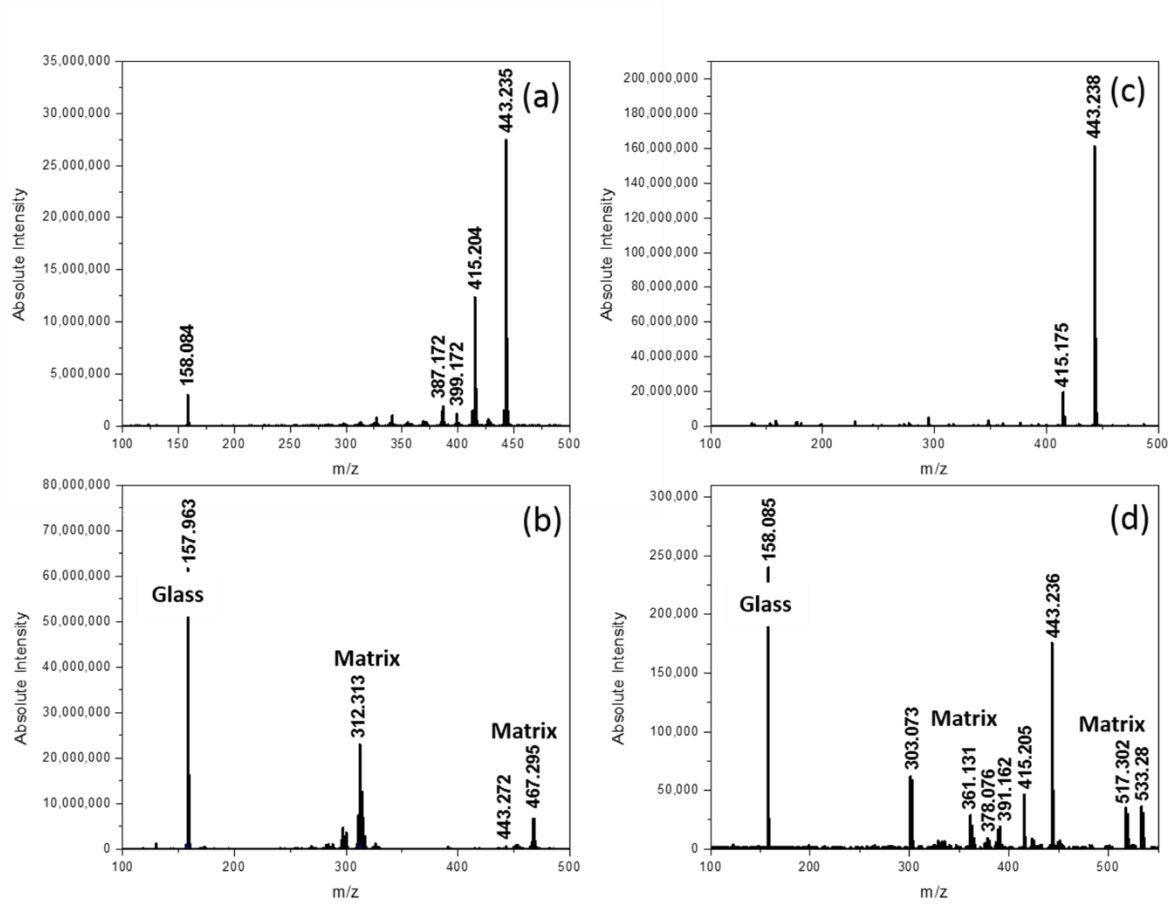

Figure 6.5. Spectra of Red BIC pen using (a) no matrix, (b) DAN, (c) DHB, and (d) silver nanoparticles.

Sample	Matrix	Peaks	*m/z* (±0.003)	Absolute Intensity
Red BIC	DAN	Rhodamine B	443.272	532,279
			415.200	227,334
			399.156	11,200
		Glass	158.963	61,504,918
	DHB	Rhodamine B	443.238	161,179,361
			415.175	19,164,619
			399.195	321,965
		Glass	158.335	3,027,284
	Ag	Rhodamine	443.236	171,806
			415.205	41,905
			399.900	1,353
		Glass	158.085	234,836
	None	Rhodamine	443.235	27,478,689
			415.204	12,290,164
			399.172	1,142,623
		Glass	158.084	2,954,098

Table 6.2. Different matrices used compared to no matrix for red BIC pen.

The spectra obtained when analyzing Uni-ball black pen is shown in Figure 6.6, where PEG was the main constituent observed. Table 6.3 indicates that using no matrix and DAN had more matrix assisting effects than using DHB and silver nanoparticles. Low-molecular-mass PEG (e.g., PEG 1000) can be analyzed in a straightforward laser desorption experiment without a matrix.[28,29] As PEG becomes more complex, by increasing the molecular mass or if the ink formula contains a mixture of polymers, a matrix will be needed. According to Figure 6.6(a), the highest mass spectrometric species detected without a matrix is *m/z* 1085.586±0.003. When a DAN and DHB is added, the number of PEG ions detected widens. Figure 6.6(c) shows an increase in

molecular weight of PEG ions detected when using DHB as a matrix. Uni-ball black pen also contained Crystal Violet dye with absolute intensities of 67,872.346 a.u., 37,716.743 a.u., and 53,728 a.u. for *m/z* 372.247±0.003, 356.215±0.003, and 343.073±0.003 respectively when no matrix was used (spectrum not shown). Huynh et al.[10] analyzed Uni-ball black pen with DAPNe-NSI-MS. Crystal Violet could only be observed when the ink was extracted with methanol:chloroform (1:1, v/v) and no peaks were observed when using methanol:water (1:1, v/v) as the extraction solvent. Although the absolute intensity values were low, the addition of DHB matrix increased the intensities values by one order of magnitude. The intensity of Crystal Violet could also be increased by using chloroform instead of methanol as the extraction solvent, but this would completely depreciate the signal of PEG.[10] This is because PEG requires heat to be soluble in chloroform. By coupling DAPNe with MALDI-MS instead of NSI-MS, signals from both Crystal Violet and PEG can be effectively observed when using DHB as a matrix and methanol as the extraction solvent.

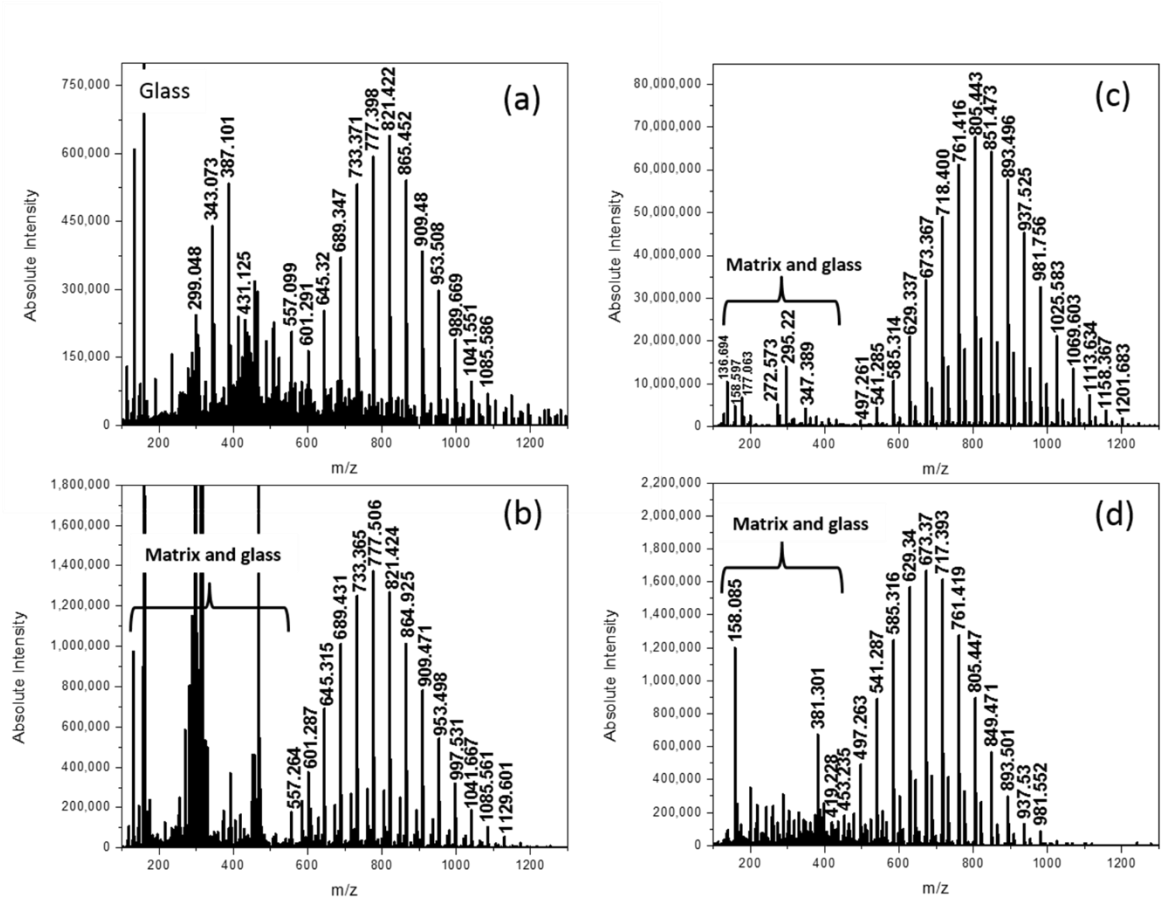

Figure 6.6. Spectra of Uni-Ball pen using (a) no matrix, (b) DAN, (c) DHB, and (d) silver nanoparticles.

Sample	Matrix	Peaks	*m/z* (±0.003)	Absolute Intensity
Uni-Ball Black	DAN	PEG *	777.506	1,370,024
		Crystal Violet	372.361	132,173
		Glass	158.666	63,390,663
	DHB	PEG *	805.443	67,361,761
		Crystal Violet	372.185	56,921
		Glass	158.597	4,648,031
	Ag	PEG *	673.370	1,631,147
		Crystal Violet	372	Not seen
		Glass	158.085	1,167,213
	None	PEG *	821.422	638,065
		Crystal Violet	372.349	67,872
		Glass	158.931	1,655,738
*The most intense peak was chosen				

Table 6.3. Different matrices used compared to no matrix for Uni-ball black pen.

6.4.2 Printer ink

Polyethylene glycol is a binding agent that was observed when analyzing HP black ink from a printer cartridge. The same constituent was found in black Epson ink cartridge.2 PEG is a popular ink solvent often used in printer inks due to its lubricating feature for the print heads.1 Different laser energies, ranging from 15 -80 μJ, were applied to prove the inefficient nature of PEG ionizing without a matrix. The molecular species of PEG ions were also not enhanced significantly when using DAN and silver nanoparticles as a matrix (Figure 6.7(a)). The matrix, DHB, greatly enriched the absolute intensity signals of the PEG distribution found in printer ink. Table 6.6 compares the most abundant PEG peak to the signal obtained from the glass substrate when using different matrices. The absolute intensity from glass (175,409,836 a.u.) was extremely

high when using DAN while it was less observed when using no matrix and silver nanoparticles. The matrix from the substrate was not seen when using DHB.

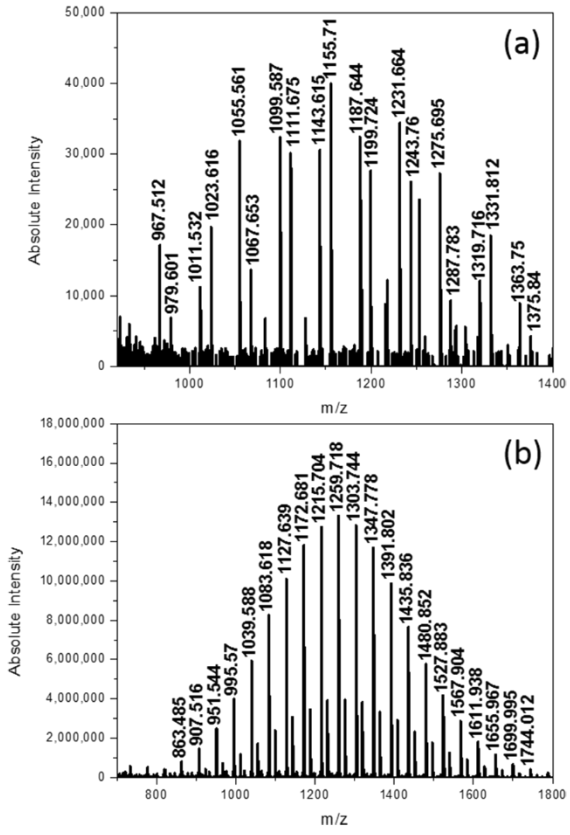

Figure 6.7. Spectra of black printer ink using (a) DAN and (b) DHB.

Sample	Matrix	Peaks	m/z (±0.003)	Absolute Intensity
Printer	DAN	PEG *	1155.710	39,877
		Glass	158.006	175,409,836
	DHB	PEG *	1259.718	13,307,377
		Glass	158	Not seen
	Ag	PEG *	n/a	Not seen
		Glass	158	373,878
	None	PEG*	n/a	Not seen
		Glass	158.242	1,347,947
*Most intense peak was chosen.				

Table 6.4. Different matrices used compared to no matrix for black printer ink.

6.5 Conclusion

For the first time, MALDI-MS can analyze ink on documents without the destructive nature of plate size constriction. Common ways to analyze ink on documents, using MALDI-MS, require removal of samples from the document or sample preparations involving evidence-altering of the paper.[30] DAPNe is a great addition for MALDI-MS and ink analysis generally due to its ability to nondestructively extract ink from a document and specifically because it can isolate specific components contained in ink. The latter is achieved by using different extraction solvents. Chloroform may be added to the extraction solvent to extract a higher volume of Crystal Violet dye from Uni-ball black pen in contrast to methanol which extracts a higher volume of PEG.[10] Not only is sample preparation time reduced, sensitivity is maintained and sample volume is not wasted. Printer ink was the only sample that could not be analyzed without a matrix. PEG could not be analyzed effectively without a matrix in printer ink, but by concurrently analyzing printer

ink with DHB this problem is solved. DHB proves to be the most proficient matrix used to enhance all molecular ion signals found in red and blue BIC pens, Uni-ball pens, and printer ink.

Acknowledgements

This project is funded by the National Institute of Justice grant no. NIJ-2013-3361.

6.6 References

(1) Heudt, L.; Debois, D.; Zimmerman, T. A.; Köhler, L.; Bano, F.; Partouche, F.; Duwez, A. S.; Gilbert, B.; De Pauw, E. *Forensic Sci. Int.* **2012**, *219*, 64–75.

(2) Donnelly, S.; Marrero, J. E.; Cornell, T.; Fowler, K.; Allison, J. *J. Forensic Sci.* **2010**, *55* (1), 129–135.

(3) Weyermann, C.; Bucher, L.; Majcherczyk, P. *Sci. Justice* **2011**, *51* (3), 122–130.

(4) Seraglia, R.; Teatino, A.; Traldi, P. *Forensic Sci. Int.* **2004**, *146S*, S83–S85.

(5) Matthews, B.; Walker, G. S.; Kobus, H.; Pigou, P.; Bird, C.; Smith, G. *Forensic Sci. Int.* **2011**, *209*, e26–e30.

(6) Baluya, D. L.; Garrett, T. J.; Yost, R. A. *Anal. Chem.* **2007**, *79* (17), 6862–6867.

(7) Wang, X.; Zhang, Y.; Wu, Y.; Yu, J.; Xie, M. *Forensic Sci. Int.* **2014**, *236*, 99–108.

(8) Weyermann, C.; Kirsch, D.; Costa-vera, C.; Spengler, B. *Am. Soc. Mass Spectrom.* **2006**, *17*, 297–306.

(9) Dunn, J. D.; Allison, J. *J. Forensic Sci.* **2007**, *52* (5), 1205–1211.

(10) Huynh, V.; Williams, K. C.; Golden, T. D.; Verbeck, G. F. *Analyst* **2015**, *140*, 6553–6562.

(11) Huynh, V.; Joshi, U.; Leveille, J. M.; Golden, T. D.; Verbeck, G. F. *Forensic Sci. Int.* **2014**, *242*, 150–156.

(12) Brown, J. M.; Hoffmann, W. D.; Alvey, C. M.; Wood, A. R.; Verbeck, G. F.; Petros, R. A. *Anal. Biochem.* **2010**, *398* (1), 7–14.

(13) Horn, P. J.; Joshi, U.; Behrendt, A. K.; Chapman, K. D.; Verbeck, G. F. *Rapid Commun.*

Mass Spectrom. **2012**, *26*, 957–962.

(14) Wallace, N.; Hueske, E.; Verbeck, G. F. *Sci. Justice* **2011**, *51* (4), 196–203.

(15) Ledbetter, N. L.; Walton, B. L.; Davila, P.; Hoffmann, W. D.; Ernest, R. N.; Iv, G. F. V.; Ph, D. *J. Forensic Sci.* **2010**, *55* (5), 1218–1221.

(16) Cole, R. B. *Electrospray and MALDI Mass Spectrometry: Fundamentals, Instrumentation, Practicalities, and Biological Applications*, Second.; John Wiley & Sons, Inc.: Hoboken, 2010.

(17) Kebarle, P.; Verkerk, U. H. *Mass Spectrom. Rev.* **2009**, *28*, 898–917.

(18) Kebarle, P.; Verkerk, U. H. *Reactive intermediates: MS Investigations in Solutions*; Santos, L. S., Ed.; Wiley-VCH: Weinheim, 2010.

(19) Glish, G. L.; Vachet, R. W. *Nat. Rev. Drug Discov.* **2003**, *2* (2), 140–151.

(20) Verbeck, G. F. IV; Davila, S. Silver and Silver Nanoparticle MALDI Matrix Utilizing Online Soft Landing Ion Mobility. US 8,610,058 B2, 2013.

(21) Walton, B. L.; Verbeck, G. F. *Anal. Chem.* **2014**, *86*, 8114–8120.

(22) Hoffmann, W.; Verbeck, G. *Appl. Spectrosc.* **2013**, *67* (6), 656–660.

(23) Verbeck, G.; Hoffmann, W.; Walton, B. *Analyst* **2012**, *137* (19), 4377–4620.

(24) Phelps, M. S.; Sturtevant, D.; Chapman, K. D.; Verbeck, G. F. *Am. Soc. Mass Spectrom.* **2015**, *10.1007/s1*, 1–7.

(25) Soltzberg, L. J.; Hagar, A.; Kridaratikorn, S.; Mattson, A.; Newman, R. *J. Am. Soc. Mass Spectrom.* **2007**, *18*, 2001–2006.

(26) Siegel, J.; Allison, J.; Mohr, D.; Dunn, J. *Talanta* **2005**, *67*, 425–429.

(27) Giurato, L.; Candura, A.; Grasso, G.; Spoto, G. *Appl. Phys. A* **2009**, *97*, 263–269.

(28) *MALDI Mass Spectrometry for Synthetic Polymer Analysis*; Liang, L., Ed.; A John Wiley & Sons, Inc.: Hoboken, 2010.

(29) Thomas, J. J.; Shen, Z.; Blackledge, R.; Siuzdak, G. *Anal. Chim.* **2001**, *442*, 183–190.

(30) Jones, R. W.; Cody, R. B.; McClelland, J. F. *Forensic Sci. Int.* **2013**, *231*, 73–81.

Graphical Abstract

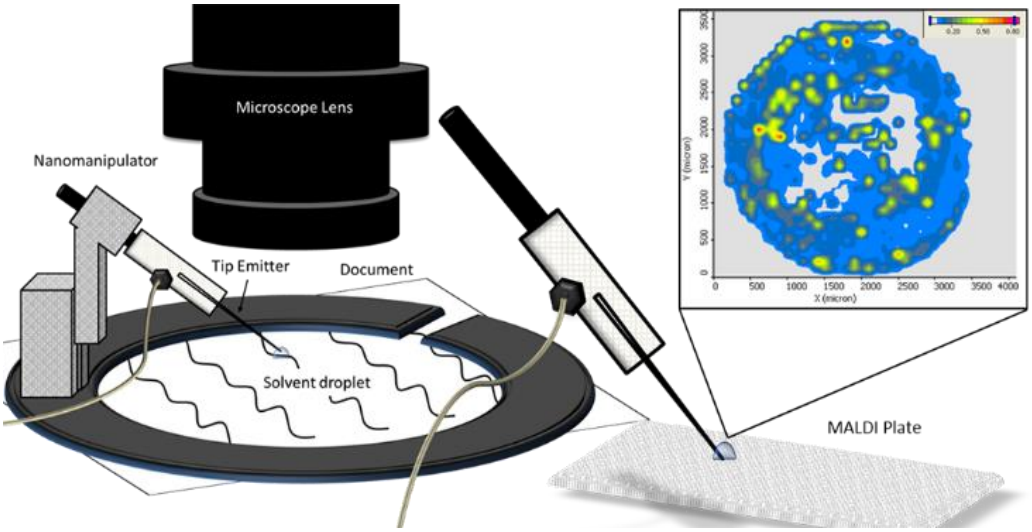

CHAPTER 7

CONCLUSIONS AND FUTURE WORK

7.1 Future Work

Although much research has been conducted in the area of ink on document analysis using DAPNe, there are still many regions that need to be explored. This chapter elaborates on these experiments as future work.

7.1.1 Liquid Phase Microextraction Interphase

The solvent droplet used as an interphase between the tip emitter and sample needs to be explored. This interphase alone contains a lot of solution chemistry that could aid in ink extractions. The purpose of the solvent droplet is to diffuse ink components into the droplet and then extract the ink-diffused droplet into the tip emitter. This technique is known as liquid phase microextraction (LPMe).

In the previously discussed chapters, only Millipore water was used as the LPMe-interphase. Many more solvent droplets need to be explored. One main problem arises when extracting ink from different paper. The solvent droplet holds its tension only for a short period of time. By expanding the amount of time the solvent droplet stays on the substrate, more components of the ink can be detected. Increasing the extraction time has many advantages such as (1) increasing analyte concentration in the solvent droplet, (2) increasing the number of different ink components diffusing into the droplet, and (3) lessening solvent absorption into the paper. Allowing more time for extraction could lead to more components from the ink to be extracted and would also give enough time to extract a higher volume, a majority of the solvent droplet, back

into the tip (i.e., leading to less solvent bleed into the writing substrate and a higher volume of sample for longer analyses). The main focus for this area of research would be to explore solvents with higher tension, but aqueous enough for nanoextraction. In addition, more types of paper can be analyzed. Thus, a solvent droplet with higher tension needs to be explored.

7.1.2 Nanoextraction Separatory Funnel

A separatory funnel is a piece of laboratory glassware used to separate a mixture into two immiscible solvent phases (e.g., chloroform and water) through liquid-liquid phase extraction. From this idea, the same concept may be used with a tip emitter via DAPNe. This technique is known as nanoextraction separatory funnel (NeSF). Figure 7.1 illustrates this technique when analyzing ink on documents. The tip emitter is first back-filled with 10 µL of chloroform. A 5 µL solvent droplet of Millipore water is then placed on the sample as shown in Figure 7.1 (inset). The tip emitter is then positioned into the droplet, propelling a miniscule amount of chloroform into the solvent droplet. This creates two immiscible phases. The analytes from the ink diffuse into the chloroform and water, depending on its solubility properties. After 10-15 s the droplet infused chloroform is then extracted into the tip for MALDI imaging analysis.

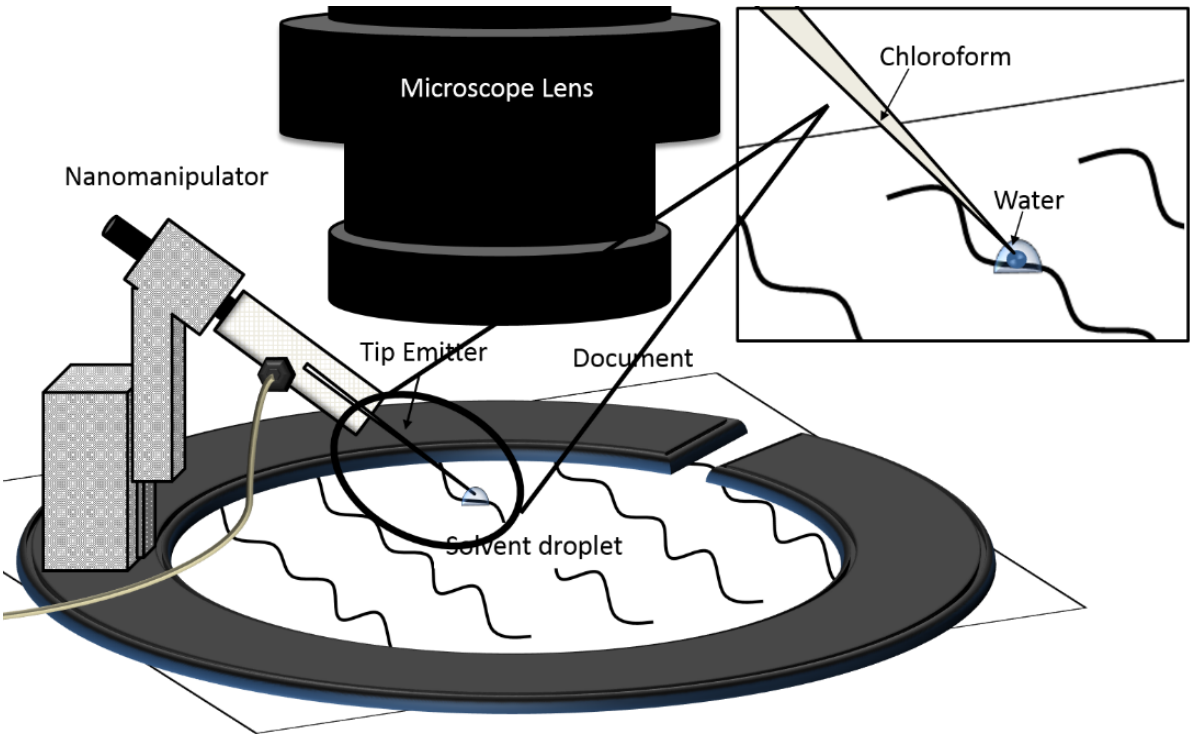

Figure 7.1. Nanomanipulator extracting ink from a document using NeSF technique where the tip emitter is filled with chloroform and Millipore water is used as the solvent droplet. Injecting chloroform into the solvent droplet creates a separate phase liquid extraction (inset).

Using MALDI-MS to analyze the sample enables the document examiner to distinguish the separation of analytes using the NeSF technique. The overall concept would be to separate the analytes within a given extraction to reduce time and enhance efficiency. The micrograph of using this technique for the extraction of ink from a Uni-ball pen is shown in Figure 7.2. A miniscule amount of chloroform is injected into the water droplet, creating an immiscible interface within. This induces the ink analytes that are more soluble in chloroform to collect in this area while the water soluble analytes collect in the aqueous phase. For example, Uni-ball black waterproof pen contains Crystal Violet and PEG. Crystal Violet is more soluble in

chloroform and PEG is more soluble in water. The ending result would be to see the separation of components in MALDI-MS spectra.

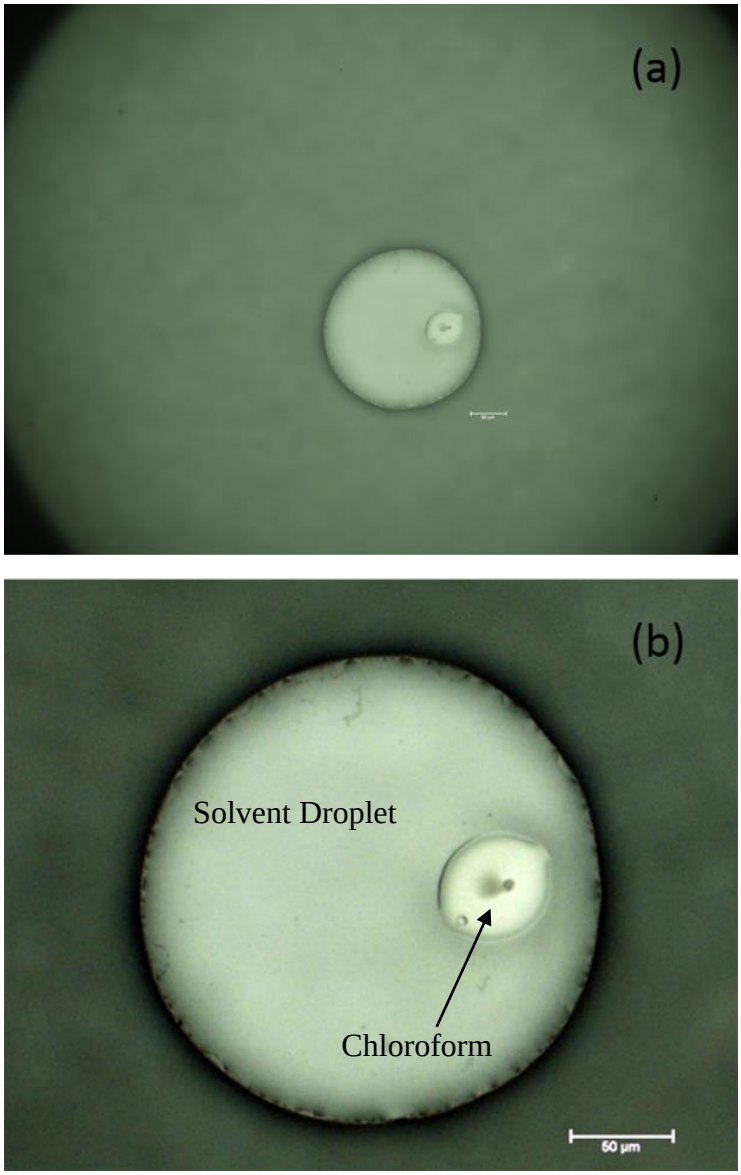

Figure 7.2. Micrograph of ink sample deposited on MALDI-MS slide using NeSF technique where (b) is a zoomed in image of (a).

7.1.3 Counterfeit Government Official Documents

As technology advances, the ability for the public to create legitimate counterfeit government documents advances. This creates a significant problem when (but not limited to) forged IDs, passports, currency, and birth certificates are approved and authorized as authentic documents. Plagiarists are able to create these documents by digitally scanning the aforementioned documents, digitally editing, and using color laser and inkjet printers to produce forged documents (i.e., scanning a passport and digitally editing the picture prior to printing). The ink cartridges used to produce these documents are proprietary to the company. Therefore, analyzing the ink chemistry can potentially lead to a specific brand ink or printer. The United States (U.S.) government has created inks with trace markers that is unique and different from in-house inks. Thus, a technique to differentiate these inks using DAPNe can determine the authenticity of government documents.

The potential of using laser ablation (LA) coupled to DAPNe has already been applied to redacted documents (Chapter 5) but needs to be extended to government official documents. The plastic layer sealing the ink of these documents needs to be removed prior to analyzing the ink underneath. Optimization of using LA to remove the plastic seal of these documents needs to be researched as well as determining an extraction method for analyzing the ink chemistry. Other items that have a plastic layer on top such as postage stamps also needs to be investigated.

7.1.4 Long Term Oxidation Studies

Long term oxidation studies of inks has yet to be explored. This includes natural aging and simulated aging in different environments. This will help investigate the authentication of back dating older documents such as ancient manuscripts and contracts or wills that are a few years old. These studies may be expanded to different kinds of pens, different brands of pens, and printer

inks. The goal of this study would be to create a library for forensic document examiners to utilize, aiding crime scene investigation and museum manuscript authentication.

7.2 Conclusion

The potential of direct analyte-probed nanoextraction is limitless. The ability for this technique to be coupled with several instruments has proven its usefulness in the forensic field of document examination. Most analysts already have one or some of the aforementioned instruments discussed in this dissertation. By having DAPNe as a new addition, these analysts can couple DAPNe with the instruments in their lab to further their studies in research and development. Not only is DAPNe an incredible tool for the forensic community, it has also expanded to biological applications such as single cell, lipid analysis, and cancer research.